nagra
National Cooperative for the
Disposal of Radioactive Waste

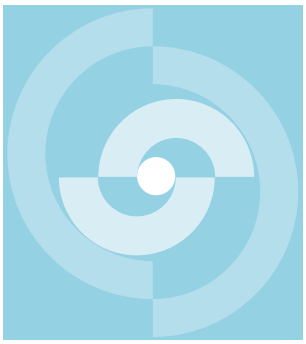

TECHNICAL REPORT 02-08

The Uptake of Eu(III) and Th(IV) by Calcite under Hyperalkaline Conditions:

The Influence of Gluconic and Isosaccharinic Acid

December 2002

J. Tits, M. Bradbury, P. Eckert,
A. Schaible, E. Wieland

Paul Scherrer Institut, Villigen PSI

Hardstrasse 73, CH-5430 Wettingen/Switzerland, Telephone +41-56-437 11 11

nagra
National Cooperative for the
Disposal of Radioactive Waste

TECHNICAL REPORT 02-08

The Uptake of Eu(III) and Th(IV) by Calcite under Hyperalkaline Conditions:

The Influence of Gluconic and Isosaccharinic Acid

December 2002

J. Tits, M. Bradbury, P. Eckert,
A. Schaible, E. Wieland

Paul Scherrer Institut, Villigen PSI

Hardstrasse 73, CH-5430 Wettingen/Switzerland, Telephone +41-56-437 11 11

This report was prepared on behalf of Nagra. The viewpoints presented and conclusions reached are those of the author(s) and do not necessarily represent those of Nagra.

PREFACE

The Laboratory for Waste Management of the Nuclear Energy and Safety Research Department at the Paul Scherrer Institut is performing work to develop and test models as well as to acquire specific data relevant to performance assessments of planned Swiss nuclear waste repositories. These investigations are undertaken in close co-operation with, and with the financial support of, the National Cooperative for the Disposal of Radioactive Waste (Nagra). The present report is issued simultaneously as a PSI-Bericht and a Nagra Technical Report.

ISSN 1015-2636

ABSTRACT

Calcite is an important component of Valanginian marl, a potential host rock for a low and intermediate level radioactive waste (L/ILW) repository in Switzerland. This mineral also forms an important component of the disturbed zone around a repository, as it remains largely unaffected by the hyperalkaline waters migrating out of the cementitious repository.

The sorption behaviour of Eu(III) and Th(IV) on Merck calcite in an artificial cement pore water (ACW) at pH 13.3 has been studied in batch-type sorption experiments. In addition, the effect of α-isosaccharinic acid (ISA) and gluconic acid (GLU) on the sorption of these two cations has been investigated.

In the absence of ISA and GLU, a strong interaction of Eu(III) and Th(IV) with Merck calcite was observed. Eu(III) and Th(IV) sorption kinetics were fast and the isotherms indicated a linear adsorption behaviour over the experimentally accessible concentration range. In the case of Eu(III), a decrease of the R_d value with increasing solid to liquid (S:L) ratio was observed indicating that, along with adsorption, other processes might influence the immobilisation of this cation by Merck calcite under ACW conditions. In the case of Th(IV), however, changes in the S:L ratio had no effect on the sorption behaviour.

High ISA and GLU concentrations in solution significantly affected the sorption of both Eu(III) and Th(IV): R_d values for Eu(III) decreased significantly at ISA concentrations higher than 10^{-5} M and at GLU concentrations higher than 10^{-7} M. The sorption of Th(IV) was reduced at ISA concentrations above $2 \cdot 10^{-5}$ M and at GLU concentrations above 10^{-6} M.

The effects of ISA and GLU on the immobilisation of Eu(III) and Th(IV) were interpreted in terms of complex formation in solution. In the case of Eu(III) the metal-ligand complexes were found to have a 1:1 stoichiometry. Complexation constants derived for the aqueous Eu(III)-ISA' and Eu(III)-GLU complexes were determined to be $\log \beta^0_{EuISA} = -31.1 \pm 0.2$ and $\log \beta^0_{EuGLU} = -28.7 \pm 0.1$.

In the case of Th(IV) it was assumed that a Th(IV) - ISA - Ca complex and a Th(IV) - GLU - Ca complex were formed both having a 1:2:1 stoichiometry. The complexation constants for these two complexes were determined to be $\log \beta^0_{ThISA} = -5.0 \pm 0.3$ and $\log \beta^0_{ThGLU} = -2.14 \pm 0.01$.

Assuming that the concentrations of ISA and GLU in the pore water of the disturbed zone are similar to the maximum concentrations estimated for the cement pore water in the near-field of the repository, i.e. 10^{-5} M ISA and 10^{-7} M GLU, then the formation of aqueous complexes with ISA or GLU would not significantly affect Eu(III) and Th(IV) sorption on calcite.

ZUSAMMENFASSUNG

Kalzit ist eine wichtiger Bestandteil des Valanginian Mergels, der als mögliches Wirtgestein für ein Tiefenlager für schwach und kurzlebig mittelaktive Abfälle (Tiefenlager SMA) in der Schweiz vorgesehen ist. Dieses Mineral ist ebenfalls ein wichtiger Bestandteil in der gestörten Zone um ein Endlager, da es durch das aus dem zementhaltigen Nahfeld austretende, hochalkalische Wasser kaum verändert wird.

Die Sorption von Eu(III) und Th(IV) auf Merck Kalzit wurde im Batchverfahren bestimmt. Dabei wurde Merck Kalzit in einem künstlichen Zementporenwasser bei pH 13.3 suspendiert. Im weiteren wurde der Einfluss von α-Isosaccharinsäure (ISA) und Gluconsäure (GLU) auf das Sorptionsverhalten der beiden Kationen untersucht.

Eine starke Wechselwirkung von Eu(III) und Th(IV) mit Merck Kalzit wurde in Abwesenheit von ISA und GLU beobachtet. Die Sorption erfolgte sehr schnell und die Isothermen entsprachen einem linearen Adsorptionsverhalten im experimentell zugänglichen Konzentrationsbereich. Eine Abnahme des Sorptionswerts (R_d Wert) mit zunehmendem Festphasen-zu-Flüssigkeitsverhältnis wurde für Eu(III) beobachtet, was darauf hindeutet, dass nebst der Adsorption weitere Prozesse das Sorptionsverhalten dieses Kations auf Merck Kalzit unter Zementporenwasserbedingungen beeinflussen. Keine Abhängigkeit des R_d Werts vom Festphasen-zu-Flüssigkeitsverhältnis wurde hingegen bei Th(IV) beobachtet.

Steigende Lösungskonzentrationen von ISA und GLU hatten einen messbaren Effekt auf die Sorptionswerten von Eu(III) und Th(IV). Die R_d Werte von Eu(III) wurden bei ISA Konzentrationen oberhalb 10^{-5} M und GLU Konzentrationen oberhalb 10^{-7} M signifikant kleiner. Die Sorption von Th(IV) nahm bei ISA Konzentrationen oberhalb $2 \cdot 10^{-5}$ M und GLU Konzentrationen oberhalb 10^{-6} M ab.

Der Einfluss von ISA und GLU auf die Immobilisierung von Eu(III) und Th(IV) wurde als Folge von Komplexbildungen in Lösung interpretiert. Im Falle von Eu(III) wurde eine 1:1 Stoichiometrie für die Metall-Ligand Komplexe gefunden. Die Komplexierungskonstanten für die gelösten Eu(III)-ISA und Eu(III)-GLU Komplexe wurden zu $\log \beta^0_{EuISA} = -31.1 \pm 0.2$ und $\log \beta^0_{EuGLU} = -28.7 \pm 0.1$ bestimmt.

Im Falle von Th(IV) wurde angenommen, dass Th(IV) - ISA - Ca Komplexe und Th(IV) – GLU - Ca Komplexe mit einer 1:2:1 Stöchiometrie gebildet werden. Die Komplexierungskonstanten für diese Komplexe wurden zu $\log \beta^0_{ThISA} = -5.0 \pm 0.3$ und $\log \beta^0_{ThGLU} = -2.14 \pm 0.01$ bestimmt.

Die Bildung von gelösten Metall-Ligand Komplexen hat keinen signifikanten Einfluss auf die Sorption von Eu(III) und Th(IV) auf Kalzit unter der Annahme, dass die ISA und GLU Konzentrationen in der gestörten Zone vergleichbar sind mit den Konzentrationen im Nahfeld des Endlagers, d.h. 10^{-5} M im Falle von ISA und 10^{-7} M im Falle von GLU.

RESUME

La calcite est un constituant important des marnes Valanginiannes, une roche envisagée pour un dépôt de déchets radioactifs de faible et moyenne activité en Suisse. Ce minéral est également un constituant important de la zone perturbée autour du dépôt car il est peu affecté par les eaux très basiques provenant du ciment du dépot.

Le comportement de sorption d'Eu(III) et de Th(IV) sur la calcite Merck dans une eau interstitielle de ciment artificielle (ACW) à pH 13.3 a été étudié par des expériences de sorption en batch. De plus, l'effet des acides α-isosaccharinique (ISA) et gluconique (GLU) sur la sorption de ces deux cations a été examiné.

En l'absence d'ISA et de GLU, une forte interaction d'Eu(III) et de Th(IV) sur la calcite Merck a été observée. Les cinétiques de sorption d'Eu(III) et de Th(IV) étaient rapides et les isothermes ont indiqué un comportement d'adsorption linéaire pour la gamme de concentration accessible. Dans le cas d'Eu(III), une diminution de la valeur du R_d avec un accroissement du rapport S:L a été observée indiquant que, parallèlement à l'adsorption, d'autres processus pourraient influencer l'immobilisation de ce cation par la calcite Merck avec des conditions ACW. Par ailleurs, le rapport S:L n'a eu aucun effet sur les valeurs de sorption pour Th(IV).

Des concentrations croissantes de ISA et de GLU en solution ont affecté de manière significative à la fois la sorption d'Eu(III) et de Th(IV): les valeurs de R_d pour Eu(III) ont diminué significativement pour des concentrations de ISA supérieures à 10^{-5} M et pour des concentrations de GLU supérieures à 10^{-7} M. La sorption de Th(IV) a été réduite pour des concentrations de ISA au-dessus de $2 \cdot 10^{-5}$ M et pour des concentrations de GLU au-dessus de 10^{-6} M.

Les effets d'ISA et de GLU sur l'immobilisation d'Eu(III) et de Th(IV) ont été interprétés en terme de formation de complexe en solution. Dans le cas d'Eu(III), les complexes métal-ligand ont été trouvés ayant une stoechiométrie 1:1. Les constantes de complexation dérivées pour les complexes aqueux Eu(III)-ISA, et Eu(III)-GLU sont $\log \beta^0_{EuISA} = -31.1 \pm 0.2$ et $\log \beta^0_{EuGLU} = -28.7 \pm 0.1$.

Dans le cas de Th(IV), il a été supposé que des complexes Th(IV) - ISA - Ca et Th(IV) - GLU – Ca se sont formés avec une stoechiometrie 1:2:1. Les constantes de complexation dérivées pour ces deux complexes sont $\log \beta^0_{ThISA} = -5.0 \pm 0.3$ et $\log \beta^0_{ThGLU} = -2.14 \pm 0.01$.

En supposant que les concentrations d'ISA et de GLU dans l'eau interstitielle de la zone perturbée sont similaires aux concentrations maximales estimées pour l'eau interstitielle du ciment dans le champ proche du dépôt, c'est à dire 10^{-5} M ISA and 10^{-7} M GLU, alors la formation de complexes aqueux avec ISA ou GLU n'affecterait pas de manière significative la sorption d'Eu(III) et de Th(IV) sur la calcite.

TABLE OF CONTENTS

LIST OF FIGURES

LIST OF TABLES

1. INTRODUCTION

1.1 Importance of measurements on calcite

In Switzerland it is proposed to dispose of low and intermediate level radioactive waste (L/ILW) in an underground repository located in a marl host rock (NAGRA, 1992). The large amounts of cementitious materials used in such a repository could release a highly alkaline fluid into the host rock. The interaction of alkaline waters with the host rock gives rise to the dissolution of its primary minerals (e.g. clays, quartz, dolomite) and the formation of secondary phases (e.g. calcium silicate hydrates, hydrotalcites, zeolites) (CRAWFORD & SAVAGE, 1994; ADLER et al., 1999). Calcite is an important component of marl and is expected to remain largely unaffected under these conditions. Furthermore, the availability of CO_3^{2-} originating from the dissolution of dolomite and ankerite, gives rise to the precipitation of calcite as a secondary phase (ADLER et al., 1999).

The safety concept for the Swiss L/ILW repository is based upon a system of safety barriers, which can be divided in two main categories (NAGRA, 1993, 1994): i) The near-field consisting of the repository caverns with the solidified waste and the backfill, and ii) the far-field consisting of the host rock. The host rock close to the repository is expected to be chemically and physically disturbed by the interaction with the repository and is called "the disturbed far-field".

Performance assessments for the planned L/ILW repository require sorption databases (SDB's) for the near and far-field. Such SDB's have been constructed at the Paul Scherrer Institute for a marl-type far-field (BRADBURY & BAEYENS, 1997a), for a cement-type near-field (BRADBURY & SAROTT, 1994; BRADBURY & VAN LOON, 1998; WIELAND & VAN LOON, 2002), and for a disturbed marl-type far-field (BRADBURY & BAEYENS, 1997b). In these databases, sorption values (R_d's) relevant to the respective environments have been evaluated and compiled. For the disturbed far-field it was noticed that very little relevant sorption data have been reported in the open literature. More specifically, information on the sorption of radionuclides under high pH conditions onto solids representative for a disturbed marl system, such as calcite and calcium silicate hydrate (CSH) phases, are generally lacking. Furthermore, radionuclide retention mechanisms under high pH conditions are

poorly understood. A more detailed understanding is required to provide the necessary information for the selection of realistic sorption values in SDB's.

Therefore, at the beginning of 1995, an experimental programme was started with the aim of measuring sorption values for radionuclides in systems representative of a disturbed marl system, and of developing a better mechanistic understanding of the uptake processes. The selection of an appropriate laboratory system appeared to be difficult because information on water chemistries to be expected during the alteration processes and the identity of the likely secondary phases was sparse at that time. As a consequence, the experimental programme was based on some simplifying assumptions:

1) The chemistry of the water migrating into the host rock was taken to be the same as that emerging from the near-field during the initial few thousand years, i.e., a (Na, K)OH solution in equilibrium with portlandite at a pH of ~13.3. (NEALL, 1994). The term "pH plume" is used for the alkaline near-field pore water migrating into the host rock. It is believed that this water may contain significant amounts of cement additives and cellulose degradation products.
2) Clay minerals in the marl within and immediately adjacent to water bearing features will disappear and the formation of CSH phases as secondary minerals under high pH conditions along the flow path will occur. There are indications from natural analogue studies (e.g., CRAWFORD & SAVAGE, 1994) that, in addition to CSH phases, zeolites may form. However, there are still some gaps of knowledge concerning stabilities of zeolites at pH values above 13.
3) Calcite remains largely unaffected by the pH plume. The alkaline water penetrating into the marl host rock is saturated with respect to calcite and portlandite. Since the Palfris marl at Wellenberg can contain up to 70 wt% calcite (NAGRA, 1993), its retention properties may be of particular significance in the disturbed zone of the repository. Furthermore, calcite may precipitate as secondary mineral due to the dissolution of dolomite (ADLER et al., 1999). Calcite will also form due to mixing of cementitious and marl pore waters in the disturbed zone and, thereby, strongly influence hydraulic and geometric properties in the disturbed host rock (BERNER, 1998; PFINGSTEN & SHIOTSUKI, 1998; PFINGSTEN, 2001).

1.2 Objectives

Based on the considerations outlined in the previous section, the experimental programme focused on the sorption behaviour of selected radionuclides on calcite and CSH phases in (Na, K)OH solutions in equilibrium with portlandite at pH 13.3. The main goal of the present investigation was to gain insight in the processes controlling the sorption of the trivalent and tetravalent actinides on the above-mentioned minerals under these extreme alkaline conditions.

In addition, the influence of organic ligands arising from the degradation of cellulose and from the use of cement additives for construction, was addressed. Organic ligands may form strong complexes with some radionuclides and, thereby, affect their sorption properties. α-Isosaccharinic acid (ISA) was selected as the main representative of the cellulose degradation products, whereas gluconic acid (GLU) represents the low molecular weight organic additives.

In a first phase the study was focused on the sorption of Am(III) on Wellenberg (WLB) calcite (TITS et al. 1996, 1997). The results from this study indicated that the uptake of Am(III) by this natural calcite sample was not simply controlled by sorption onto the calcite surface, but, also by coprecipitation with CSH phases. CSH phases are formed due to the dissolution of quartz in alkaline Ca-rich fluids. Note that quartz impurities can make out up to 8 wt% of the solid material in the WLB calcite.

In this report, the results of sorption studies with Eu(III) and Th(IV) on a synthetic calcite are presented. The experimental programme included the determination of sorption kinetics and isotherms as well as studies of the effect of the solid to liquid ratio (S:L ratio). Moreover, the effect of ISA and GLU on the short term sorption behaviour of Eu(III) and Th(IV) on calcite was investigated. These data were used to evaluate stoichiometries and complexation constants of the metal-ligand complexes. Moreover, the results allowed us to assess the effect of ISA and GLU on Eu(III) and Th(IV) mobilisation in the pH plume.

2. THEORY

2.1 Definitions

In the literature terms like "sorption", "adsorption", "surface precipitation" and "precipitation" are defined in different ways. In order to avoid confusion, the terms used in the present paper are defined as follows:

"*Sorption*" is used as a general expression for processes in which chemicals become associated with pre-existing solid phases (SCHWARZENBACH et al., 1993). Typical examples of such processes are ion exchange and surface complexation (**ad**sorption) as well as incorporation (**ab**sorption). Adsorption is defined as the net accumulation of matter at the interface between a pre-existing solid phase and an aqueous solution phase (SPOSITO, 1989). It is a two-dimensional process. Absorption or incorporation involves processes through which a radionuclide is trapped in the body of a pre-existing solid phase (e.g., solid state diffusion). It is a three dimensional process.

The simplest case of sorption is that one type of sorption sites, S, on a solid phase becomes occupied by the sorbing species, M. Note that S includes adsorption sites on the surface of a solid phase as well as, in the case of absorption, sites in the bulk phase of the solid. Assuming a 1:1 stoichiometry, the sorption process can be described by the following Langmuir equation (STUMM & MORGAN, 1996):

$$[M_s] = [S_T] \cdot \frac{K_{ads} \cdot [M]}{1 + K_{ads} \cdot [M]} \quad . \qquad (2.1)$$

$[M_s]$: concentration of material associated with the sorption sites on the surface [mol L^{-1}],

$[S_T]$: total concentration of sorption sites [mol L^{-1}],

$[M]$: concentration of sorbing species in solution [mol L^{-1}],

K_{ads}: sorption equilibrium constant.

Equation 2.1 shows that a typical characteristic of sorption processes is the positive correlation between the concentration of sorbed species, $[M_s]$, and the concentration of sorption sites present in the system, $[S_T]$. Note that, in this case, $[S_T]$ is proportional to the S:L ratio of the system.

"*Precipitation*" is defined as an accumulation of a material to form a new bulk solid phase (SPOSITO, 1984).

The solubility of a solid phase M_xL_y, consisting of a cation "M" and an anion L, can be described by the solubility product, K_{s0}:

$$K_{s0} = (a_M)^x \cdot (a_L)^y \qquad (2.2)$$

where "a" represents the activity of the chemical species in solution in equilibrium with the solid phase and x and y represent the stoichiometric coefficients of the solid phases involved in the reaction.

The state of saturation of a solution with respect to a solid can be evaluated by comparing the ion activity product (IAP) of this solution with K_{s0}. The IAP is defined as the weighted product of the individual ionic activities in solution:

$$IAP = \left(a_M^*\right)^x \cdot \left(a_L^*\right)^y \quad , \qquad (2.3)$$

where "a*" represents the actual activity of the chemical species in solution. A solution is supersaturated with respect to a solid phase when

$$IAP > K_{s0} \qquad (2.4)$$

It is evident that the concentrations of the species M and L in solution are only controlled by the solubility product and are independent of the amount of any substrate already present in the system. However, this is not true in case that an independent substrate contains dissolvable impurities, which have an influence on the solubility equilibrium. In such a case, increasing amounts of substrate result in increasing impurity concentrations (either M or L) and, consequently, in decreasing solution concentrations of M and L.

A special case is the formation of solid solutions. Solid solutions are formed when a cation, M, substitutes for A to the lattice of a solid composed of cation A and L (McBRIDE, 1994). The end-members of such a solid solution are A_pL_q and M_rL_s. The chemical formula of the solid solution is $A_{p(1-x)}M_{rx}L_{q(1-x)+sx}$ with x as variable between 0 and 1. In contrast to pure solids, the concentration of M in solution is not constant but depends on the solid solution composition.

2.2 Presentation of sorption data

In this study, the sorption of a radionuclide onto a solid is quantified in terms of a distribution ratio, R_d. The R_d describes the partitioning of a radionuclide between the liquid and the solid phase and is defined as:

$$R_d = \frac{\{M_s\}}{[M]} = \frac{[M_s]}{[M]} \cdot \frac{V}{m} = \frac{[M_T] - [M]}{[M]} \cdot \frac{V}{m} \quad [L\ kg^{-1}] \ . \tag{2.5}$$

$\{M_s\}$ is the quantity of radionuclide on the solid phase [mol kg^{-1}] and [M] and $[M_s]$ are the radionuclide concentration in the liquid phase and on the solid phase [mol L^{-1}], respectively. $[M_T]$ is the total radionuclide concentration in the suspension [mol L^{-1}]. V is the volume of the liquid phase [L] and m is the mass of solid phase [kg].

Practically, R_d values were determined from batch-type experiments using radiotracers. They were calculated from the ratio of the activity of the radionuclide on the solid phase and its activity in solution. The activity on the solid phase was obtained by subtracting the activity determined in the supernatant (equilibrium solution) after centrifugation from the total activity measured in the suspension before centrifugation.

$$R_d = \frac{A_s}{A_l} = \left(\frac{A_{susp} - A_l}{A_l} \right) \cdot \frac{V}{m} \quad [L\ kg^{-1}] \ . \tag{2.6}$$

A_s: radionuclide activity on the solid phase [cpm kg^{-1}],
A_{susp}: radionuclide activity in the suspension [cpm L^{-1}],
A_l: radionuclide activity in the equilibrium solution [cpm L^{-1}].

The radionuclide concentration in solution, [M], was calculated by dividing the activity determined in solution, A_l, by the specific activity of the tracer solution, A_{spec}:

$$[M] = \frac{A_l}{A_{spec}} \quad [mol\ L^{-1}] \ . \tag{2.7}$$

A_{spec} is defined as follows:

$$A_{spec} = \frac{A_{std}}{[M_{std}]} [cpm\ mol^{-1}] \ . \tag{2.8}$$

A_{std}: measured activity of the standard [cpm L^{-1}].

$[M_{std}]$: radionuclide concentration in the standard [mol L^{-1}]

Thus, A_{spec} was obtained by measuring the activity of an aliquot of the tracer solution (the standard).

The quantity of a radionuclide sorbed $\{M_s\}$, expressed in mol kg^{-1}, was calculated as follows:

$$\{M_s\} = \frac{\left(A_{susp} - A_l\right)}{A_{spec}} \cdot \frac{V}{m} \quad [\text{mol kg}^{-1}] \ . \qquad (2.9)$$

2.3 Analysis of sorption processes

Information on a sorption process can be obtained by studying the effect of different experimental parameters on the sorption. Typical experimental parameters are: the reaction time, the aqueous radionuclide concentration and the S:L ratio. The information obtained from each of these parameters is discussed briefly below.

Reaction time:

An adsorption process is generally characterised by short reaction times (typically less then 24 hours). Larger reaction times are characteristic for incorporation and precipitation processes (time scales ranging from weeks to months) (SPOSITO, 1984; SPOSITO, 1986).

Sorption isotherms:

Radionuclides sorb onto solids via sorption sites. The sorption sites can have the same affinity for the radionuclide (linear sorption) or can have different affinities (non-linear sorption). Furthermore, a radionuclide can be present in solution as different species each of them having a different affinity for the sorption sites. The presence of different sorption sites or different sorbing species is expressed in the shape of the sorption isotherm: In the case where sorption is dominated by only one type of sites and no site saturation occurs, the sorption isotherm is linear; i.e., the amount of radionuclide sorbed increases proportionally to its concentration in solution. The resultant R_d value is constant.

In the case when different sites with decreasing affinity are occupied sequentially with increasing radionuclide concentration in solution, the sorption isotherm is non-linear; i.e., the R_d decreases with increasing radionuclide concentration in solution. In this case, the site with the highest affinity for the sorbing radionuclide is occupied at very low radionuclide concentrations corresponding to the linear part of the isotherm. At high radionuclide concentrations, however, this site is saturated and sites with lower affinities are occupied giving rise to lower R_d values. The sorption process evolves from linear (slope of the isotherm = 1), to non-linear (slope of the isotherm<1). Note that the sorption isotherm has a similar shape when more than one sorbing species are involved.

It is realistic to assume that, in the case of Eu(III) and Th(IV) sorption under the given experimental conditions, the concentrations of the radionuclides generally are much lower than the concentrations of sorption sites, so that only the site with the highest affinity for the radionuclide will be involved in the sorption process (linear sorption). Hence, non-linear sorption, i.e., sorption on several different types of sorption sites, will not be considered further in this discussion.

It is noted that information obtained from sorption isotherms does not enable us to differentiate between adsorption and incorporation process because the amount of sorbed radionuclides increases with the concentration of radionuclides in solution in the same manner (equation 2.1) for both processes.

Precipitation of a solid containing the radionuclide of interest occurs if its solubility product is exceeded. Considering the high pH and the carbonate concentrations in ACW the potential counterions of solid compounds with Eu(III) and Th(IV) are OH^- and CO_3^{2-}. As the pH is kept constant in all the sorption tests, both OH^- and CO_3^{2-} concentrations are constant. Application of the solubility product expression (equation 2.2) shows that precipitation of Eu(III) or Th(IV) with one of these two ligands must result in a constant aqueous concentration at equilibrium. In those cases, however, where Eu(III) and Th(IV) form mixed precipitates (solid solutions), e.g., mixed Ca, Eu hydroxides, the solubility product may depend on the solid composition. Changes in the radionuclide content of the precipitate thus cause variation in the aqueous radionuclide concentration at equilibrium.

S:L ratio:

In the case of linear sorption the concentration of the radionuclides sorbed increases proportionally to the S:L ratio (m/V). Therefore, the R_d is constant (see equation 2.5).

Precipitation processes under ACW conditions are characterised by constant radionuclide concentrations in solution, irrespective of the amount of solid phase present. Thus, the ratio, $(A_{susp}-A_l)/A_l$, in equation 2.6 takes a constant value over the whole solid concentration range for a constant initial radionuclide concentration. Under these conditions, the R_d value is expected to be inversely proportional to the S:L ratio. Note that in the case of co-precipitation the radionuclide concentration is not necessarily constant as the solubility of the co-precipitate (solid-solution) depends on its composition.

2.4 The effect of complexing organic ligands on the immobilisation of radionuclides

Complex formation in solution may affect the radionuclide concentration in the aqueous phase irrespective of the uptake process involved. In the case of sorption, the aqueous radionuclide concentration in solution is expected to increase due to competition between the complexing ligands and sorption sites for the radionuclide.

In the absence of a complexing ligand, the distribution ratio of a sorbing radionuclide, R_d^0, is given by equation 2.5. The aqueous concentration, $[M_l]$, is the sum of the free radionuclide concentration, the concentration of the metal hydroxy complexes and the concentration of the metal carbonate complexes in solution.

Hydrolysis reactions, complexation reactions with carbonate, and the formation of mixed hydroxy carbonate complexes can be described by the following equations:

$$M^{z+} + mOH^- \Leftrightarrow M(OH)_m^{z-m} \qquad \text{with:} \qquad \beta_m^{OH} = \frac{\left[M(OH)_m^{z-m}\right]}{\left[M^{z+}\right]\cdot\left[OH^-\right]^m}, \tag{2.10}$$

$$M^{z+} + nCO_3^{2-} \Leftrightarrow M\left(CO_3\right)_n^{z-2n} \quad \text{with:} \qquad \beta_n^{CO_3} = \frac{\left[M\left(CO_3\right)_n^{z-2n}\right]}{\left[M^{z+}\right]\cdot\left[CO_3^{2-}\right]^n} \quad , \tag{2.11}$$

$$M^{z+} + pCO_3^{2-} + qOH^- \Leftrightarrow M\left(CO_3\right)_p\left(OH\right)_q^{y-2p-q} \quad \text{with:}$$

$$\beta_{pq} = \frac{\left[M\left(CO_3\right)_p\left(OH\right)_q^{z-2p-q}\right]}{\left[M^{z+}\right]\cdot\left[CO_3^{2-}\right]^p\cdot\left[OH^-\right]^q} \quad . \tag{2.12}$$

Using these expressions, equation 2.5 can be rewritten as:

$$R_d^0 = \frac{\left\{M_s\right\}}{\left[M^{z+}\right]\cdot\left(1+\sum_m \beta_m^{OH}\cdot\left[OH^-\right]^m + \sum_n \beta_n^{CO_3}\cdot\left[CO_3^{2-}\right]^n + \sum_p\sum_q \beta_{pq}\left[CO_3^{2-}\right]^p\cdot\left[OH\right]^q\right)} \quad [L\ kg^{-1}] \quad . \tag{2.13}$$

The expression between brackets in the denominator of equation 2.13 is the so-called side reaction coefficient, A. A is constant for a given pH and carbonate concentration in the experiment. Hence, equation 2.13 can be simplified to:

$$R_d^0 = \frac{\left\{M_s\right\}}{\left[M^{z+}\right]\cdot A} \tag{2.14}$$

In the presence of a ligand L, additional complexation reactions in solution take place:

$$M^{z+} + xL^{y-} \Leftrightarrow ML_x^{z-y} \qquad \text{with: } \beta_x^y = \frac{\left[ML_x^{z-y}\right]}{\left[M^{z+}\right]\cdot\left[L^{y-}\right]^x} \quad . \tag{2.15}$$

The distribution coefficient R_d can then be rewritten as:

$$R_d = \frac{\left\{{}^*M_s\right\}}{\left[{}^*M^{z+}\right]\cdot\left(A+\sum_x \beta_x^y\cdot\left[L^{y-}\right]^x\right)} \quad . \tag{2.16}$$

Note that the amount of radionuclide sorbed, $\{M_s\}$ and $\{^*M_s\}$, and the free radionuclide concentration, $[M^{z+}]$ and $[^*M^{z+}]$, are different in the absence and in the presence of ligand L (equation 2.14 and 2.16). For linear sorption, however, the following equation holds:

$$\frac{\{M_s\}}{[M^{z+}]} = \frac{\{^*M_s\}}{[^*M^{z+}]} \quad . \tag{2.17}$$

Combining equation 2.14, 2.16 and 2.17, enables us to write the R_d as a function of R_d^0:

$$R_d = R_d^0 \cdot \left(\frac{A}{A + \sum_x \beta_x^y \left[L^{y-}\right]^x} \right) \quad . \tag{2.18}$$

Expression 2.18 shows that the sorption reduction caused by the complexing ligand L depends on the stability constant of the complexes and on the concentration of the free ligand L^{y-}. It is worth emphasizing that equation 2.18 is only valid when the two following conditions are fulfilled:

1) Sorption of the radionuclide is linear and reversible.
2) Neither the ligand nor the metal - ligand complex sorb.

3. ANALYTICAL METHODS

3.1 Radiotracers and radio-assay

Radionuclide sorption was measured using solutions labelled with radiotracers. ^{152}Eu tracers were purchased from Amersham Pharmacia Biotech, Dübendorf, Switzerland, and from Isotopendienst Blasek GmbH, Waldburg, Germany. ^{228}Th was purchased from CIS Medipro AG, Teufen, Switzerland. The ^{152}Eu and ^{228}Th source solutions were diluted in 50 ml 5% HCl to produce a stock solution. Small aliquots (0.1-1 ml) of the stock solution were further diluted with 0.1 M HCl to give tracer solutions with required initial concentrations. ^{152}Eu and ^{228}Th activities were measured on a Packard Minaxi 5530 gamma counter and a Packard Cobra 5003 auto gamma counter using the energy window between 15 keV and 400 keV. The background activity measured in this window for an ^{152}Eu measurement was typically ~150 cpm/5ml, while the background activity for a ^{228}Th measurement was ~350 cpm/5ml. For the most critical experiments (samples with very low activity), the ^{152}Eu activity was determined with a Canberra Packard Tri-Carb 2250CA liquid scintillation counter using an energy window between 6 keV and 70 keV. For these measurements the background activity was typically ~30 cpm/5ml.

Solutions containing ^{228}Th were analysed by measuring the total activity, i.e., activities due to γ decay of ^{228}Th and its daughters, mainly ^{224}Ra. Note that the other daughters, ^{220}Rn, ^{216}Po, ^{212}Pb, ^{212}Bi, ^{212}Po, ^{208}Tl, have a half-life of less than 1 day while ^{224}Ra has a half-life of 3.66 days. Prior to radio-assay, the solutions were stored for at least one month to allow secular equilibrium of ^{228}Th with the daughters to be established. This secular equilibrium is disturbed after uptake of the tracer by the solid due to the much higher sorption of ^{228}Th (R_d = ~ 10^5 L kg^{-1}) compared to its main daughter ^{224}Ra (R_d < 10^3 L kg^{-1})[1].

^{14}C labelled GLU was purchased from Amersham Pharmacia Biotech as a potassium salt of D-[U-^{14}C] gluconic acid. The tracer was stored at -20° C in a refrigerator to avoid microbial decomposition. The purity of the tracer was determined by the manufacturer using high performance liquid chromatography. The tracer contained 96.6 wt% GLU whereas the remaining 3.4 wt% was

---

[1] The R_d value for ^{224}Ra was assumed to be of the same order of magnitude as the R_d values of ^{85}Sr. The R_d value of ^{85}Sr on calcite in ACW was determined to be well below 10^3 L kg^{-1}.

reported as unknown low molecular weight organics. Before use, the tracer was diluted with deionised water to produce a stock solution. This stock solution was transferred to the glove box and used to label stable GLU solutions. The fraction of ^{14}C labelled GLU in the GLU solutions was at maximum 5%. Thus, the concentration of the unknown low molecular weight organics was at least a factor 500 lower than the GLU concentration. We therefore anticipate that the low molecular weight organics had no significant influence on the experiments.

^{14}C labelled GLU was measured using a Canberra Packard Tri-carb 2250 CA liquid scintillation analyser. The ^{14}C labelled GLU solutions were prepared for radio-assay by mixing 5 ml aliquots with 15 ml scintillator (Insta-gel II Plus®, Packard Bioscience S.A.).

3.2 Chemical analyses

The pH of the samples was controlled using a WTW Microprocessor 535 pH meter combined with either Orion 8103 Ross combination pH electrodes or Ingold combination pH electrodes.

Ionic compositions (Na, K, Ca, Al, Si, Eu, Th) of equilibrium solutions were determined by plasma emission spectrometry (ICP-OES) and plasma mass spectrometry (ICP-MS).

ISA was measured by ion exchange chromatography using a Dionex DX-500 system, consisting of a quaternary gradient pump (GP40), a Carbopac PA-100 separation column and an electrochemical detector (ED 40) in the pulsed amperometric mode (GLAUS et al., 1999). It is noted that the same method did not allow precise measurements of GLU to be conducted, prompting us to use ^{14}C labelled GLU.

3.3 Experimental uncertainties and reproducibility

Sorption measurements are subject to several sources of uncertainties giving rise to an overall uncertainty on the sorption values. In the present study the uncertainty on the activity measurements for specific experimental conditions was evaluated in three steps: 1) Determination of the maximum measurable sorption value, $R_{d,max}$. 2) Determination of the minimum measurable sorption value, $R_{d,min}$. 3) Determination of the 95% confidence interval of the measurements which fall within the range limited by $R_{d,max}$ and $R_{d,min}$. Each of these steps is explained in detail in appendix A.

4. MATERIALS AND EXPERIMENTAL METHODS

4.1 Calcite

Powdered analytical grade calcite was purchased from Merck AG (Dietikon, Switzerland) and used without any further treatment. The average surface area from 6 replicates was determined to be 0.31±0.05 m^2 g^{-1} based on N_2 sorption measurements (BET method). The measurements were conducted with a Micrometrics Gemini 2360 analyzer. However, the value has to be used with caution because the reliability of N_2 sorption measurements for low surface area samples, i.e., samples with a specific surface area below 1 m^2 g^{-1}, has been questioned (DAVIS & KENT, 1990).

The composition of Merck calcite was determined by dissolution in 1 M HCl followed by ICP-OES and ICP-MS analysis of the acidic solution. The chemical composition including the most important elements is given in Table 1. The Ca concentration agrees well with the theoretically expected value of 0.4 g Ca per g calcite. The concentrations of Eu(III) and Th(IV) in the acid solutions were below the detection limits (ICP-MS analyses). Thus, calcite does not appear to be an important source of both Eu(III) and Th(IV). Note the presence of small concentrations of unidentified Na and Si impurities.

Table 1: Chemical composition of Merck calcite.

Element	Concentration [ppm]
Na	72±4
K	$<5\cdot10^{-3}$
Ca	$(4.0\pm0.2)\cdot10^{5}$
Mg	65±4
Al	$<5\cdot10^{-3}$
Si	151±7
Eu	$<10^{-4}$*
Th	$<10^{-4}$*

In the sorption experiments, Merck calcite was not pre-equilibrated prior to adding the tracer. The radionuclides were added immediately after suspending calcite in ACW. Therefore, the nature of the calcite surface structure may change due to recrystallisation processes coinciding with the adsorption of radionuclides (STIPP et al., 1994). Surface recrystallisation may cause partial incorporation of radionuclides into the calcite structure. Note that the Ca concentration in ACW remained constant in the sorption experiments, showing that, on a macroscopic scale, calcite was stable (see Figure 1). A constant Ca concentration is expected because the ACW was equilibrated with the same calcite material (see section 4.2). The Ca concentration of the ACW in equilibrium with calcite was found to be approximately $(1.6\pm0.2)\cdot10^{-3}$ M (Figure 1). This value agrees very well with the predicted value obtained from thermodynamic calculations.

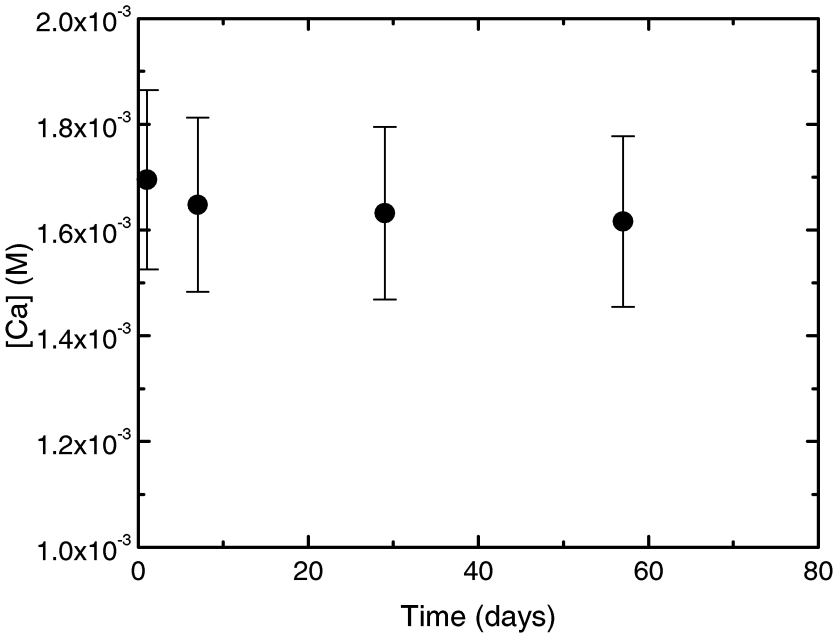

Figure 1: Aqueous Ca concentration in suspensions of Merck calcite equilibrated with ACW. The S:L ratio was 0.01 kg L^{-1}.

4.2 Artificial cement pore water (ACW)

An artificial cement pore water ACW) was employed for all experiments. The composition of ACW was determined based on an estimate of the pore water composition in a hardened cement paste before any degradation of the material had occurred (BERNER, 1990). The pore water is a highly alkaline (K, Na)OH

solution saturated with respect to portlandite (pH=13.3). The ACW was prepared under CO_2-free conditions in a glovebox by dissolving 11.9 g KOH and 4.6 g NaOH in 1 L of deionised water and adding 1 g of $Ca(OH)_2$ and 1 g of $CaCO_3$ to this solution. It was found that the chemicals used for the preparation of the ACW always contained an unknown, but significant amount of Na_2CO_3 and K_2CO_3 as impurities, which could not be removed. Therefore, the ACW was equilibrated with $CaCO_3$ in order to fix the CO_3^{2-} concentration at a known level corresponding to saturation with respect to $CaCO_3$. The final carbonate concentration of ACW was calculated to be $1.2 \cdot 10^{-4}$ M. The ACW was shaken for one week and filtered over a 0.1μm Criticap™ filter (Gelman Science) prior to be used in the experiments.

The concentrations of the major elements (Na, K, Ca, Mg, Al, Si) in the ACW were determined using ICP-OES (Table 2). Eu(III) and Th(IV) concentrations were measured with ICP-MS. The concentrations of these elements in ACW were found to be below the respective detection limits, i.e., $6.6 \cdot 10^{-11}$ M and $4.3 \cdot 10^{-11}$ M.

4.3 α-Isosaccharinic acid and gluconic acid

Gluconic acid was purchased as a Na salt (Merck AG, Dietikon, Switzerland). The synthesis of α-isosaccharinic acid was reported by VAN LOON et al. (1997). Stock solutions of ISA and GLU were prepared in ACW. Labelled GLU stock solutions were prepared by adding an aliquot of ^{14}C labelled GLU to obtain an activity of approximately 10^6 cpm ml^{-1}.

Table 2: Concentrations of selected elements in ACW.

Element	Concentration (M)
Na	0.114±0.002
K	0.182±0.006
Mg	$(4.7 \pm 0.4) \cdot 10^{-7}$
Ca	$(1.6 \pm 0.2) \cdot 10^{-3}$
Al	$(3.7 \pm 0.7) \cdot 10^{-6}$
Si	$(6 \pm 1) \cdot 10^{-5}$
Eu	$< 6.6 \cdot 10^{-11}$
Th	$< 4.3 \cdot 10^{-11}$

4.4 Experimental stability tests for Eu(III) and Th(IV) solutions

The stability of ^{152}Eu and ^{228}Th tracer solutions was studied in ACW. Solutions containing total tracer concentrations ranging from 10^{-11} M to 10^{-6} M were prepared. One series of samples was shaken for 1 day, the others for 30 days in a glove box under controlled N_2 atmosphere (O_2 and CO_2 concentrations < 5 ppm). After these ageing periods, the radionuclide activities were measured before and after centrifugation (1 hour at 95 000 *g* (max)). Calculations using Stokes law indicate that any colloidal material with a diameter greater than ~ 20 nm should settle during the centrifugation step. Applying this stepwise procedure allowed the radionuclide fraction in "true" solution to be distinguished from the radionuclide fraction present as colloidal material.

4.5 Batch sorption tests

All sorption experiments were carried out in a glovebox under a controlled N_2 atmosphere (O_2 and CO_2 concentrations < 5 ppm).

Batch sorption tests were carried out in 50 ml polyallomere centrifuge tubes, which were thoroughly washed and left overnight in a solution of 0.1 M HNO_3. This acid treatment was followed by thorough rinsing with de-ionised water.

4.5.1 Sorption of radionuclides

Calcite suspensions were prepared in polyethylene beakers by mixing Merck calcite with 1 L of ACW. The amount of Merck calcite used to prepare the suspensions varied according to the experimental set-up. The suspensions were thoroughly mixed and homogenised with a shear mixer and equilibrated for approximately one hour using a magnetic stirrer. 40 ml aliquots were taken from the vigorously stirred suspensions and pipetted into 50 ml polyallomere centrifuge tubes. These samples were then spiked with 0.4 ml tracer solution containing the radionuclide of interest. Standards for the determination of the total activity inventory and of the specific activity of the tracer solutions were prepared by adding 0.4 ml aliquots of the radionuclide tracer solution into counting vials and diluting them to 5 ml with ACW.

For the kinetic tests with Eu(III), total radionuclide concentrations of $2.5 \cdot 10^{-9}$ M and $5 \cdot 10^{-10}$ M, and S:L ratios of $2 \cdot 10^{-4}$ kg L^{-1} and $2 \cdot 10^{-3}$ kg L^{-1} were used. For

the kinetic tests with Th(IV), total radionuclide concentrations were $8.6 \cdot 10^{-11}$ M and $8.2 \cdot 10^{-12}$ M, and the S:L ratios were $4 \cdot 10^{-4}$ kg L^{-1} and $2 \cdot 10^{-3}$ kg L^{-1}. The experimental conditions for the kinetics tests are summarised in Table 3.

For the sorption isotherms, a S:L ratio of $5 \cdot 10^{-4}$ kg L^{-1} was chosen with Eu(III) and a S:L ratio of 10^{-3} kg L^{-1} with Th(IV). The equilibration time was 2 weeks. The experimental conditions for the sorption isotherms are summarised in Table 4.

To determine the effect of the S:L ratio, sorption experiments were performed at an initial Eu(III) tracer concentration of 10^{-9} M and initial Th(IV) tracer concentrations of 10^{-10} M or 10^{-11} M. The equilibration time was 1 day. The experimental conditions for these sorption experiments are summarised in Table 5.

For the experiments with GLU and ISA, 2 ml aliquots of a calcite suspension were transferred to 50 ml polyallomere centrifuge tubes. Appropriate quantities of ISA or GLU stock solutions were then added. The suspensions were diluted to 40 ml with ACW to give S:L ratios of $4 \cdot 10^{-4}$ kg L^{-1}, $2 \cdot 10^{-3}$ kg L^{-1} and $4 \cdot 10^{-3}$ kg L^{-1} in the experiments with Eu(III) and $4 \cdot 10^{-4}$ kg L^{-1}, $2 \cdot 10^{-3}$ kg L^{-1}, $4 \cdot 10^{-3}$ kg L^{-1} and 10^{-2} kg L^{-1} in the experiments with Th(IV). ISA concentrations varied between $2 \cdot 10^{-7}$ M and $2.5 \cdot 10^{-2}$ M, and GLU concentration varied between 10^{-8} M and 10^{-4} M. A summary of the experimental conditions for the sorption experiments in the presence of ISA and GLU is given in Table 6.

The centrifuge tubes were shaken on an end-over-end shaker for an appropriate period of time, depending on the type of experiment. After shaking, duplicate samples were taken from the vigorously stirred suspension to determine the total activity involved in the sorption process. Measuring the radionuclide activity in the suspension allows artefacts due to sorption of the tracers on the walls of centrifuge tubes to be avoided.

Phase separation between the solid and liquid phase was achieved by centrifuging the samples for 1 hour at 95 000 g (max). After centrifugation, samples in duplicates were taken from the supernatant solution. The samples withdrawn from the suspensions and from the supernatant solutions were analysed together with the standards. Finally, pH was checked at the end of each sorption test.

Table 3: Experimental conditions for the Eu(III) and Th(IV) kinetic experiments.

Eu(III) experiments			Th(IV) experiments		
$[^{152}Eu]_{tot}$ [M]	S:L ratio [kg L^{-1}]	V [ml]	$[^{228}Th]_{tot}$ [M]	S:L ratio [kg L^{-1}]	V [ml]
$2.5 \cdot 10^{-9}$	$2 \cdot 10^{-4}$	40	$8.6 \cdot 10^{-11}$	$2 \cdot 10^{-3}$	40
$5 \cdot 10^{-10}$	$2 \cdot 10^{-4}$	40	$8.6 \cdot 10^{-12}$	$4 \cdot 10^{-4}$	40
$5 \cdot 10^{-10}$	$2 \cdot 10^{-3}$	40			

Table 4: Experimental conditions for the Eu(III) and Th(IV) sorption isotherms.

Eu(III) experiments			Th(IV) experiments		
Equilibration time [days]	S:L ratio [kg L^{-1}]	V [ml]	Equilibration time [days]	S:L ratio [kg L^{-1}]	V [ml]
14	$5 \cdot 10^{-4}$	40	14	10^{-3}	40

Table 5: Experimental conditions for the sorption experiments with varying S:L ratio.

Eu(III) experiments				Th(IV) experiments			
$[^{152}Eu]_{tot}$ [M]	Pre-equil. time [days]	Equil. time [days]	V [ml]	$[^{228}Th]_{tot}$ [M]	Pre-equil. time [days]	Equil. time [days]	V [ml]
10^{-9}	0.042	1	40	10^{-10}	-	1	40
10^{-9}	30	1	40	10^{-11}	-	1	40

Table 6: Experimental conditions for the sorption experiments in the presence of ISA and GLU.

	Eu(III) experiments				Th(IV) experiments			
	Equil. time [days]	$[^{152}Eu]_{tot}$ [M]	S:L ratio [kg L^{-1}]	V [ml]	Equil. time [days]	$[^{228}Th]_{tot}$ [M]	S:L ratio [kg L^{-1}]	V [ml]
ISA	3	10^{-9}	$4 \cdot 10^{-4}$	40	3	10^{-11}	$4 \cdot 10^{-4}$	40
	3	10^{-9}	$4 \cdot 10^{-3}$	40	3	10^{-11}	$2 \cdot 10^{-3}$	40
					3	10^{-11}	$4 \cdot 10^{-3}$	40
					3	10^{-11}	10^{-2}	40
GLU	3	10^{-9}	$4 \cdot 10^{-4}$	40	3	10^{-11}	$4 \cdot 10^{-4}$	40
	3	10^{-9}	$2 \cdot 10^{-3}$	40	3	10^{-11}	$2 \cdot 10^{-3}$	40
	3	10^{-9}	$4 \cdot 10^{-3}$	40	3	10^{-11}	$4 \cdot 10^{-3}$	40

4.5.2 Sorption of ISA and GLU

The sorption behaviour of ISA and GLU was examined as function of time and by measuring sorption isotherms. For the sorption kinetic tests, Merck calcite suspensions containing 0.05 kg L^{-1} solid material were prepared in ACW. Centrifuge tubes were filled with 40 ml calcite suspension. Then, 0.4 ml of a 10^{-2} M ISA or GLU solution, respectively, was added to give a final concentration of 10^{-4} M. The centrifuge tubes were shaken on an end-over-end shaker. At regular time intervals, two tubes were removed from the shaker and centrifuged. The sorption time varied between one and 42 days. The ISA and GLU ligand concentrations in the supernatant solutions were determined using ion exchange chromatography.

Parallel to the sorption samples four samples were run to test the stability of ISA and GLU in ACW over the experimental period of time. Two of them were filled with 40 ml ACW and 0.4 ml ISA stock solution, whereas the other contained 0.4 ml GLU stock solution instead of ISA. These solutions were analysed for ISA and GLU after 42 days.

The experimental procedure was slightly changed for the determination of the GLU sorption isotherm. Instead of pipetting calcite suspensions in the centrifuge tubes, 4 g Merck calcite was directly weighted into the tubes. Then, increasing amounts of a ^{14}C labelled GLU solution were added. The centrifuge tubes were filled up to 40 ml by adding ACW and put on an end-over-end shaker for 24 hours. After this time period, the tubes were centrifuged for 1 hour at 95,000 g (max), and 5 ml aliquots were taken from the supernatant solution and analysed for ^{14}C activity. The pH was checked in each supernatant solution.

5. RESULTS AND DISCUSSION

5.1 Thermodynamic modelling and speciation

5.1.1 Calcite/ACW/GLU/ISA systems

SCHUBERT & LINDENBAUM (1952) and VERCAMMEN et al. (1999) showed that ISA and GLU can form weak complexes with Ca. This reaction could cause dissolution of calcite in experiments at high ISA or GLU concentrations. The solubility of calcite was modelled using the code MEDUSA (PUIGDOMENECH, 1983) and the Nagra Chemical Thermodynamic Database (HUMMEL et al., 2002). The complexation constants for $Ca(ISA)^0$, $Ca(ISA)^+$, $Ca(GLU)^0$ and $Ca(GLU)^+$ as well as the solubility products for $Ca(ISA)_2(s)$ and $Ca(GLU)_2(s)$ are given in Table 7. VAN LOON et al. (1999) assumed that the complexation constant of $Ca(ISA)^+$ is similar to the complexation constant of $Ca(GLU)^+$. This estimate is justified based on the chemical similarities between the two ligands. For the same reasons we assumed the existence of a $Ca(GLU)^0$ complex with a complexation constant similar to the complexation constant of $Ca(ISA)^0$ which was previously reported by VERCAMMEN et al. (1999).

Figure 2 shows the speciation of Ca with increasing ISA and GLU concentrations. Ca-ISA and Ca-GLU complexes become dominant only at ligand concentrations larger than approximately 10^{-2} M. Note that, below ~$3 \cdot 10^{-3}$ M, the system is slightly supersaturated with respect to portlandite. Hence, it is possible that portlandite precipitates under these conditions.

The calculated Ca concentrations in calcite-ISA-ACW and calcite-GLU–ACW systems are presented as solid lines in Figure 3a and Figure 3b. The model calculations show that solubilities remain constant up to ligand concentrations of approximately 10^{-2} M. Solubilities are expected to increase above 10^{-2} M due to the formation of Ca-ISA and Ca-GLU complexes in solution.

The Ca concentrations in ACW solutions containing ISA or GLU were also determined experimentally. The tests showed that the presence of ISA and GLU at concentrations up to $3 \cdot 10^{-2}$ M and 10^{-4} M, respectively, did not significantly enhance the solubility of Merck calcite (Figure 3a and Figure 3b). Moreover, modelling and experimental data fairly agree in this concentration

ranges. The predicted influence of ISA on the calcite solubility at ISA concentrations above $2 \cdot 10^{-3}$ M, however, was not confirmed experimentally. This suggests that the thermodynamic constants used to model Ca-ISA complexation may be too high.

Table 7: Thermodynamic complexation constants for Ca-ISA and Ca-GLU complexes and formation constants for Ca-ISA and Ca-GLU solid phases.

Species	$\log\beta$ (I=0)	Reference	Reaction
$Ca(ISA)^0$	-10.4	(VERCAMMEN et al., 1999)	$Ca^{2+} + H_4ISA^- \Leftrightarrow Ca(H_3ISA)^0 + H^+$
$Ca(H_5GLU)^0$	-10.4	estimated (VAN LOON et al., 1999)	$Ca^{2+} + H_5GLU^- \Leftrightarrow Ca(H_4GLU)^0 + H^+$
$Ca(H_4ISA)^+$	1.7	estimated	$Ca^{2+} + H_4ISA^- \Leftrightarrow Ca(H_4ISA)^+$
$Ca(H_5GLU)^+$	1.7	(SCHUBERT & LINDENBAUM, 1952)	$Ca^{2+} + H_5GLU^- \Leftrightarrow Ca(H_5GLU)^+$
$Ca(H_4ISA)_2(s)$	-6.53	(VAN LOON et al., 1999)	$Ca(H_4ISA)_2(s) \Leftrightarrow Ca^{2+} + 2H_4ISA^-$
$Ca(H_5GLU)_2(s)$	-4.19	(VAN LOON et al., 1999)	$Ca(H_5GLU)_2(s) \Leftrightarrow Ca^{2+} + 2H_5GLU^-$

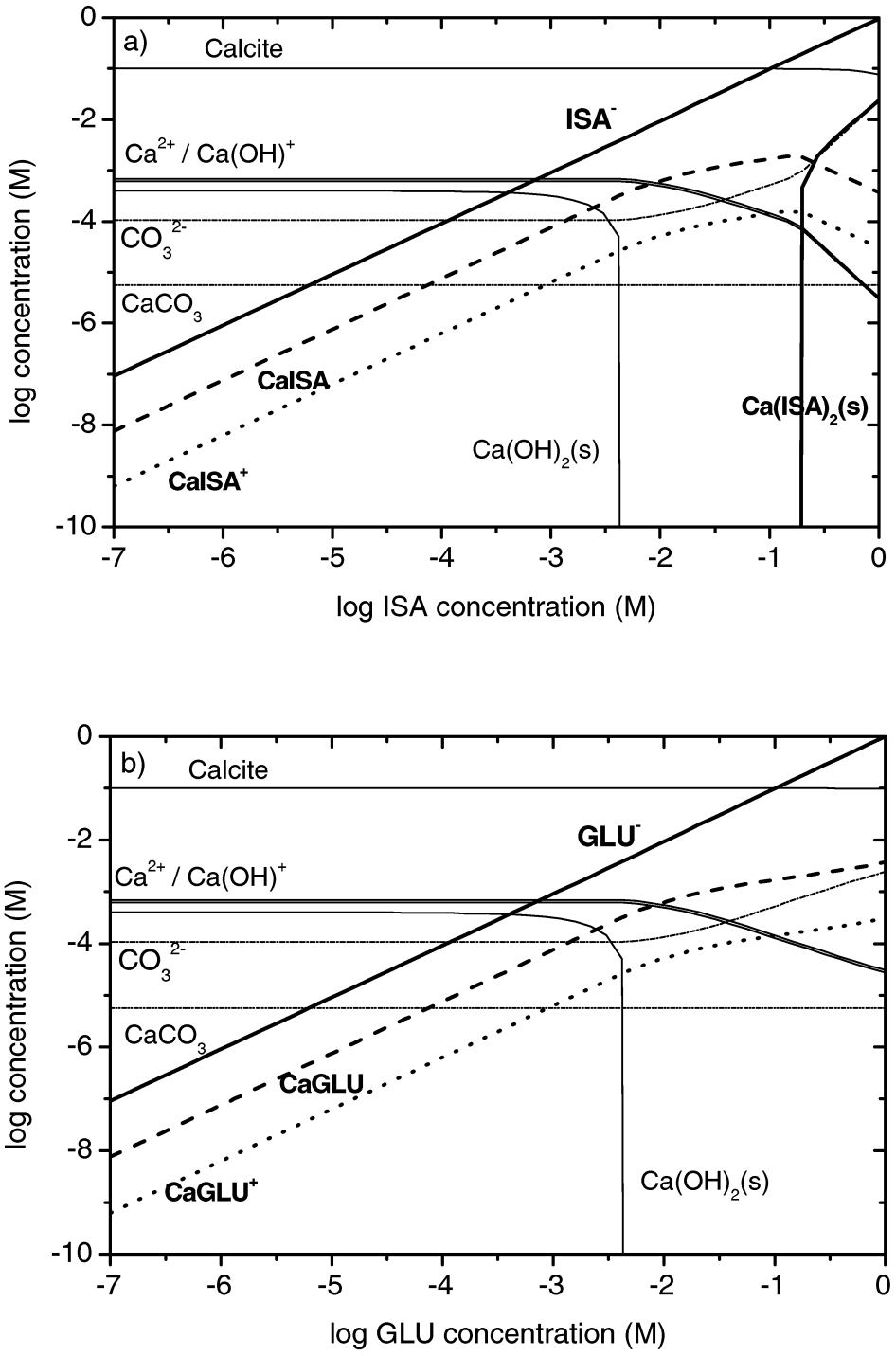

Figure 2: Ca speciation in a calcite-ACW system at pH 13.3 (0.1 kg L^{-1} calcite). a) Influence of ISA. b) Influence GLU.

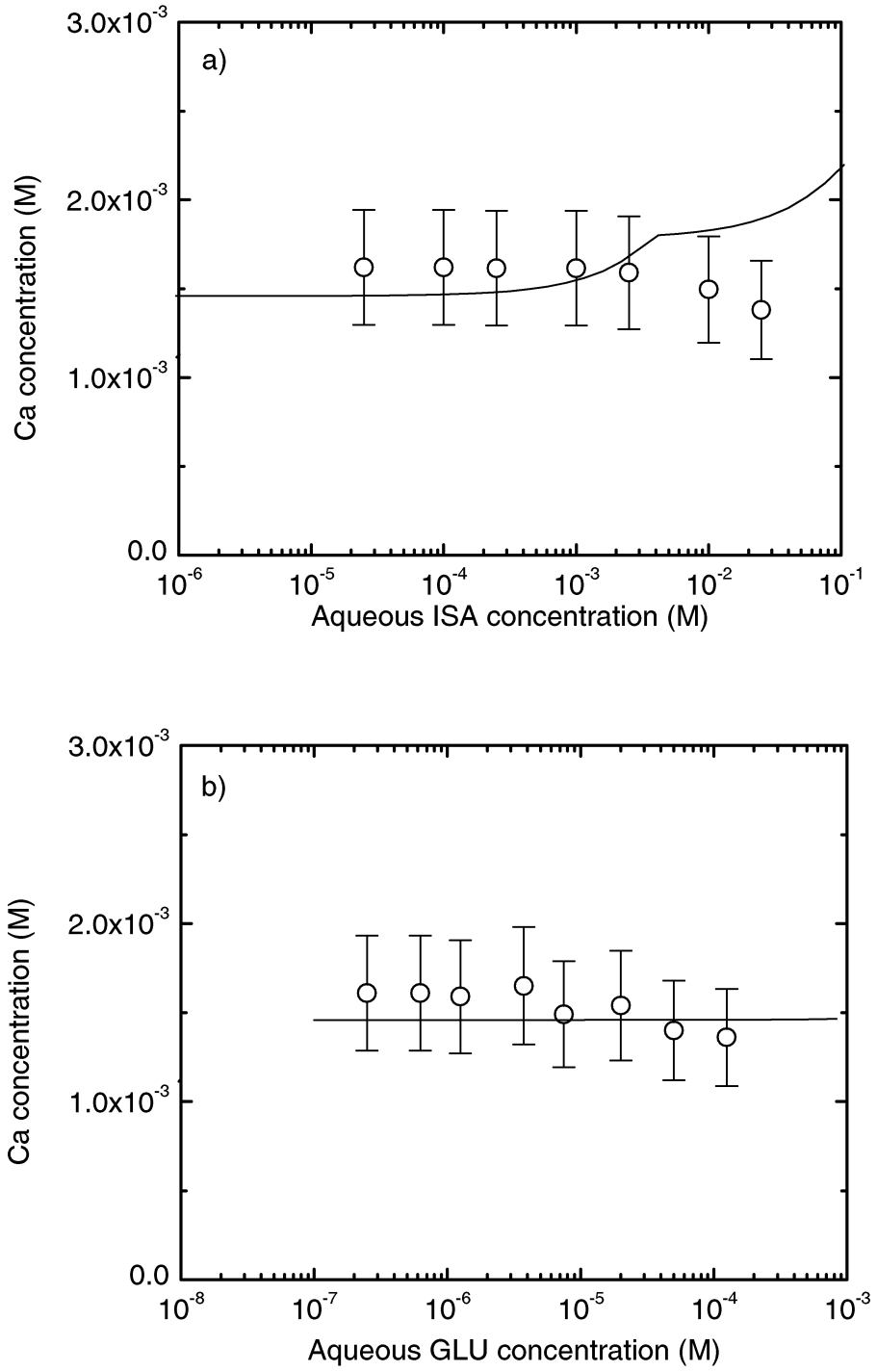

Figure 3: Solubility of Merck calcite in ACW at pH 13.3 as function of a) ISA and b) GLU concentrations. The S:L ratio was $4 \cdot 10^{-3}$ kg L^{-1}. The equilibration time was 3 days. The solid lines represent solubilities of calcite under these conditions using the complexation constants and solubility products listed in Table 7.

5.1.2 Speciation of Eu(III) and Th(IV) in ACW

The solution chemistry of Eu(III) and Th(IV) under conditions of high pH and high ionic strength is complex and not yet well understood. Often, speciation calculations have to be performed using thermodynamic data measured at much lower pH values. In this section the speciation and solubilities of Eu(III) and Th(IV) are discussed using thermodynamic data reported in the literature.

Relevant Eu(III) species in ACW are the hydroxy complexes, carbonate complexes and mixed hydroxy carbonate complexes. The stability constants of these complexes were taken from HUMMEL et al. (2002) and are summarised in Table 8. Extrapolation to I=0.3 was carried out using the Davies equation. The solubility of Eu(III) in ACW at pH 13.3 was calculated using the values for the solubility products of amorphous and crystalline $Eu(OH)_3$ reported by (HUMMEL et al. (2002) (see Table 8).

Speciation calculations show that the dominant aqueous species in ACW is $Eu(OH)_4^-$. The maximum concentration of Eu(III), soluble in ACW at pH 13.3, is estimated to be $8.6 \cdot 10^{-6}$ M assuming $Eu(OH)_3$(am) to be the solubility limiting phase and $1.8 \cdot 10^{-8}$ M assuming $Eu(OH)_3$(cr) to be the solubility controlling phase.

Th(IV) species relevant to the present experimental study are hydroxy complexes and mixed hydroxy carbonate complexes. The stability constants for these complexes were taken from HUMMEL et al. (2002). The solubility of Th(IV) in ACW at pH 13.3 was calculated using the solubility products for ThO_2(s) and $Th(OH)_4$(cr) reported by HUMMEL et al. (2002). The constants are listed in Table 9. Extrapolation to I = 0.3 was done with the help of the Davies equation.

Speciation calculations using these constants show that the dominant aqueous Th(IV) species in ACW at pH 13.3 is $Th(OH)_4$. The maximum concentration of Th(IV) soluble in ACW at pH 13.3 was estimated to be $3.1 \cdot 10^{-9}$ M assuming ThO_2(s) to be the solubility limiting phase and $2.3 \cdot 10^{-5}$ M assuming $Th(OH)_4$(cr) to be the solubility controlling phase.

Table 8: Thermodynamic complexation constants for Eu(III) hydroxy and Eu(III) carbonate complexes (HUMMEL et al. 2002).

Species	$\log\beta$ (I=0)	$\log\beta^{1)}$ (I=0.3)	Reaction
$Eu(OH)^{2+}$	6.36	5.59	$Eu^{3+} + OH^- \Leftrightarrow EuOH^{2+}$
$Eu(OH)_2^+$	12.9	11.58	$Eu^{3+} + 2OH^- \Leftrightarrow Eu(OH)_2^+$
$Eu(OH)_3^0$	18.3	16.7	$Eu^{3+} + 3OH^- \Leftrightarrow Eu(OH)_3^0$
$Eu(OH)_4^-$	19.8	18.2	$Eu^{3+} + 4OH^- \Leftrightarrow Eu(OH)_4^-$
$EuCO_3^+$	8.1	6.52	$Eu^{3+} + CO_3^{2-} \Leftrightarrow EuCO_3^+$
$Eu(CO_3)_2^-$	12.1	9.99	$Eu^{3+} + 2CO_3^{2-} \Leftrightarrow Eu\left(CO_3\right)_2^-$
Species	**Log K_s (I=0)**	**Log K_s (I=0.3)**	**Reaction**
$Eu(OH)_3$(am)	-24.4	-22.8	$Eu(OH)_3(am) \Leftrightarrow Eu^{3+} + 3OH^-$
$Eu(OH)_3$(cr)	-27.1	-25.5	$Eu(OH)_3(cr) \Leftrightarrow Eu^{3+} + 3OH^-$
$Eu_2\left(CO_3\right)_3$(cr)	-35.0	-31.0	$2Eu^{3+} + 3CO_3^{2-} \Leftrightarrow Eu_2\left(CO_3\right)_3(cr)$
$EuOHCO_3$(cr)	-21.7	-19.9	$Eu^{3+} + OH^- + CO_3^{2-} \Leftrightarrow EuOHCO_3(cr)$

1) Ionic strength correction based on the Davies equation.

Table 9: Relevant thermodynamic complexation constants for Th(IV) hydroxy complexes and Th(IV) hydroxy carbonate complexes (HUMMEL et al., 2002).

Species	logβ (I=0)	logβ [1)] (I=0.3)	Reaction
$ThOH^{3+}$	11.6	10.8	$Th^{4+} + OH^- \Leftrightarrow ThOH^{3+}$
$Th(OH)_4^0$	37.6	34.9	$Th^{4+} + 4OH^- \Leftrightarrow Th(OH)_4^0$
$Th(CO_3)(OH)_3^-$	39.8	36.8	$Th^{4+} + CO_3^{2-} + 3OH^- \Leftrightarrow Th(CO_3)(OH)_3^-$
Species	**Log K_s (I=0)**	**Log K_s (I=0.3)**	**Reaction**
$ThO_2(s)$	46.1	43.5	$Th^{4+} + 4OH^- \Leftrightarrow ThO_2(s) + 2H_2O$
$Th(OH)_4(cr)$	42.2	39.6	$Th^{4+} + 4OH^- \Leftrightarrow Th(OH)_4(cr)$

1) Ionic strength correction based on the Davies equation.

5.1.3 Experimental stability tests for Eu(III) and Th(IV) solutions

Because of the uncertainties associated with the thermodynamic constants at high pH, the stabilities of Eu(III) and Th(IV) tracer solutions were determined experimentally prior to performing the sorption experiments.

The results of these tests are presented in Figure 4 to Figure 7. The error bars indicate 95% confidence intervals calculated from 5 replicates. In both the Eu(III) and Th(IV) solutions, activity losses between 40% and 80% were observed over the entire concentration range before centrifugation, due to wall sorption (Figure 4 and Figure 6). The percentages of the Eu(III) and Th(IV) inventories measured in solution before centrifugation are lower after 30 days than after 1 day, indicating that sorption on the container walls is a slow process. For both elements, centrifugation (1 hour at 95 000 g (max)) caused additional losses at radionuclide concentrations above approximately 10^{-9} M (Figure 4 and 6). The loss of activity is explained by the presence of Eu(III) and Th(IV) colloids, which were generated in ACW and settled during centrifugation. The data in Figure 5 and Figure 7 show the equilibrium radionuclide concentrations as function of the input concentration. The solid lines with slope 1

represent the case where the input concentration is completely recovered in the equilibrium solution. Both the datasets measured before and after centrifugation lie below this line and parallel to it, indicating sorption of the radionuclides on the container walls. The formation of radiocolloids was observed at a total Eu(III) and Th(IV) concentration of approximately 10^{-9} M and higher, indicated by increasing differences in the measured activities before and after centrifugation. In the case of Eu(III), the presence of radiocolloids is observed at aqueous concentrations of approximately $2 \cdot 10^{-10}$ to $5 \cdot 10^{-10}$ M which is more than four orders of a magnitude below the calculated solubility limit for $Eu(OH)_3(am)$ (not shown) and about a factor 50 to 100 below the calculated solubility limit for $Eu(OH)_3(cr)$ represented by the dashed horizontal line in Figure 5.
In the case of Th(IV), radiocolloids started forming at aqueous concentration values of approximately $5 \cdot 10^{-9}$ M. This concentration agrees well with the calculated solubility for $ThO_2(s)$ in ACW.

The conclusions drawn from these tests are:

1) Using the thermodynamic constants given in Table 8 Eu(III) solutions are predicted to be stable up to concentrations corresponding to the thermodynamically calculated solubility limit for $Eu(OH)_3$ ($1.5 \cdot 10^{-8}$ M). Th(IV) solutions are predicted to be stable up to concentrations corresponding to the theoretically calculated solubility limit for $ThO_2(s)$ ($3 \cdot 10^{-9}$ M).

2) Under the experimental conditions employed in this study, the critical radionuclide concentrations are found to be approximately $2 \cdot 10^{-10}$ M to $5 \cdot 10^{-10}$ M for Eu(III) and $5 \cdot 10^{-9}$ M for Th(IV).

Based on the these findings, the initial input ^{152}Eu concentrations used in the sorption experiments were optimised considering, on the one hand, the stability of Eu(III) solutions, and, on the other hand, the detection limits for ^{152}Eu activity measurements. In some experiments the chosen ^{152}Eu input concentration was slightly higher than the critical concentration of $2 \cdot 10^{-10}$ M to $5 \cdot 10^{-10}$ M in order to obtain better counting statistics. Sorption measurements are correct under these conditions, if the formation of colloidal precipitates is significantly slower than the sorption process. Arguments in favour of this assumption will be provided in section 5.2.2.

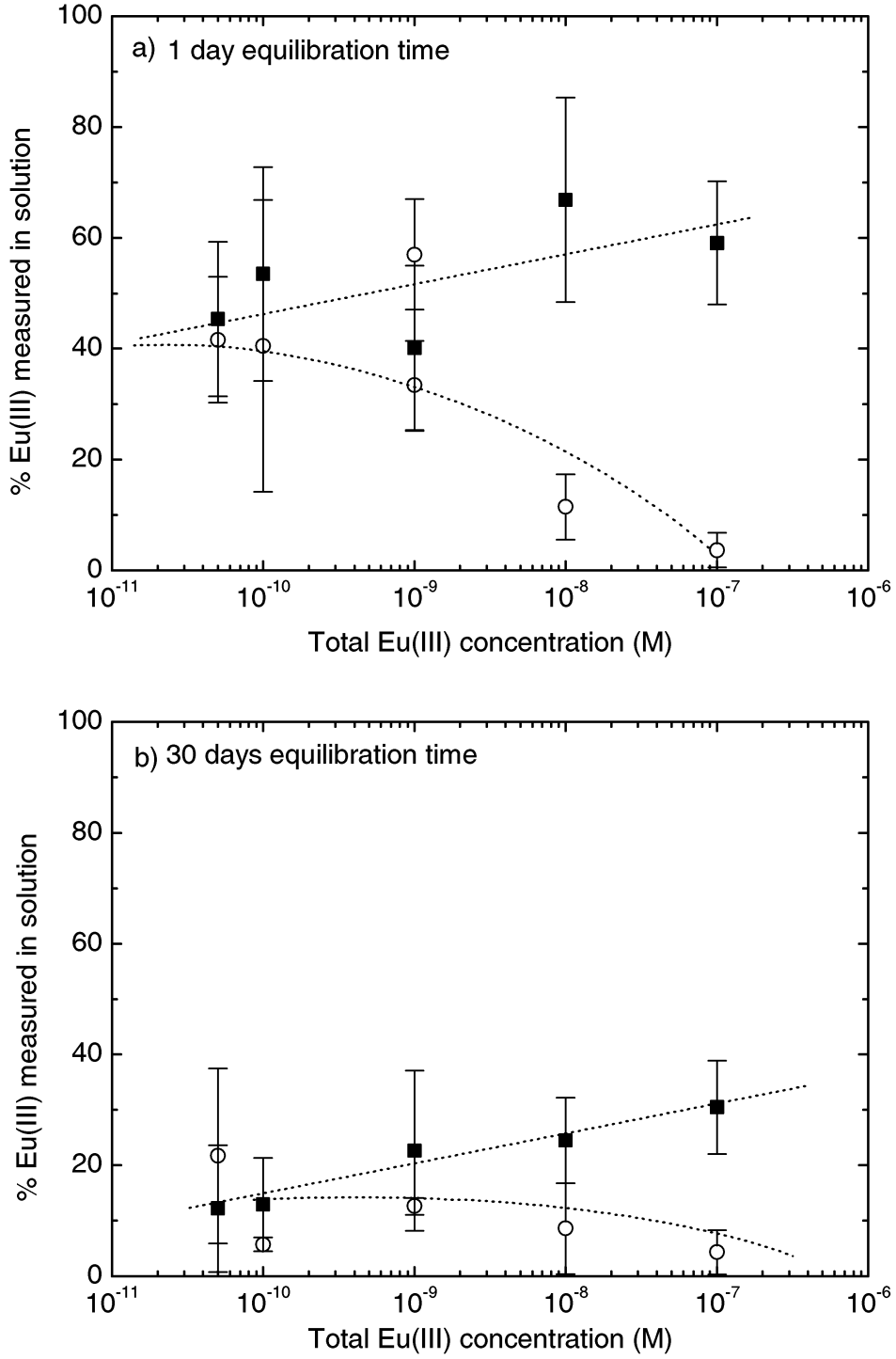

Figure 4: Percentage of the Eu(III) input concentration measured in solution before (■) and after centrifugation (○) as a function of the input Eu(III) concentration. Measurements were conducted for 1 day (a) and 30 days equilibration (b). The dotted curves only serve as a guide to the eye.

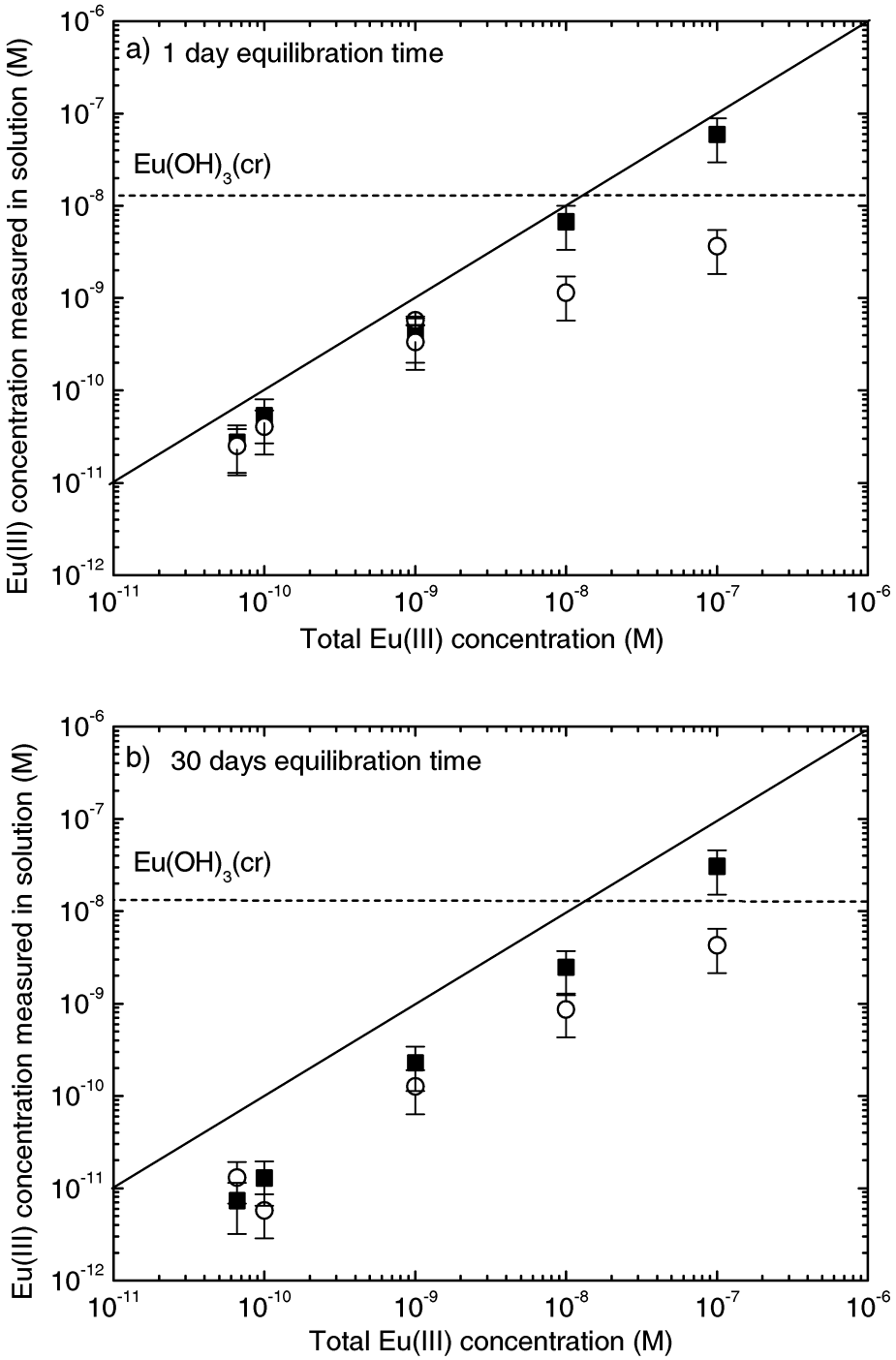

Figure 5: Eu(III) concentration measured in solution before (■) and after centrifugation (○) as a function of the input Eu(III) concentration. Measurements were conducted after 1 day (a) and 30 days equilibration (b). The dashed lines represent the calculated Eu(III) solubility limit in ACW.

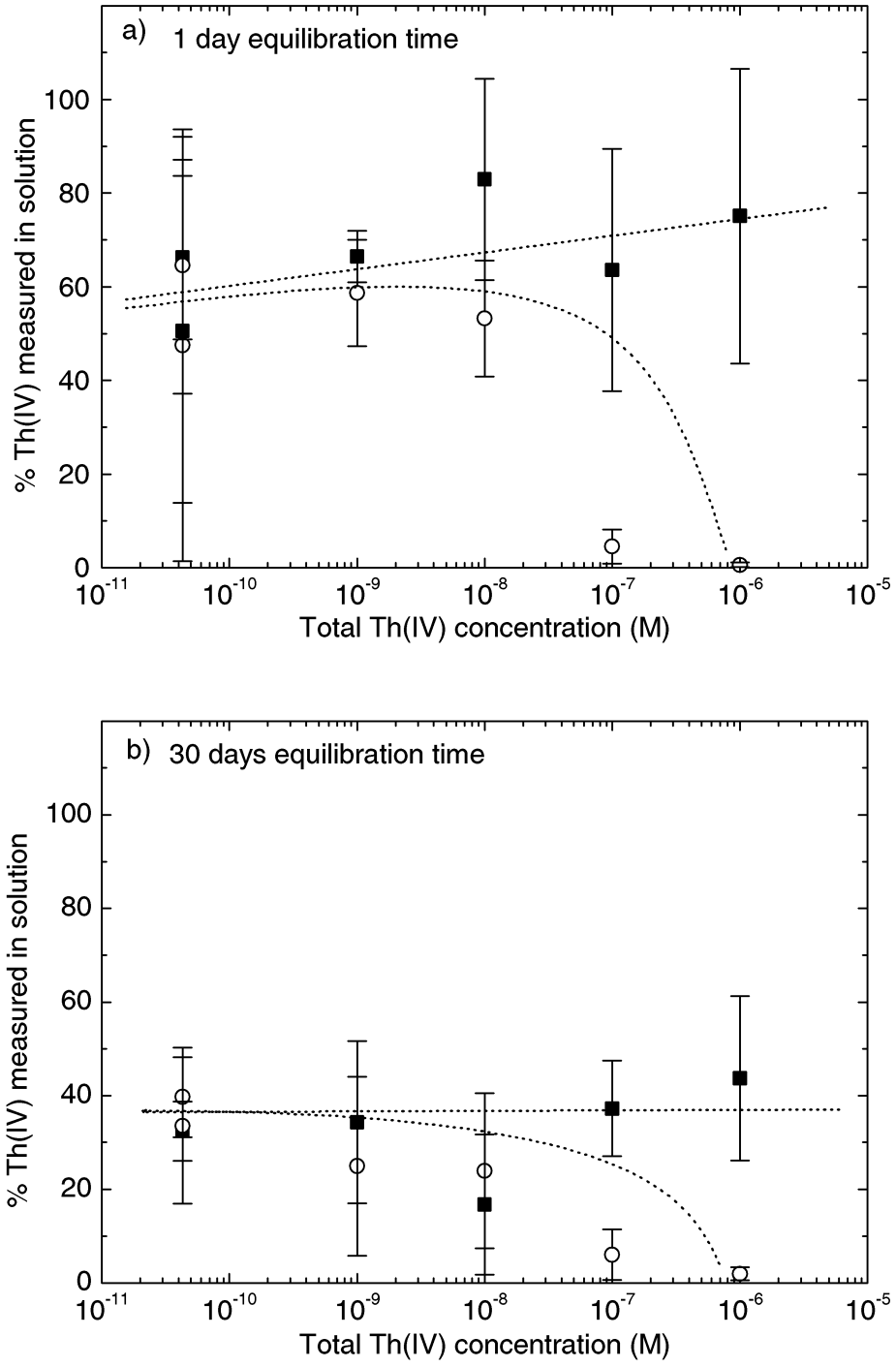

Figure 6: Percentage of the Th(IV) input concentration measured in solution before (■) and after (○) centrifugation as a function of the input Th(IV) concentration. Measurements were conducted after 1 day (a) and 30 days equilibration (b). The dotted curves only serve as a guide to the eye.

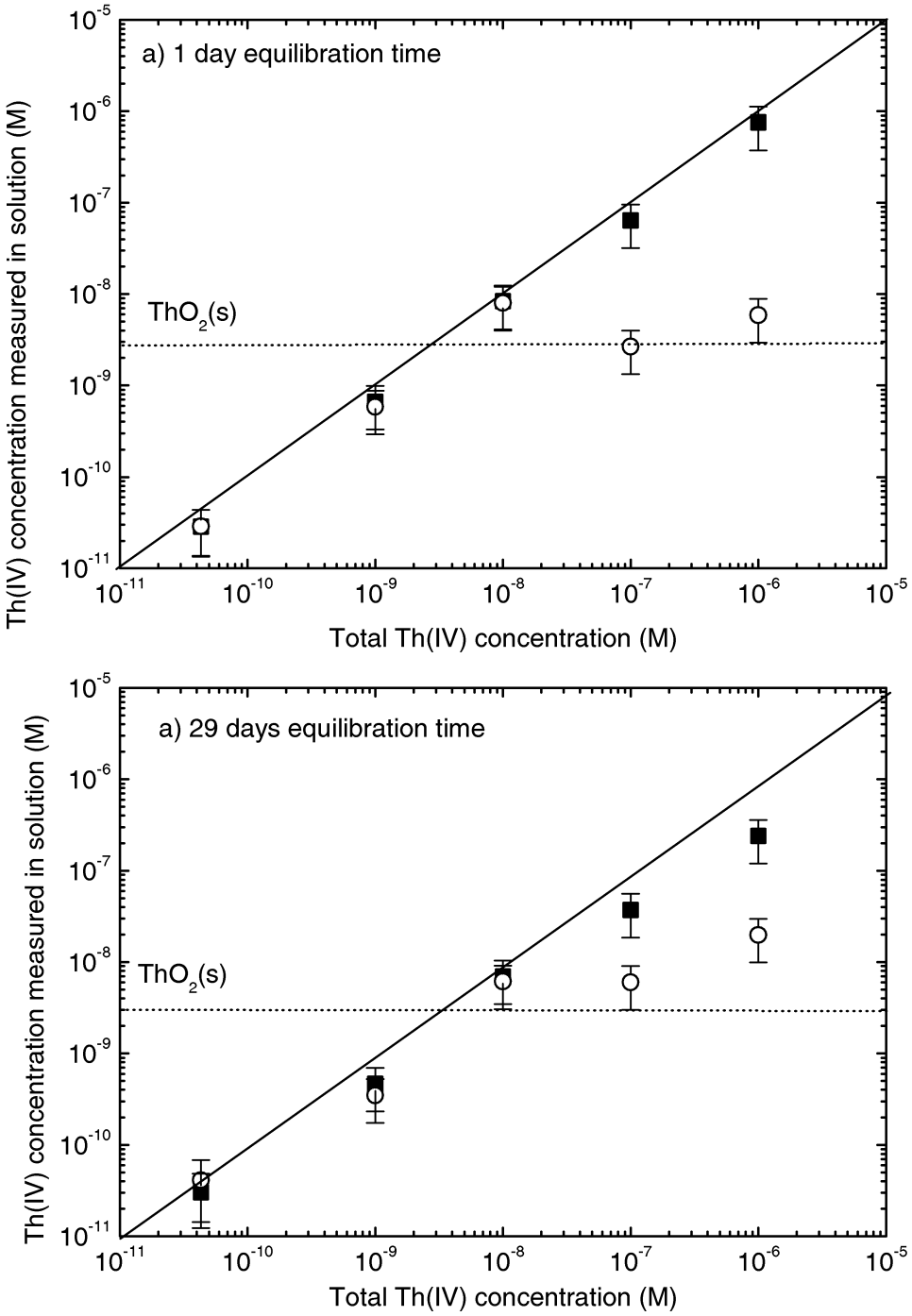

Figure 7: Th(IV) concentration measured in solution before (■) and after (○) centrifugation as a function of the total Th(IV) inventory. Measurements were conducted after 1 day (a) and 30 days equilibration (b). The dashed lines represent the calculated Th(IV) solubility limit in ACW.

5.2 Uptake of Eu(III) and Th(IV) by Merck calcite in the absence of complexing ligands

5.2.1 Kinetics

The results of kinetic tests for Eu(III) and Th(IV) sorption on Merck calcite in the absence of organic ligands are presented in Figure 8 and Figure 9. Figure 8a and Figure 9a show the R_d values and Figure 8b and Figure 9b show the aqueous Eu(III) and Th(IV) concentrations as a function of the equilibration time. The total Eu(III) and Th(IV) concentrations used in the sorption experiments were between $5.0 \cdot 10^{-10}$ M and $2.5 \cdot 10^{-9}$ M for Eu(III) and between $8.6 \cdot 10^{-12}$ M and $8.6 \cdot 10^{-11}$ M for Th(IV).

According to the stability tests discussed in section 4.1, Merck calcite was, at least from a macroscopic point of view, in equilibrium with the ACW when the sorption experiments were started. It was observed that the ACW composition did not change with time during the kinetic tests.

Very high distribution ratios were determined for both radionuclides. In the case of Eu(III), R_d values of $(1.0 \pm 0.6) \cdot 10^5$ L kg^{-1} and $(3 \pm 2) \cdot 10^4$ L kg^{-1} were measured at S:L ratios of 0.2 g L^{-1} and 2 g L^{-1}, respectively (Figure 8a). In the case of Th(IV), a value of $(6 \pm 4) \cdot 10^4$ L kg^{-1} was determined irrespective of the S:L ratio (Figure 9a). Note that the high R_d values are statistically acceptable. The $R_{d,max}$ and $R_{d,min}$ values given in Figure 8a and Figure 9a were estimated as described in appendix A.

Although the scatter of the data is quite large, a trend towards increasing R_d values with decreasing S:L ratios appears from the Eu(III) data. In the case of Th(IV), however, R_d values agree for the two S:L ratios.

Figure 8a and Figure 9a further show that sorption of both Eu(III) and Th(IV) on calcite in ACW was fast. Steady state was reached after approximately 1 day. No further increase in the sorption values was observed after this time period. Earlier studies reported in the open literature show that the uptake of divalent and trivalent metals by calcite occurs in two steps: a fast step followed by a much slower uptake step (e.g. DAVIS et al., 1987; ZACHARA et al., 1988; ZHONG & MUCCI, 1995). The fast step is usually assumed to be a diffusion-controlled adsorption reaction that takes minutes to hours to reach steady state on condition that transport in the bulk solution is not limiting (SPOSITO, 1986).

The slow step has been attributed to processes such as matrix diffusion into the adsorbent, structural rearrangements of surface species, cluster formation or surface precipitation, which can continue over time scales from weeks to months. Surprisingly, a two-step process was not observed in the present experiments. Nevertheless, this can be explained taking into account the relative importance of the two processes. It was reported that kinetic effects attributed to the slow step are more pronounced at high surface coverages (WERSIN et al., 1989; DZOMBAK & MOREL, 1986; DZOMBAK & MOREL, 1990). Moreover, the study by DZOMBAK & MOREL (1986) clearly demonstrated that the rate-limiting process can change as adsorption density increases. The sorption experiments reported in this study were carried out at low surface coverages favouring monolayer adsorption. Assuming a surface site density for calcite of 5 sites per nm^2 (DAVIS & KENT, 1990) and a specific surface area of 0.3 $m^2\ g^{-1}$ (see section 4.1), the site concentration amounts to $2.6 \cdot 10^{-3}$ mol kg^{-1} or $5.15 \cdot 10^{-7}$ mol sites L^{-1} at a S:L ratios of $2 \cdot 10^{-4}$ kg L^{-1}. This value is ten times higher at an S:L ratio of $2 \cdot 10^{-3}$ kg L^{-1}. Thus, site concentrations are significantly higher than the total Eu(III) concentration in our systems, i.e. $2.5 \cdot 10^{-9}$ M and $5 \cdot 10^{-10}$ M. Even on the assumption that all Eu(III) sorbs, the surface coverages are still extremely low. Therefore, in agreement with the previous studies, we conclude that the slow step of the sorption process is not important under the given experimental conditions.

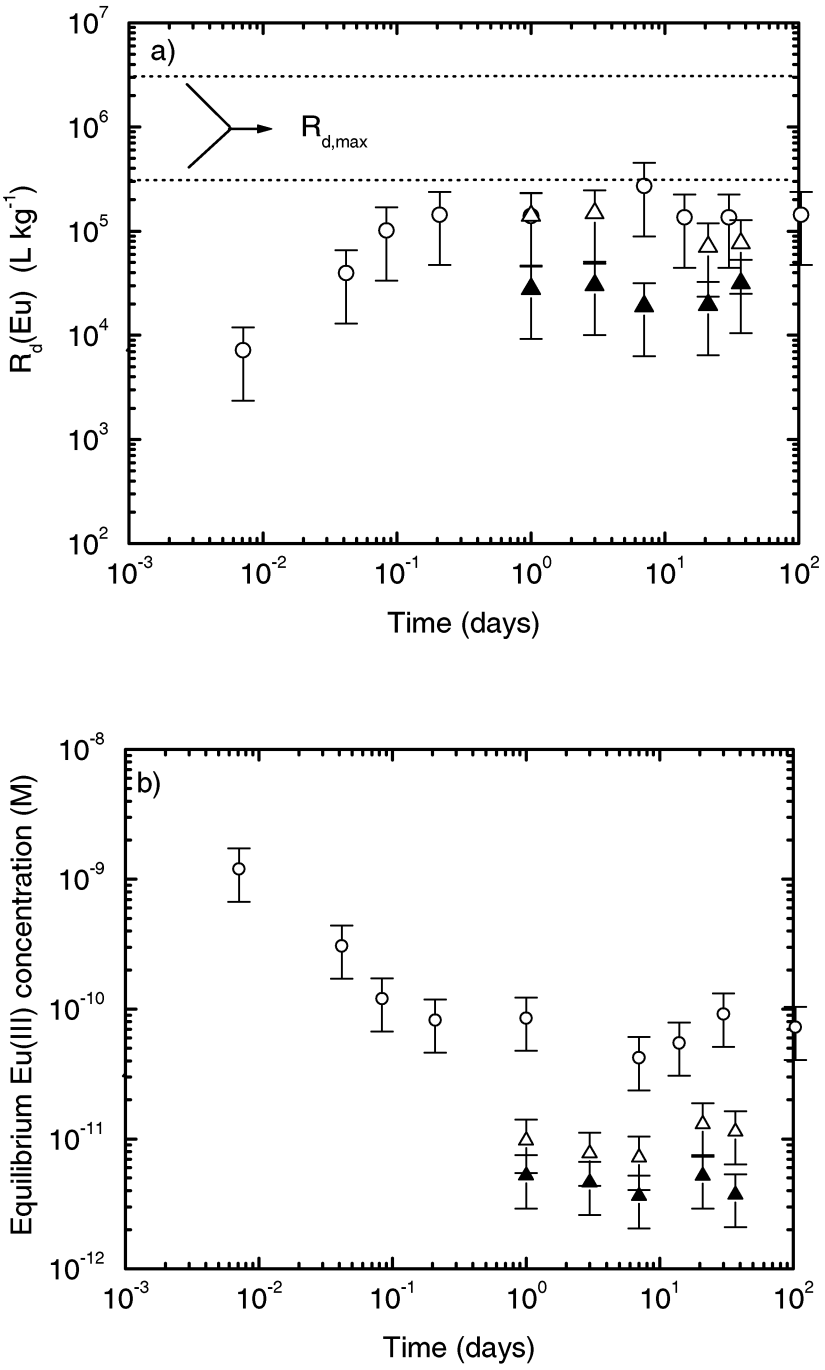

Figure 8: Eu(III) sorption kinetics on Merck calcite in ACW at pH 13.3. a) R_d values; b) Aqueous Eu(III) concentration at equilibrium. The initial Eu(III) concentrations were $5 \cdot 10^{-10}$ M (▲, △) and $2.5 \cdot 10^{-9}$ M (○). The S:L ratios were $2 \cdot 10^{-4}$ kg L^{-1} (○, △) and $2 \cdot 10^{-3}$ kg L^{-1} (▲). The dashed lines indicate the highest measurable distribution ratio, $R_{d,max}$, under the given experimental conditions.

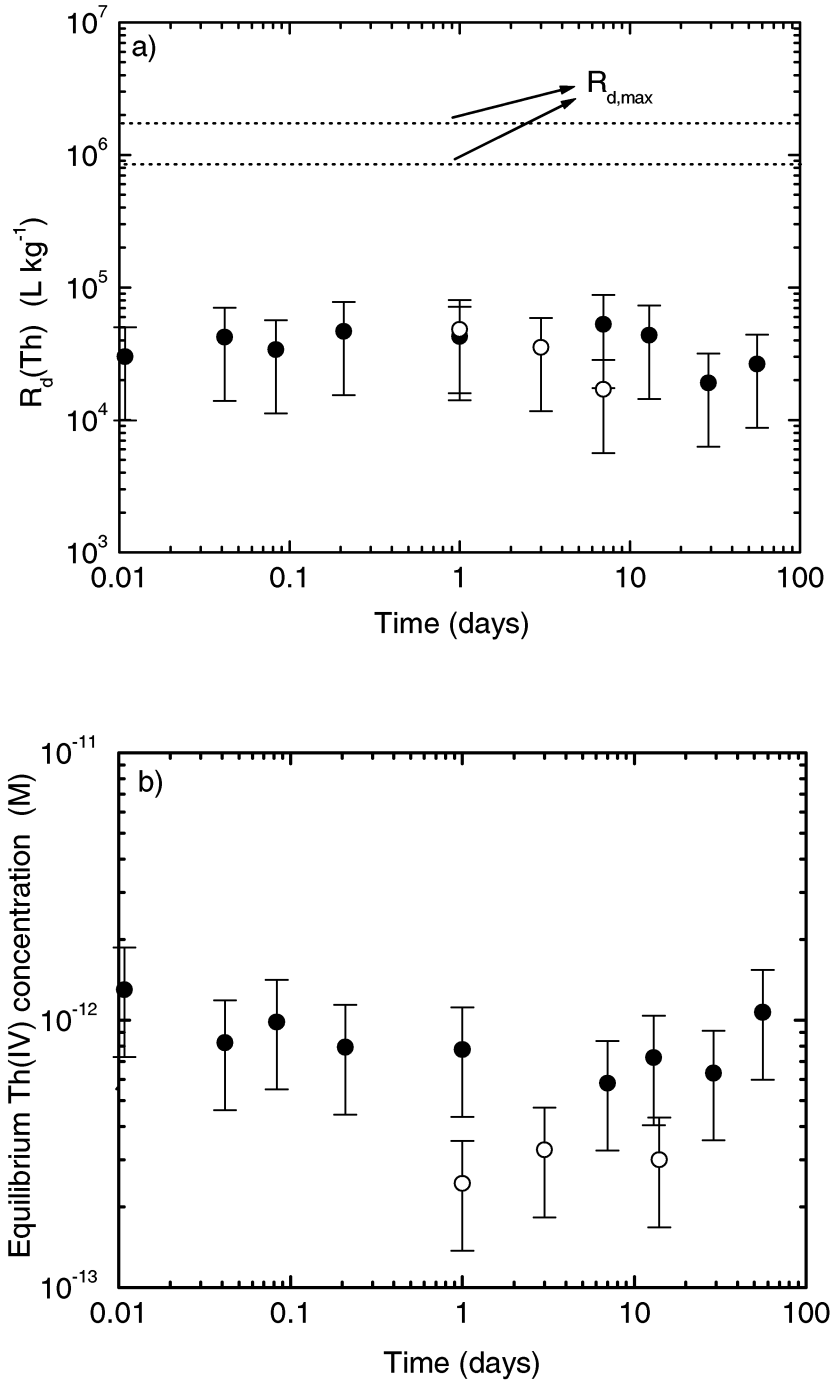

Figure 9: Th(IV) sorption kinetics on Merck calcite. a) R_d values; b) Aqueous Th(IV) concentration at equilibrium. The initial Th(IV) concentrations were $8.6 \cdot 10^{-11}$ M (●) and $8.2 \cdot 10^{-12}$ M (○). The S:L ratio were $2 \cdot 10^{-3}$ kg L^{-1} (●) and $4 \cdot 10^{-4}$ kg L^{-1} (○). The dashed lines indicate the highest measurable distribution ratio, $R_{d,max}$, under the given experimental conditions.

5.2.2 Eu(III) and Th(IV) sorption isotherms

Eu(III) and Th(IV) sorption isotherms are shown in Figure 10 and Figure 11. Calculation of the $R_{d,max}$ values (solid lines in Figure 10a and Figure 11a) and $R_{d,min}$ values (not shown) for these experimental conditions are discussed in appendix A.

Both isotherms were found to be linear over the concentration range employed in the experiments. However, for a sound interpretation of the data, the upper and lower limits of the concentration range, over which the isotherm is valid, must be taken into account. The upper limits of the isotherms for Eu(III) and Th(IV) are determined by the tracer stability in solution and corresponds to 10^{-9} M for both radionuclides. The lower limits are determined by the presence of non-radioactive impurities of Eu(III) and Th(IV) present both in ACW and in Merck calcite. The maximum non-radioactive Eu(III) and Th(IV) concentrations in the calcite-ACW system can be obtained from a mass balance considering Eu(III) and Th(IV) impurities both in ACW and Merck calcite. The mass balance is given by:

$$V \cdot I_M^{ACW} + m \cdot I_M^C = m \cdot R_d \cdot C_{eq} + V \cdot C_{eq} \quad , \tag{5.1}$$

m: mass of solid [kg],

I_M^C: intrinsic inventory of element M in the Merck calcite [mol kg^{-1}],

I_M^{ACW}: intrinsic inventory of element M in the ACW solution [M],

C_{eq}: aqueous equilibrium concentration [M],

V: volume of the suspension [L].

Eu(III) and Th(IV) impurities of Merck calcite were determined to be < 10^{-4} ppm (Table 1). This corresponds to < $6.6 \cdot 10^{-10}$ mol kg^{-1} for Eu(III) and < $4.3 \cdot 10^{-10}$ mol kg^{-1} for Th(IV). Thus, the concentrations of both cations in ACW after equilibration with Merck calcite can be calculated with equation 5.2 assuming a R_d value of 10^5 L kg^{-1} for both Eu(III) and Th(IV) (Figure 8a and Figure 9a), intrinsic inventories in ACW, I_M^{ACW}, of $6.6 \cdot 10^{-11}$ M for Eu(III) and $4.3 \cdot 10^{-11}$ M for Th(IV) (Table 2) and intrinsic inventories in Merck calcite, I_M^C, of $6.6 \cdot 10^{-10}$ mol kg^{-1} for Eu(III) and $4.3 \cdot 10^{-10}$ mol kg^{-1} for Th(IV). With this, the equilibrium concentration in solution can be estimated to be at most $3.1 \cdot 10^{-12}$ M in the case of Eu(III) and $2.1 \cdot 10^{-12}$ M in the case of Th(IV). This indicates that sorption isotherms in ACW can be evaluated over the concentration range between

$3.1 \cdot 10^{-12}$ M and 10^{-9} M for Eu(III) and between $2.1 \cdot 10^{-12}$ M and 10^{-9} M for Th(IV). The isotherms in Figure 10 and Figure 11 were constructed from the activity of radiotracer sorbed and the activity of radiotracer in solution neglecting Eu(III) and Th(IV) impurities of the system. Hence, all datapoints with equilibrium concentrations below the maximum non-radioactive element concentration must be interpreted as having the same total (radioactive isotope + non-radioactive isotope) aqueous concentration and refer to the same point on the isotherm.

The data in Figure 10 further show that the Eu(III) sorption isotherm remains linear above the concentration limit for stable Eu(III). This indicates that the kinetics of Eu(III) sorption on the calcite surface is faster than the kinetics of radiocolloid formation observed in the stability experiments (section 5.1.3).

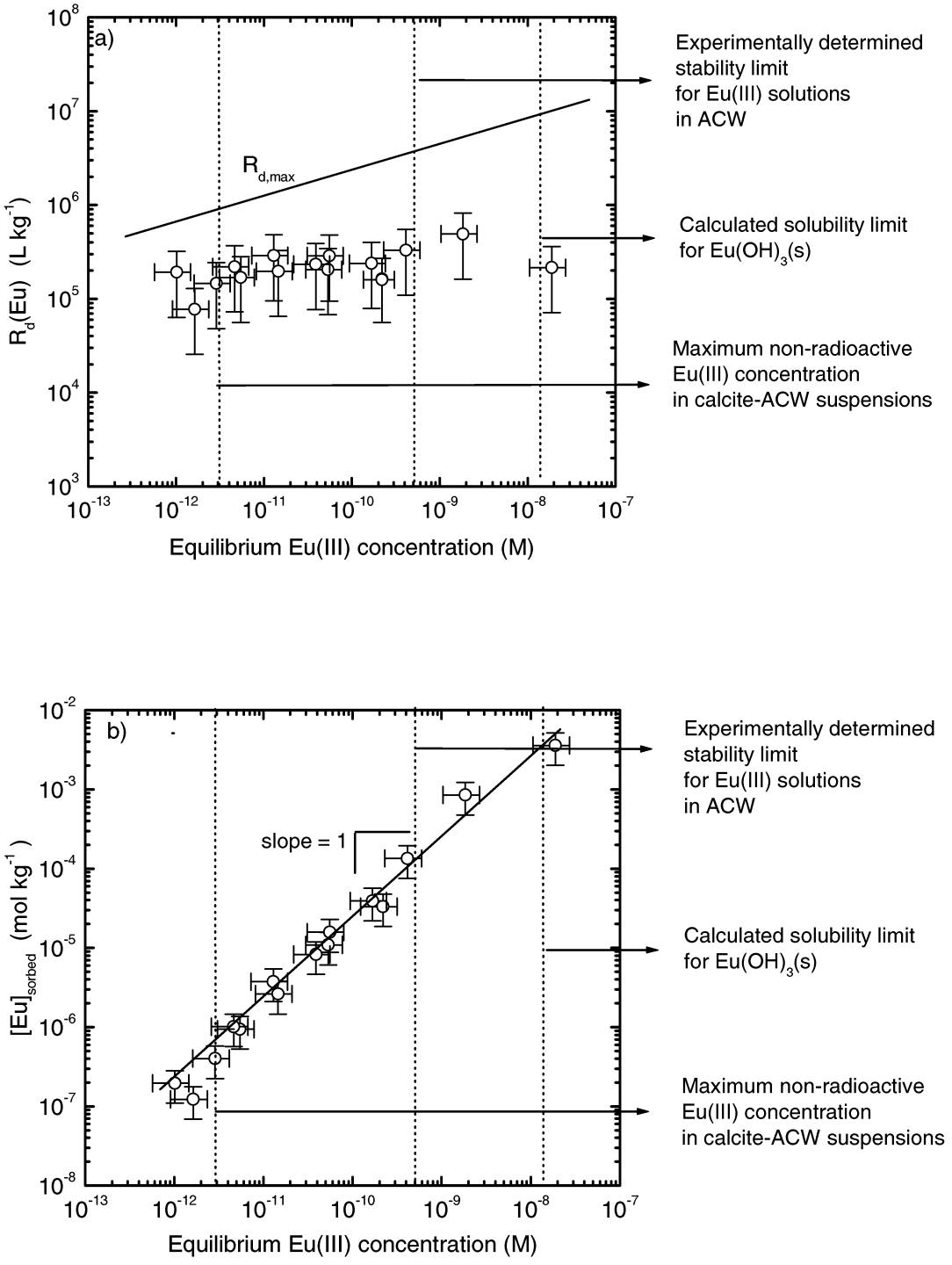

Figure 10: Eu(III) sorption isotherm on Merck calcite in ACW at pH 13.3. The S:L ratio was $5 \cdot 10^{-4}$ kg L^{-1}. The equilibration time was 2 weeks. The solid line in a) represents the maximum measurable sorption value, $R_{d,max}$.

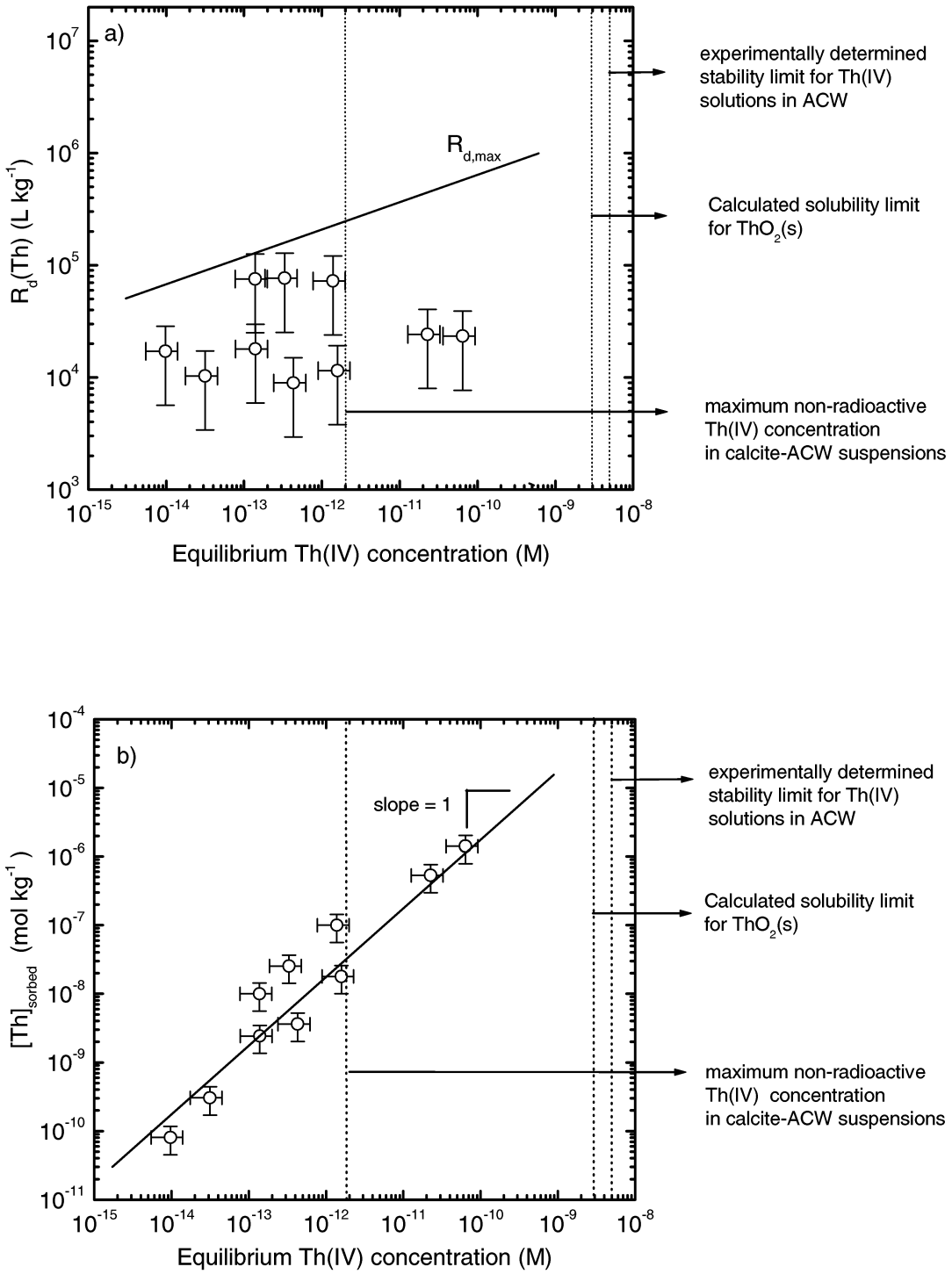

Figure 11: Th(IV) sorption isotherm on Merck calcite in ACW at pH 13.3. The S:L ratio was 10^{-3} kg L. The equilibration time was 2 weeks. The solid line in a) represents the maximum measurable sorption value, $R_{d,max}$.

5.2.3 Dependence of Eu(III) and Th(IV) sorption on the S:L ratio

Figure 12 and Figure 13 show the results of a series of Eu(III) and Th(IV) sorption tests on Merck calcite at S:L ratios varying from 10^{-4} L kg^{-1} to $2 \cdot 10^{-2}$ L kg^{-1}. For both radionuclides, two independent experiments were performed (triangles and squares in Figure 12 and Figure 13). Note that all experimental data points are well within the $R_{d,max}$ and $R_{d,min}$ values (appendix A) and therefore, the data are statistically acceptable.

The results show that the R_d value for Th(IV) is independent of the S:L ratio. By contrast, the R_d value for Eu(III) decreases with increasing S:L ratio. Note that the calcite in one series of tests (squares) was pre-equilibrated with ACW for one month before ^{152}Eu was added. Using the least-squares method to obtain solutions for the best linear fits give a slope of -0.5±0.1. The Eu(III) concentration in the equilibrium solution was found to decrease slightly with increasing S:L ratio, exhibiting a slope of -0.4±0.1.

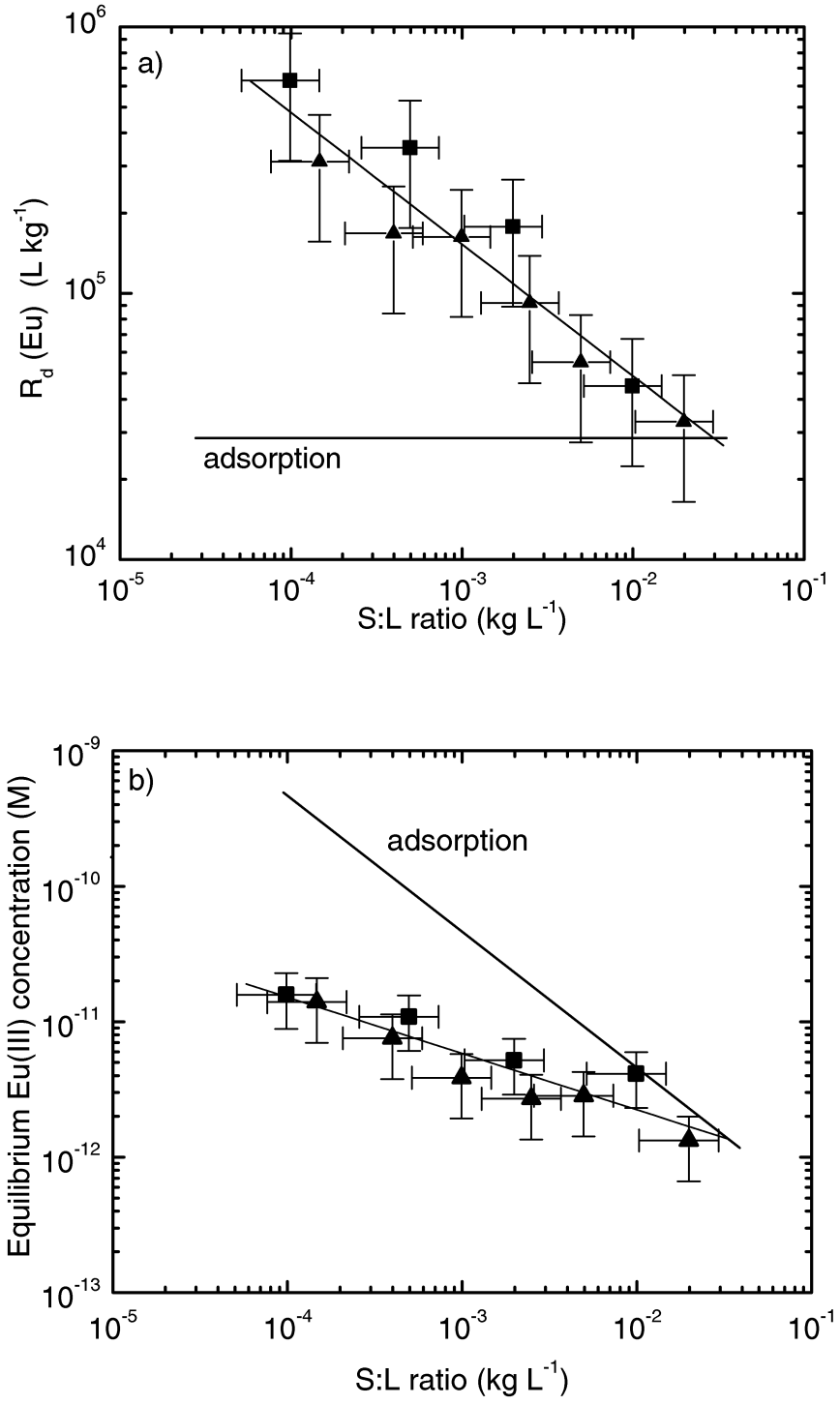

Figure 12: Sorption of Eu(III) by Merck calcite in ACW at pH 13.3. a) Dependence of R_d values on the S:L ratio. b) Eu(III) concentration at equilibrium. The total Eu(III) concentration in the systems was 10^{-9} M. The equilibration time was 1 day. (■) Calcite pre-equilibrated with ACW for 1 month. (▲) Calcite not pre-equilibrated with ACW.

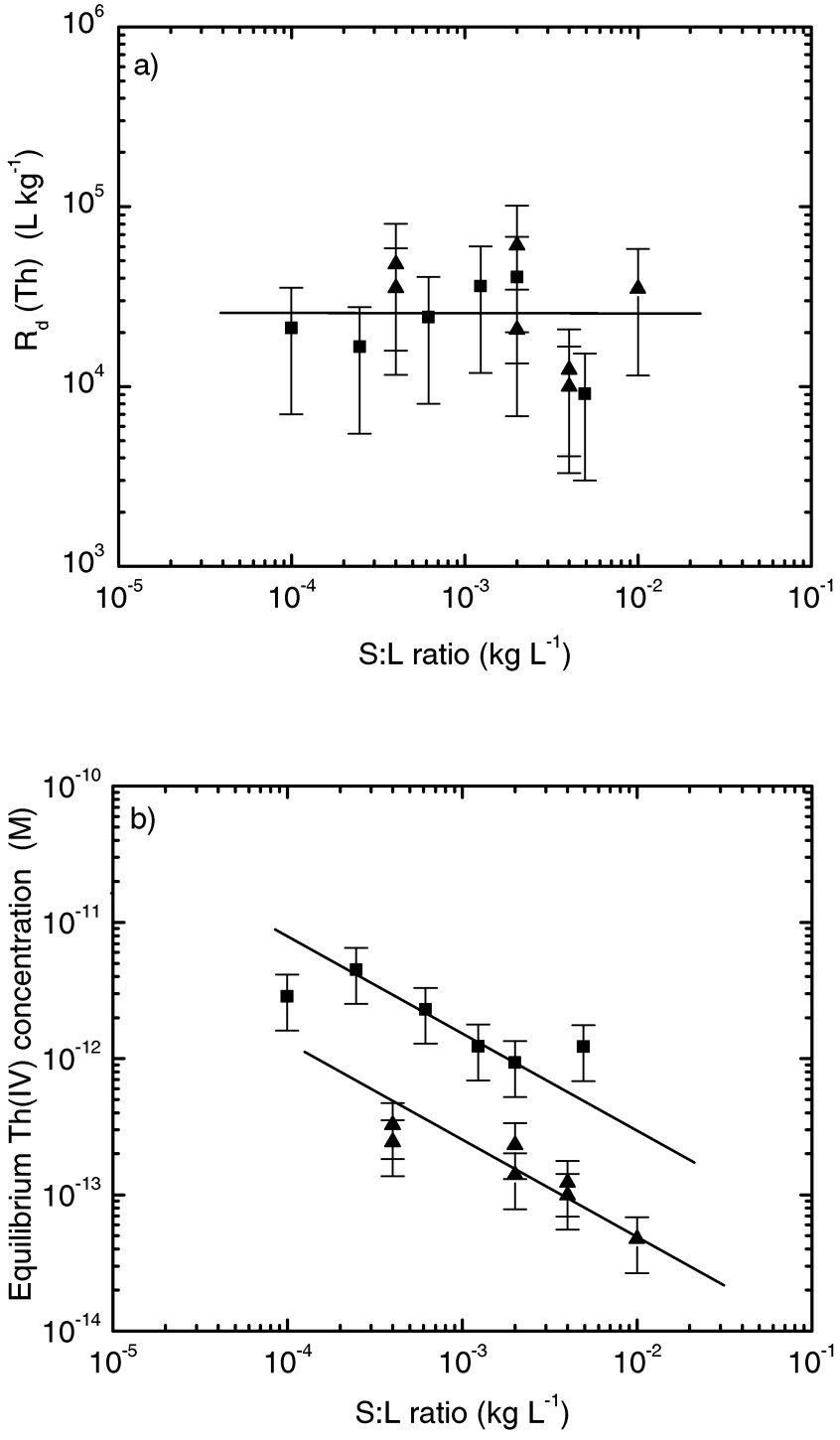

Figure 13: Sorption of Th(IV) by Merck calcite in ACW at pH 13.3.
a) Dependence of the R_d value on the S:L ratio. b) Th(IV) concentration at equilibrium. The total Th(IV) concentration in the systems was 10^{-10} M (■) and 10^{-11} M (▲), respectively. The equilibration time was 1 day.

5.2.4 Interpretation of the sorption tests

Both Eu(III) and Th(IV) sorb very strongly on Merck calcite under ACW conditions, R_d values range from $3 \cdot 10^4$ L kg^{-1} to $2 \cdot 10^5$ L kg^{-1} for Eu(III) and amount $3 \cdot 10^4$ L kg^{-1} for Th(IV). Although very high, such values are compatible with the results obtained from sorption studies with trivalent actinides on clay minerals under high pH conditions: GORGEON (1994) measured the sorption of Am(III) on Na-illite, Na-montmorillonite and Na-kaolinite. The author found that the R_d value for Am(III) increases with pH from 10^3 L kg^{-1} to 10^4 L kg^{-1} at pH 6 to values up to 10^6 L kg^{-1} in the pH range 10 to 12. BASTON et al. (1992) determined the sorption of Th(IV) on several clay samples in the pH range from 8 to 12. The authors deduced R_d values ranging from 10^3 L kg^{-1} to $3 \cdot 10^3$ L kg^{-1}.

Th(IV) uptake by Merck calcite can be described in terms of an adsorption process. Uptake is fast and follows linear sorption. Moreover, a constant R_d at varying S:L ratio corroborates a linear sorption process.

In the case of Eu(III), the fast sorption kinetics and the linear sorption isotherm also suggest adsorption as uptake controlling process. Figure 10b shows that the sorption process is linear over a concentration range of more than 4 orders of magnitude (10^{-7} mol kg^{-1} sorbed Eu(III) to $4 \cdot 10^{-3}$ mol kg^{-1} sorbed Eu(III)). Note that the number of sorption sites on the surface of calcite was estimated to be at maximum $2.6 \cdot 10^{-3}$ mol kg^{-1} (section 5.2.1). These two values are very similar suggesting that, at maximum surface coverage, all sorption sites on the calcite surface are occupied. Moreover, as a consequence of the linear sorption behaviour, all the sorption sites have the same affinity for Eu(III). These findings are not consistent with the notion of an adsorption-type process but suggest incorporation into the calcite structure. Therefore, we infer that other processes such as solid-solution formation may control the uptake of Eu(III) by calcite.

A further indication that processes other than adsorption are involved, is the effect of the S:L ratio in the Eu(III) sorption experiments. Both the R_d value and the Eu(III) concentration at equilibrium decrease with increasing S:L ratio (slopes -0.5 and -0.4), which is not consistent with an adsorption process.

A possible explanation for the S:L ratio effect arises from the speciation calculations shown in section 5.1.1. The calculations indicate that the ACW solution in contact with calcite is slightly supersaturated with respect to

portlandite, which may result in the formation of, at maximum, 0.0295 g L^{-1} portlandite. Experiments performed in our laboratory show that Eu(III) strongly sorbs on portlandite (R_d = $5 \cdot 10^5$ L kg^{-1}). An overall R_d value for the calcite-portlandite mixture can be calculated, assuming that the actual R_d value for Eu(III) sorption on calcite corresponds to the value obtained at the highest calcite concentrations, i.e., approximately $3 \cdot 10^4$ L kg^{-1}, and assuming that the following relation exists between the overall R_d value of a mixture and the R_d values for the components of the mixture:

$$R_d^{overall} = (1-x) \cdot R_d^{calcite} + x\, R_d^{portlandite} \quad , \qquad (5.2)$$

Where x denotes the portlandite fraction in the calcite-portlandite mixture. The overall R_d value increases with increasing portlandite – calcite ratios because the R_d value for Eu(III) sorption on portlandite is more than a factor 10 higher than the R_d value on calcite.

The effect of portlandite on the overall R_d value is demonstrated in Figure 14. The dotted line represents predicted changes in the R_d value assuming portlandite precipitation (0.0295 g L^{-1}). Based on this assumption, a decrease of the R_d value with increasing S:L ratios is expected. Nevertheless, the linear trend in the experimental data cannot be explained. Furthermore, it is noticed that, if portlandite precipitation would play a role, a similar trend should be observed for the Th(IV)-calcite system. This is not the case (R_d (Th-portlandite) = $6 \cdot 10^5$ L kg^{-1}; R_d (Th-calcite) = $6 \cdot 10^4$ L kg^{-1}). We thus conclude that sorption on precipitating portlandite does not account for the S:L ratio effect observed in the Eu(III)-calcite system.

Another possible explanation could be that kinetic effects interfere with the sorption process, e.g., Eu(III) forming a solid solution with calcite via a surface recrystallisation process. It can be shown that it is necessary to postulate a stoichiometry with twice as much Eu(III) ions in the trace end-member as Ca(II) ions in calcite, in order to explain the slope of –0.5 by means of an ideal solid-solution model (CURTI, pers. comm.). This seems very unlikely. However, the S:L ratio effect might be explained assuming changes in recrystallisation rate of calcite as function of the S:L ratio. Testing this hypothesis, however, requires a more detailed understanding of recrystallisation processes under strongly alkaline conditions and resultant effects on radionuclide uptake. Certainly, this calls for a new experimental program beyond the scope of the present study.

To explain the conflicting results obtained in the wet chemistry studies it is recommended to use complementary methods in future studies. Spectroscopic methods such as X-ray absorption spectroscopy (XAS) or laser-induced fluorescence spectroscopy (LIFS) may provide more detailed information on Eu(III) speciation at the calcite surface.

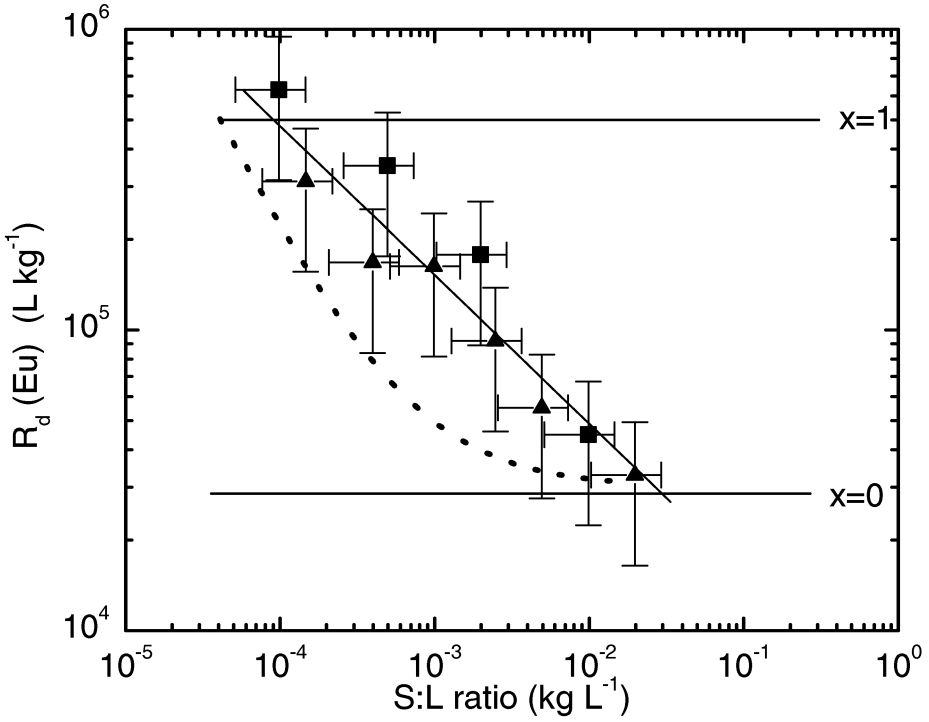

Figure 14: Sorption of Eu(III) onto Merck calcite in ACW at pH 13.3. Dependence of R_d values on the S:L ratio. The dashed line represents the calculated R_d value assuming precipitation of 0.0295 g L^{-1} portlandite. x = the portlandite fraction in the calcite-portlandite mixture.

5.3 The effect of ISA and GLU on the uptake of Eu(III) and Th(IV) by calcite

Organic ligands originating from the degradation of cellulose and from cement additives in a cementitious near-field may influence the sorption behaviour of radionuclide in the pH-plume altered zone of a repository far-field. Isosaccharinic acid (ISA) and gluconic acid (GLU) have been taken as representatives of each of the above mentioned groups of organic ligands. The former is the main degradation product of cellulose under alkaline conditions (VAN LOON & GLAUS, 1998), and the latter is a low molecular weight cement additive, regularly used as a plasticizer in cement (RAMACHANDRAN, 1984). Their structures are shown in Figure 15.

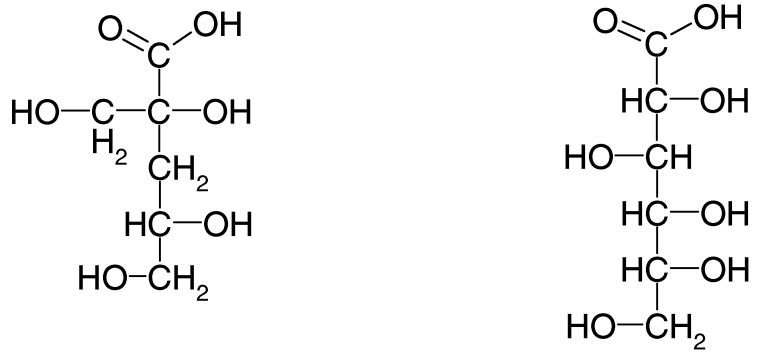

Figure 15: Chemical structures of α-isosaccharinic acid and gluconic acid .

The formation of aqueous radionuclide-ligand complexes could decrease the sorption of radionuclides and, consequently, increase their mobility. VAN LOON & GLAUS (1998) showed that ISA strongly reduces the sorption of several radionuclides such as Ni(II), Eu(III) and Th(IV) on feldspar in ACW, indicating that this organic ligand may act as a strong complexant under ACW conditions. WIELAND et al. (1998) observed only a minor effect of ISA on Eu(III) uptake by hardened cement paste in ACW which was tentatively attributed to the formation of ternary Eu(III)-ISA surface complexes. The same authors observed a decrease in the R_d values for Th(IV) at ISA concentrations greater than 10^{-4} M.

NORDEN & ALLARD (1994) found that GLU strongly reduces the Eu(III) sorption on a standard Portland cement in a cement pore water at pH 12.5 at GLU concentration greater than $3 \cdot 10^{-5}$ M. The authors further observed that the effect decreased with time, which was tentatively explained by the decomposition of GLU under the high pH conditions. BERRY et al. (1991) and BASTON et al. (1992) studied the effect of GLU on the sorption of uranium, plutonium and thorium on several clay materials at pH 11 using GLU concentrations of $2 \cdot 10^{-3}$ M and in the range between $2 \cdot 10^{-6}$ M and $4 \cdot 10^{-7}$ M, respectively. These authors found that the presence of this organic ligand markedly reduced the R_d values for these radioelements.

In the present study the effect of ISA and GLU on the sorption of Eu(III) and Th(IV) on Merck calcite has been examined. First, the sorption of ISA and GLU on Merck calcite was investigated and, second, the effect of increasing GLU and ISA concentrations on Eu(III) and Th(IV) uptake was studied. From these experiments conditional complexation constants for Eu(III)-GLU, Th(IV)-GLU, Eu(III)-ISA and Th(IV)-ISA complexes were determined.

5.3.1 Sorption of ISA and GLU on Merck calcite

Sorption kinetics and sorption isotherms were determined for ISA and GLU on Merck calcite. Stability tests showed that both ligands are stable in ACW over the time period relevant to the experiment, i.e., up to 42 days. The kinetic tests did not give any evidence for GLU or ISA sorption on the Merck calcite over this time period. These tests were performed at ISA and GLU concentrations of 10^{-4} M. In the case of GLU, additional sorption measurements were carried out in the concentration range between 10^{-7} M and 10^{-4} M. The results corroborate the findings from the kinetic tests that ISA and GLU sorption on Merck calcite is negligibly small.

5.3.2 The effect of ISA and GLU on Eu(III) sorption

The effect of ISA and GLU on Eu(III) sorption was studied at calcite concentrations ranging between $4 \cdot 10^{-4}$ kg L^{-1} and $4 \cdot 10^{-3}$ kg L^{-1}. The concentration of ISA varied between $2.0 \cdot 10^{-7}$ M and $2.5 \cdot 10^{-2}$ M, and the concentration of GLU varied between 10^{-4} M and 10^{-8} M. Note that the calcite

solubility in these experiments is not affected by ISA at concentrations up to $2 \cdot 10^{-2}$ M and by GLU for concentrations up to $2 \cdot 10^{-4}$ M (section 5.1.1). The total ^{152}Eu concentration was 10^{-9} M.

The effects of ISA and GLU on the R_d value and on the aqueous Eu(III) concentration are shown in Figure 16 and Figure 17. The data clearly show that aqueous ISA concentrations above 10^{-5} M and aqueous GLU concentrations above 10^{-7} M significantly reduce the sorption of Eu(III) under the given experimental conditions. Note that only experimental data which fall within the $R_{d,max}$ and $R_{d,min}$ limits are displayed in Figure 16 and Figure 17. The values for $R_{d,max}$ and $R_{d,min}$ are given in appendix A for each set of experiments together with the parameters necessary for the calculations. The measured R_d value approaches $R_{d,max}$, which is approximately $3 \cdot 10^5$ L kg^{-1} for both ISA and GLU, when the ligand concentration is very low. The measured R_d approaches $R_{d,min}$ (approximately 40 L kg^{-1} for both ISA and GLU) with increasing ligand concentration.

A close inspection of the data for ISA (Figure 16) reveals a possible dependence of the R_d values on the S:L ratio, especially at lower ISA concentrations. A decrease of the S:L ratio from $4 \cdot 10^{-3}$ L kg^{-1} to $4 \cdot 10^{-4}$ L kg^{-1} results in an increase in the R_d value by approximately a factor 5. This effect of the S:L ratio on the R_d values is even more pronounced in the experiments with GLU (Figure 17). An increase in the S:L ratio by one order of magnitude results in a proportional decrease of the R_d value.

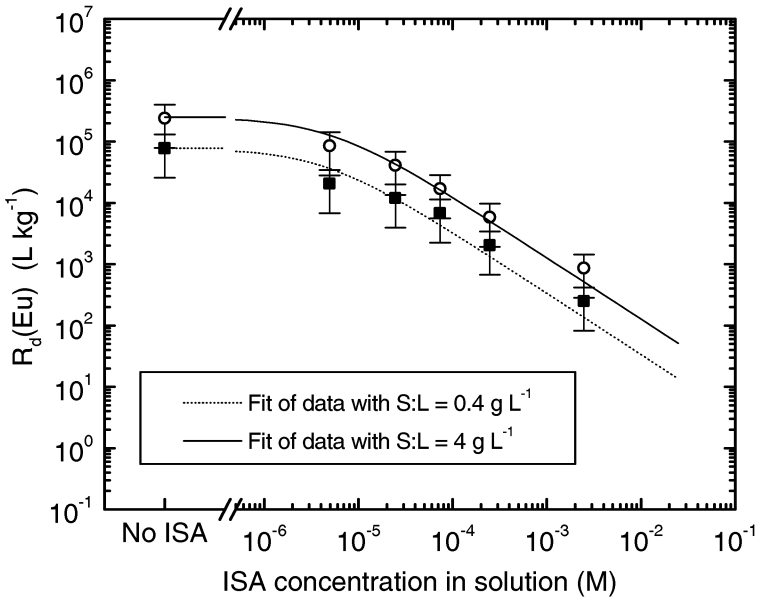

Figure 16: Influence of ISA on the uptake of Eu(III) by Merck calcite in ACW at pH 13.3. The S:L ratios were $4{\cdot}10^{-4}$ kg L^{-1} (○)and $4{\cdot}10^{-3}$ kg L^{-1} (■). The equilibration time was 3 days. The total Eu(III) concentration was 10^{-9} M. The continuous lines represent best fits obtained from the data at each S:L ratio.

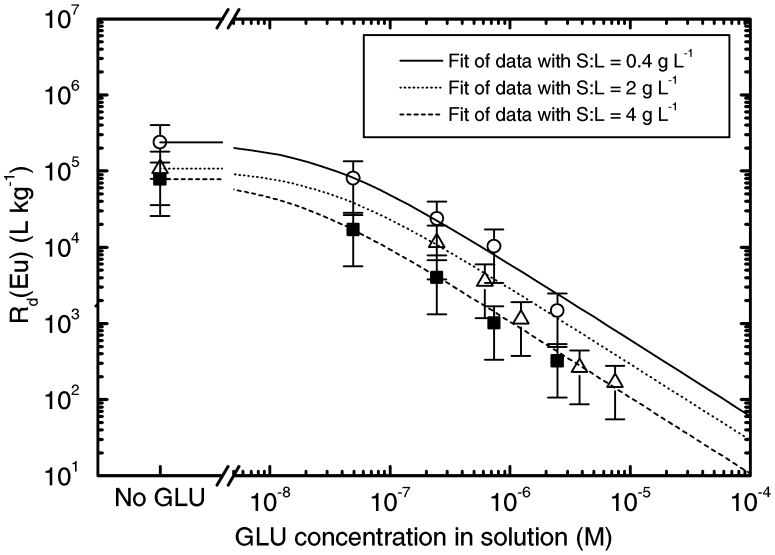

Figure 17: Influence of GLU on Eu(III) sorption onto Merck calcite in ACW at pH 13.3. S:L ratios = $4{\cdot}10^{-4}$ kg L^{-1} (○), $2{\cdot}10^{-3}$ kg L^{-1} (Δ) and $4{\cdot}10^{-3}$ kg L^{-1} (■). The equilibration time was 3 days. The total Eu(III) concentration was 10^{-9} M. The continuous lines represent best fits obtained from the data at each S:L ratio.

5.3.2.1 The stoichiometries of the Eu(III)-ISA and Eu(III)-GLU complexes

The following general reaction scheme for the formation of complexes between Eu(III) and ISA or GLU, respectively, was proposed by VAN LOON & GLAUS (1998):

$$Eu^{3+} + nH_qL^- + mH_2O \Leftrightarrow Eu(OH)_m(H_{q-p}L)_n^{3-m-n(1+p)} + (m+np)H^+ \quad . \qquad (5.3)$$

"H_qL^-" stands for deprotonated ISA or GLU. "n" represents the number of ligands involved in the complexation reaction. The negative charge originates from the deprotonated carboxyl group (Figure 15). "H_q" represents the protons of q hydroxyl groups of the organic ligands. q is equal to 4 in the case of ISA and 5 in the case of GLU. p represents the number of protons released when Eu(III)-ISA and Eu(III)-GLU complexes are formed.

VERCAMMEN (2000) showed that a 1:1 complex is formed between ISA and Eu(III) (n=1) in the pH range between 10.7 and 13.3. The formation of the complex was found to be coupled with the release of 4 protons. There is, however, no experimental evidence whether these protons are released due to deprotonation of the hydroxyl groups of ISA (p=4) or from the water molecules associated with the central trivalent cation (m=4). VAN DUIN et al. (1989) proposed a general coordination - ionisation scheme for polyhydroxy carboxylic acids. This reaction scheme relates the coordination of cations to polyhydroxy carboxylic acids with the acidity of the complexing cation. With this approach it is predicted that, at this high pH, cations with a high charge density and a large polarisation potential, such as the trivalent lanthanides and actinides, coordinate with two or more hydroxyl-groups of polyhydroxy carboxylic acids. The coordination reaction causes the release of an equivalent number of protons from the hydroxyl-groups of the ligand, which is supported by the work of VERCAMMEN (2000). The model suggests the formation of tetradentate Eu(III)-ISA or Eu(III)-GLU complexes in which the central Eu(III) cation is coordinated to 4 deprotonated hydroxyl groups. Finally, the model of VAN DUIN et al. (1989) implies that the protons released in the complexation reaction originate from the hydroxyl groups and not from water molecules associated with the central trivalent cation. Based on the above findings, it is assumed that m and p are equal to 0 and 4, for both ligands. Thus, the general reaction scheme proposed in equation 5.3. is adapted for the present study using m=0 and p=4.

5.3.2.2 Determination of the Eu(III)-ISA complexation constant

In the case of Eu(III), complexation with ISA can be written as:

$$Eu^{3+} + H_4ISA^- \Leftrightarrow EuISA^{2-} + 4H^+ \quad . \tag{5.4}$$

The sorption value, R_d, in the presence of ISA can be expressed in accordance with equation 2.17:

$$R_d = R_d^0 \cdot \left(\frac{A}{A + \frac{\beta_{EuISA} \cdot \left[H_4ISA^-\right]}{[H]^4}} \right) \quad , \tag{5.5}$$

R_d^0: R_d value in the absence of ISA,

$[H_4ISA^-]$: equilibrium concentration of H_4ISA^- in solution,

β_{EuISA}: stability constant of the complex $EuISA^{2-}$,

A: side-reaction coefficient defined in section 2.4.

Use of equation 5.5 requires that the sorption of Eu(III) is linear and reversible and that neither the organic ligand nor the complex sorb on the solid phase. The latter assumption is justified as previously discussed in section 5.2.1.

The side-reaction coefficient, A, and the proton concentration are constant, as a result of constant pH and ionic strength in the experiments. Thus, the following expression holds:

$$\frac{\beta_{EuISA}}{\left[H^+\right]^4 \cdot A} = C_{EuISA} = \text{constant} \quad . \tag{5.6}$$

Furthermore, the total Eu(III) concentration in the experiments was ~ 10^{-9} M, which is much lower than the ligand concentrations used. With this and the finding that ISA does not sorb onto the calcite surface, the concentration of the free ligand in solution can be approximated by the total ligand concentration ($[H_4ISA^-]_{tot}$). Taking into account these simplifications, equation 5.5 can be written as follows:

$$R_d = \frac{R_d^0}{1 + C_{EuISA} \cdot \left([H_4ISA^-]_{tot}\right)} \quad . \qquad (5.7)$$

The data displayed in Figure 16 were fitted with equation 5.7 (continuous lines). However, it was impossible to fit the data of both datasets (S:L ratio of 0.4 g L^{-1} and 4.0 g L^{-1}) with one single mean R_d^0 value. As a consequence, each dataset was fitted separately using a unique R_d^0 value taken from the sorption experiments carried out in the absence of the organic ligand (section 5.2.3). The R_d^0 values used in the fitting procedures are listed in Table 10 together with the constants, C_{EuISA}, obtained from the best fit of each dataset. Figure 16 shows that the fits correctly represent the trend in the experimental data on the assumption that a 1:1 Eu:ISA complex (n=1) is formed.

C_{EuISA} was determined to be $(2.0\pm0.7)\cdot10^5$ M^{-1} and $(2.3\pm1.0)\cdot10^5$ M^{-1} for S:L ratios of $4\cdot10^{-4}$ L kg^{-1} and $4\cdot10^{-3}$ L kg^{-1}, respectively. These values can be transformed into conditional complexation constants, β_{EuISA}, using equation 5.6. The side-reaction coefficient was estimated to be $10^{16.17}$ (I=0.3 M), considering $Eu(OH)_4^-$ as the only relevant Eu(III) complex in ACW ($\log K^{0.3}_{Eu(OH)_4^-}$ = 18.2). The conditional complexation constants, β_{EuISA}, were extrapolated to I=0 by means of the Davies equation.

The resulting complexation constants are listed in Table 10. The mean value for the complexation constant (I=0) was determined to be:

$\log\beta^0_{EuISA} = -31.1\pm0.2$.

The complexation constant for the Eu(III)–ISA complex obtained in this study can be compared with values previously reported by VAN LOON & GLAUS (1998), VERCAMMEN (2000) and VERCAMMEN et al. (2001). The former authors report a conditional complexation constant (I=0.3) for the Eu(III)-ISA complex, $\log K_{EuISA}$, of (-18.8±0.3). However, this constant was estimated by VAN LOON & GLAUS (1998) assuming the release of only 3 protons in the complexation reaction. In the present study, however, the release of 4 protons is assumed. Furthermore, VAN LOON & GLAUS (1998) used a different set of hydrolysis constants to estimate the side-reaction coefficient, A, of 10^{17}. Recalculating their value assuming the release of 4 protons and using a value of $10^{16.17}$ for A, yields $\log\beta^{0.3}_{EuISA^-}$ = -32.6.

VERCAMMEN et al. (2001) used the complexation model described in the present study (release of 4 protons) to interpret their data. The Eu(III)–ISA complexation constant at I = 0.3, $\log K_{EuISA}$, was determined to be -30.6 by these authors. The calculation, however, was based on a value of $10^{17.8}$ for A . Using $A=10^{16.17}$ yields $\log \beta^{0.3}_{EuISA^-} = -32.2$.

Thus, the complexation constants reported by VAN LOON & GLAUS (1998) and VERCAMMEN et al. (2001) are consistent and approximately one order of magnitude lower than the value deduced in the present study.

Table 10: R_d^0 values for Eu(III) used to fit the data in Figure 16, the resulting fitting parameter, C_{EuISA}, and the corresponding complexation constants.

S:L ratio [kg L^{-1}]	R_d^0 [kg L^{-1}]	C_{EuISA}	$\log \beta^{0.3}_{EuISA^-}$	$\log \beta^{0}_{EuISA^-}$	Mean $\log \beta^{0}_{EuISA^-}$
$4\cdot10^{-4}$	$2.4\cdot10^{5}$	$(2.0\pm0.7)\cdot10^{5}$	-31.4±0.2	-31.1±0.2	-31.1±0.2
$4\cdot10^{-3}$	$7.8\cdot10^{4}$	$(2.3\pm1.0)\cdot10^{5}$	-31.3±0.2	-31.1±0.2	

5.3.2.3 Determination of the Eu(III)-GLU complexation constant

Because ISA and GLU belong to the same group of polyhydroxy ligands, the complexation of Eu(III) with GLU under high pH conditions is postulated to follow the reaction scheme previously presented for ISA (equation 5.3):

$$Eu^{3+} + H_5GLU^- \Leftrightarrow EuHGLU^{2-} + 4H^+ \quad . \qquad (5.8)$$

The sorption value, R_d, in the presence of ISA can be expressed in accordance with equation 2.17:

$$R_d = R_d^0 \cdot \frac{A}{\left(A + \frac{\beta_{EuGLU} \cdot \left[H_5GLU^- \right]}{[H^+]^4} \right)} \quad . \qquad (5.9)$$

Assuming that the side-reaction coefficient, A, and the proton concentration are constant, and that the free ligand concentration, $[H_5GLU^-]$, is equal to the total ligand concentration, $[H_5GLU^-]_{tot}$, equation 5.9 can be simplified to:

$$R_d = \frac{R_d^0}{1 + C_{EuGLU} \cdot \left([H_5GLU^-]_{tot}\right)} \quad , \tag{5.10}$$

with:

$$C_{EuGLU} = \frac{\beta_{EuGLU}}{\left[H^+\right]^4 \cdot A} = constant \quad . \tag{5.11}$$

The data in Figure 17 were fitted (continuous lines) with equation 5.10. Each dataset was fitted separately using different R_d^0 values based on the sorption experiments in the absence of the organic ligand, (section 5.2.3). The R_d^0 values used in the fitting procedures are listed in together with the constants, C_{EuGLU}, obtained from the best fit of each dataset. The fits correctly represent the trend in the experimental data confirming that the assumption of a 1:1 Eu:GLU complex (n=1) is justified.

The corresponding conditional complexation constants were estimated with equation 5.15 using a value of $10^{16.17}$ for A. Recalculation to zero ionic strength by means of the Davies equation yields the complexation constant, β^0_{GLU}, listed in Table 11.

The mean value for the complexation constant (I=0) amounts to:

$\log\beta^0_{EuGLU^-} = (-28.7 \pm 0.1)$.

Table 11: R_d^0 values for Eu(III) used to fit the data in Figure 17, the resulting fitting parameter, C_{EuGLU}, and the corresponding complexation constants.

S:L ratio kg L^{-1}	R_d^0 L kg^{-1}	C_{EuGLU}	log $\beta^{0.3}_{EuGLU^-}$	log $\beta^{0}_{EuGLU^-}$	Mean log $\beta^{0}_{EuGLU^-}$
$4\cdot10^{-4}$	$2.4\cdot10^{5}$	$(7.3\pm0.2)\cdot10^{7}$	-28.8±0.1	-28.6±0.1	-28.7±0.1
$2\cdot10^{-3}$	$1.08\cdot10^{5}$	$(3.7\pm0.3)\cdot10^{7}$	-29.1±0.1	-28.9±0.1	
$4\cdot10^{-3}$	$7.8\cdot10^{4}$	$(3.9\pm0.3)\cdot10^{7}$	-29.1±0.1	-28.8±0.1	

5.3.3 The effect of ISA and GLU on Th(IV) sorption

The effect of ISA and GLU on the uptake of Th(IV) by Merck calcite was studied in a similar way to that described for Eu(III). The concentration of ISA varied between $2.5\cdot10^{-2}$ M and $5\cdot10^{-7}$ M, whereas the concentration of GLU varied between 10^{-4} M and $7\cdot10^{-8}$ M. The effect of ISA and GLU on Th(IV) sorption are shown in Figure 18 and Figure 19. Note that only experimental data which fall within the $R_{d,max}$ and $R_{d,min}$ limits are shown. The limits were calculated for the given experimental conditions as shown in appendix A. For GLU and ISA concentrations above 10^{-6} M and $5\cdot10^{-5}$ M, respectively, significant reduction in the sorption of Th(IV) on calcite was observed. The sorption reduction is due to the formation of Th(IV) - ligand complexes in solution. In contrast to the interpretation of the Eu(III) data, Th(IV) uptake by calcite can be attributed to an adsorption process.

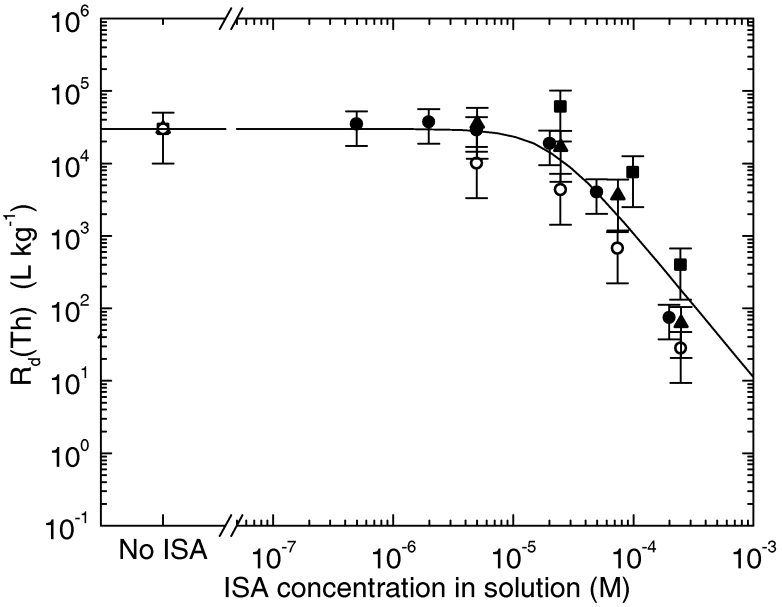

Figure 18: Influence of ISA on Th(IV) sorption onto Merck calcite in ACW at pH 13.3. The S:L ratios used in the experiments were $4{\cdot}10^{-4}$ kg L^{-1} (▲), $2{\cdot}10^{-3}$ kg L^{-1} (■), $4{\cdot}10^{-3}$ kg L^{-1} (○) and 10^{-2} kg L^{-1} (●). The equilibration time was 3 days. The added Th(IV) concentration was 10^{-11} M. The solid line represents the best fit obtained from the data.

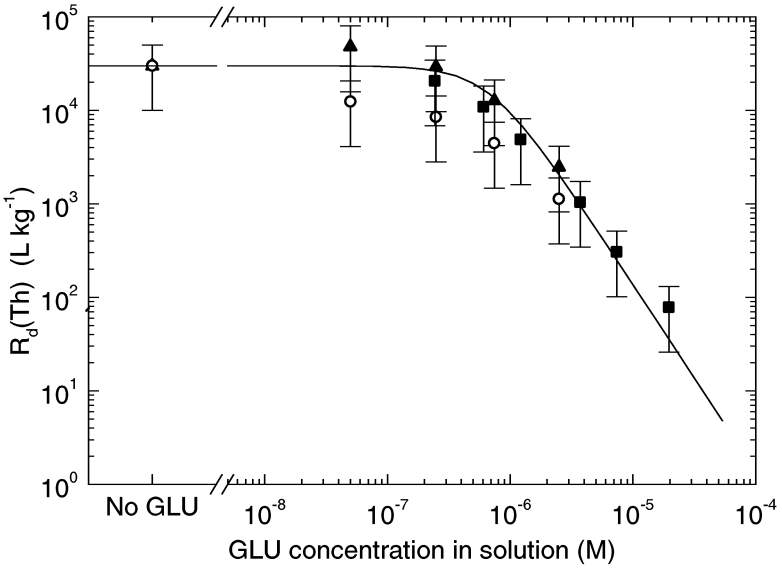

Figure 19: Influence of GLU on Th(IV) sorption onto Merck calcite in ACW at pH 13.3. The S:L ratios used in the experiments were $4{\cdot}10^{-4}$ kg L^{-1} (▲), $2{\cdot}10^{-3}$ kg L^{-1} (■) and $4{\cdot}10^{-3}$ kg L^{-1} (○). The equilibration time was 3 days. The added Th(IV) concentration was 10^{-11} M. The solid line represents the best fit obtained from the data.

5.3.3.1 Stoichiometries of the Th(IV)-ISA and Th(IV)-GLU complexes

The literature concerning the complexation of tetravalent metal cations with GLU or ISA under alkaline conditions is sparse. SAWYER & AMBROSE (1962) studied the complexation of Ce(IV) with GLU using an excess of Ce(IV) compared to GLU. The authors concluded that the most stable complex contained 2 Ce(IV) ions per 3 GLU ions under alkaline conditions. The formula proposed by these authors for Ce(IV)-GLU complexes formed at pH 11 was $Ce_2(H_4GLU)_3(OH)_{11}^{6-}$. MACAROVICI & CZEGLEDI (1964) precipitated Th(IV)-GLU solids under acid and alkaline conditions with Th(IV):GLU ratios of 0.5 and 0.33. They found that Th(IV) forms a 1:1 complex with GLU above pH 9 and proposed a structure in which GLU coordinates with Th(IV) via 2 hydroxyl groups to form a bidentate complex $Th(OH)_3{\cdot}H_2GLU{\cdot}4H_2O^-$. The authors also presented evidence for the formation of Th(IV)-GLU polymers with a Th(IV):ligand ratio of 3:4 above pH 11. Note that these experiments were performed at high Th(IV) and GLU concentrations and only Th(IV)-GLU precipitates were analysed.

WIELAND et al. (1998) and (WIELAND et al., 2002) studied the complexation of Th(IV) with ISA via batch sorption experiments on sulphate-resisting Portland cement in ACW at pH 13.3. The authors suggest the formation of a 1:2 complex between Th(IV) and ISA.

VERCAMMEN (2000), VERCAMMEN et al. (2000) and VERCAMMEN et al. (2001) studied the formation of Th(IV)-ISA complexes in solution between pH 12.8 and 13.3 using high performance ion exchange chromatography and batch sorption experiments. These authors showed that, under alkaline conditions and in the absence of Ca, a 1:1 Th(IV)-ISA complex is formed causing the release of 4 protons. In the presence of Ca, however, Th(IV) coordinates with 2 ISA ligands and 1 or 2 Ca ions[2] causing the release of 4 protons (2 protons per ISA ligand). These observations confirm the 1:2 Th(IV)-ISA stoichiometry proposed by WIELAND et al. (1998, 2002). Note that both studies were carried out in ACW of similar chemical composition (Ca concentration ~ 1.6 mM).

---

[2] VERCAMMEN (2000) and VERCAMMEN et al. (2001) found evidence for a 1:2:2 Th(IV):ISA:Ca complex from high performance anion exchange chromatography experiments. In contrast, results from batch sorption studies gave evidence for a 1:2:1 Th(IV):ISA:Ca complex. The author could not exclude either stoichiometry based upon her results.

The following discussion of Th(IV)-ISA and Th(IV)-GLU complexation in ACW is based upon the findings reported by WIELAND et al. (1998) and VERCAMMEN et al. (2001). It is assumed that Th(IV)-ISA-Ca complexes and Th(IV)-GLU-Ca complexes with a 1:2:1 stoichiometry are formed in ACW and that Th(IV)-ISA and Th(IV)-GLU complexes can be ignored under the given experimental conditions. The model with one Ca cation was chosen because it results from experiments similar to those presented in this study and it allows comparisons with the complexation constants reported by VERCAMMEN et al. (2001) to be made.

Thus, the following reaction scheme for Th(IV)-ISA and Th(IV)-GLU complex formation under ACW conditions is assumed:

$$Th^{4+} + nH_qL^- + rCa^{2+} + mH_2O \Leftrightarrow Th(OH)_m(Ca)_r(H_{q-p}L)_n^{4-m+2r-n(1+p)} + (m+np)H^+. \quad (5.12)$$

H_qL^- represents the organic ligands ISA or GLU. This scheme is proposed in analogy to the one used for Eu(III)-ISA and Eu(III)-GLU complexes (equation 5.3).

5.3.3.2 Determination of the Th(IV)-ISA complexation constant

According to VERCAMMEN et al. (2001), n, r, m and p in equation 5.12 take values of 2, 1, 0 and 4, respectively, in the case of ISA. Thus, equation 5.12 can be simplified to:

$$Th^{4+} + 2H_qL^- + Ca^{2+} \Leftrightarrow Th(H_{q-4}L)_2Ca^0 + 4H^+ \quad , \quad (5.13)$$

The structure of ISA contains 4 hydroxyl groups, q=4. With this, equation 5.13 can be rewritten:

$$Th^{4+} + 2H_4ISA^- + Ca^{2+} \Leftrightarrow Th(H_2ISA)_2Ca^0 + 4H^+ \quad . \quad (5.14)$$

The effect of ISA on Th(IV) sorption can be expressed as follows:

$$R_d = R_d^0 \cdot \left(\frac{A}{A + \frac{\beta_{ThISA} \cdot \left[H_4ISA^-\right]^2 \left[Ca^{2+}\right]}{\left[H^+\right]^4}} \right) , \qquad (5.15)$$

with β_{ThISA} as the stability constant of the complex $Th(H_2ISA)_2Ca^0$. A denotes the side-reaction coefficient.

Assuming that the solution composition is constant, i.e. [Ca] and $[H^+]$ are constant, that the sorption of ISA on Merck calcite is negligible, and that the equilibrium ligand concentration equals the total ligand concentration ($[Th]_{tot} <<< [H_4L^-]_{tot}$), equation 5.15 can be simplified to:

$$R_d = \frac{R_d^0}{1 + C_{ThISA} \cdot \left([H_4ISA^-]_{tot}\right)^2} . \qquad (5.16)$$

in which C_{ThISA} is given by:

$$C_{ThISA} = \frac{\beta_{ThISA} \cdot \left[Ca^{2+}\right]}{\left[H^+\right]^4 \cdot A} . \qquad (5.17)$$

The data in Figure 18 were fitted using a R_d^0 value of $(3\pm2)\cdot10^4$ L kg^{-1} (solid lines). This value was taken from the experimental data shown in Figure 13a. The fit to the experimental data is good, indicating that the assumption of a 1:2 stoichiometry for the Th(IV)-ISA complex is justified. The constant C_{ThISA}, obtained for the Th(IV)-ISA complex was determined to be $(2.7\pm1.4)\cdot10^9$ M^{-2}. This value can then be used to estimate a conditional complexation constant (equation 5.17). The free Ca^{2+} concentration was calculated to be $7.1\cdot10^{-4}$ M (section 5.1.1). The side reaction coefficient, A, was estimated to be $7.26\cdot10^{32}$ considering $Th(OH)_4$ as the only relevant Th(IV) complex in ACW ($\log K^{0.3}_{Th(OH)_4} = 34.9$).

With this, the conditional complexation constant for the Th(IV)-ISA complex (I = 0.3) can be calculated. The value amounts to:

$\beta^{0.3}_{ThISA} = (4\pm2)\cdot10^{-8}$, or $\log\beta^{0.3}_{ThISA} = (-7.4\pm0.3)$,

which corresponds to

$\beta^{0}_{ThISA} = (9\pm5)\cdot10^{-6}$, or $\log\beta^{0}_{ThISA} = (-5.0\pm0.3)$,

at zero ionic strength.

VERCAMMEN et al. (2001) reported a value for $\log\beta^{0.3}_{ThISA}$ of -3.6±0.2 which was derived from sorption tests on a Biorad 50W-X2 resin converted to the Na^+ form and on feldspar and from high performance anion-exchange chromatography studies in the pH range between 10.7 and 13.3. Note that these authors used a different hydrolysis constant for $Th(OH)_4$: at I=0.3, log $\beta_{Th(OH)4}$ was 39.44 compared to 34.9 in the present work. Furthermore, the total Ca concentration in the experiments of VERCAMMEN et al. (2001) was $3.5\cdot10^{-4}$ M compare to $1.6\cdot10^{-3}$ M in the present study. Recalculation of the complexation constant of VERCAMMEN et al. (2001) using the hydrolysis constant for $Th(OH)_4$ reported by HUMMEL et al. (2000) and taking into account a lower total Ca concentration, yields $\log\beta^{0.3}_{ThISA} = -7.4\pm0.1$. Thus, the complexation constant for the Th(IV)-ISA complex determined in the present study agrees very well with the value recalculated from the data reported by VERCAMMEN et al. (2001) .

5.3.3.3 Determination of the Th(IV)-GLU-Ca complexation constant

Because ISA and GLU belong to the same group of polyhydroxy ligands, it is assumed that the same reaction scheme can be adopted. Hence, the following equation is proposed for Th(IV)-GLU complexation:

$$Th^{4+} + 2H_5GLU^{-} + Ca^{2+} \Leftrightarrow Th(H_3ISA)_2Ca^{0} + 4H^{+} \qquad (5.18)$$

The effect of increasing GLU concentrations in solution on the sorption value can be expressed by:

$$R_d = R_d^0 \cdot \left(\frac{A}{A + \frac{\beta_{ThGLU} \cdot [H_5GLU]^2 [Ca^{2+}]}{[H^+]^4}} \right) , \qquad (5.19)$$

with β_{ThGLU} as the stability constant of the complex $Th(H_2GLU)_2Ca^0$.

The proton concentration, $[H^+]$, the free Ca concentration, $[Ca^{2+}]$, and the A term are constant. Furthermore, the free ligand concentration, $[H_5GLU^-]$, is replaced by the total ligand concentration, $[H_5GLU^-]_{tot}$. On these assumptions, equation 5.19 can be simplified to:

$$R_d = \frac{R_d^0}{1 + C_{ThGLU} \cdot \left([H_5GLU^-]_{tot}\right)^2} \quad , \tag{5.20}$$

in which C_{ThGLU} is given by:

$$C_{ThGLU} = \frac{\beta_{ThGLU} \cdot \left[Ca^{2+}\right]}{\left[H^+\right]^4 \cdot A} \quad . \tag{5.21}$$

The sorption data displayed in Figure 19 were fitted with a R_d^0 value of $(3\pm2)\cdot10^4$ L kg^{-1}. Figure 19 reveals that the assumption of a 1:2 stoichiometry for the Th(IV)-GLU complex holds. The constant C_{ThGLU} was determined to be $(2.1\pm0.5)\cdot10^{12}$ M^{-2}. This value can be used to estimate a conditional complexation constant assuming a free Ca^{2+} concentration of $7.1\cdot10^{-4}$ M and a value for the A term of $4.81\cdot10^{32}$:

$\beta^{0.3}_{ThGLU} = (3.02\pm0.06)\cdot10^{-5}$, or $\log\beta^{0.3}_{ThGLU} = (-4.52\pm0.01)$.

This value was extrapolated to zero ionic strength by means of the Davies equation:

$\beta^{0}_{ThGLU} = (7.2\pm0.2)\cdot10^{-3}$, or $\log\beta^{0}_{ThGLU} = (-2.14\pm0.01)$.

5.3.4 The effect of ISA and GLU on Eu(III) and Th(IV) speciation in ACW

The complexation constants obtained in this study were used to calculate the effect of ISA and GLU on the speciation of Eu(III) and Th(IV) under conditions relevant to the disturbed zone of a cementitious repository.

The calculations were based on a series of assumptions:

1. The total radionuclide concentration:
   The free Eu(III) and Th(IV) concentrations in solution were fixed by the solubilities of their relevant oxides, i.e., $Eu(OH)_3$(cr) (log K_s=14.9 at I=0) and ThO_2(s) (log K_s= 9.9 at I=0). These solid phases were chosen because their calculated solubilities corresponded well with the experimental results (section 5.1.3). Note that, in contrast to the present calculations, the radionuclide concentrations in the pore water of a repository environment are expected to be controlled by the radionuclide inventory and by retardation processes such as sorption on cement and the host rock. Thus, the total Eu(III) and Th(IV) concentration obtained from the calculations are not relevant to repository conditions. Nevertheless, the speciation calculations show under which conditions ISA and GLU have an influence on Eu(III) and Th(IV) speciation in cement pore waters.

2. The pore water composition:
   The cement pore water leaving the repository is expected to be in equilibrium with the portlandite present in the cement matrix. In the alkaline disturbed zone around the repository, however, no portlandite is available. In this zone Ca bearing phases in the host rock will control the Ca concentration. To simplify the speciation calculations, it was assumed that the Ca and CO_3^{2-} concentrations are controlled by the dissolution of calcite. The Na and K concentrations were assumed to correspond to their concentrations in cement pore water.

3. The pH:
   The pore water leaving the repository during the initial few thousand years after closure is expected to have a pH of approximately 13.3. Due to the buffering capacity of the host rock, the pH of the pore water will drop with time and with increasing distance to the repository until the pH equals the equilibrium pH of the host rock. For the speciation calculations, the pH was fixed at 13.3 to simulate the situation in a pore water leaving the repository. Additional calculations were made to simulate the effect of the pH on the speciation. For this, the pH range was varied between 9.0 and 13.3.

4. The ligand concentration:
   The ISA and GLU concentrations in solution were varied between two limits: The upper limit was fixed at the highest possible ligand concentration in a cement pore water at pH 13.3. This concentration is defined by the solubilities of $Ca(ISA)_2(s)$ and $Ca(GLU)_2(s)$, i.e., approximately 0.05 M and 1 M, respectively. The lower limit was fixed as follows: Taking into account realistic numbers for the amounts of ISA and GLU present in the radioactive waste and the cement, and taking into account retardation processes such as sorption, the maximal concentration of ISA and GLU are expected to be 10^{-5} M and 10^{-7} M, respectively (GLAUS, pers. comm.). Therefore the minimum concentration in the speciation calculations was fixed at 10^{-7} M.

5.3.4.1 Effect of the ligand concentration

The results of the speciation calculations under conditions relevant to cement systems are shown in

Figure 20 and Figure 21 for Eu(III) and in Figure 22 and Figure 23 for Th(IV) . The thermodynamic complexation constants for ISA and GLU complexes with Eu(III) and Th(IV) are summarised in Table 12 and Table 13.

Figure 20 and Figure 21 show that Eu(III)–ISA complexes dominate above total ISA concentrations of $4 \cdot 10^{-6}$ M whereas Eu(III)–GLU complexes dominate over the whole GLU concentration range.

Th(IV)–ISA complexes are dominant above a total ISA concentration of ~$3 \cdot 10^{-}$M and Th(IV)–GLU complexes above a total GLU concentration of 10^{-6} M.

VAN LOON & GLAUS (1998) estimated the ISA concentration in the pore water of a cementitious repository. They found that the free ISA concentration in the pore water of that compartment of the repository, which contains large amounts of cellulose, is in the order of 10^{-5} M. Assuming that this pore water leaves the repository as such, the ISA concentration is expected to to take a similar value in the pore water of an altered near field. This is a conservative assumption because the cement pore water leaving this compartment of the repository still has to pass the cavern backfill and, depending on the flow path, even other compartments of the repository. Thus, the ISA concentration is further reduced

due to sorption on cementitious materials outside the waste matrix before arriving in the altered far-field.

At concentrations of 10^{-5} M, the dominant Eu(III) species are the Eu(III)-ISA complex and the $Eu(OH)_4^-$ complex. In the case of Th(IV), the dominating species at an ISA concentration of 10^{-5} M is $Th(OH)_4$. The data in Figure 16 and Figure 18 show that an ISA concentration of 10^{-5} M reduces the R_d value for Eu(III) by a factor of 3. However, at this concentration level, the R_d value for Th(IV) is not significantly reduced.

The GLU concentration in the cement pore water of a cementitious repository was estimated to be ≤ 10^{-7} M (GLAUS, pers. comm.). Assuming that this cement pore water leaves the repository as such, the GLU concentration is expected to take a similar value in the altered far-field pore water. Such GLU concentrations are beyond the region where $Th(GLU)_2Ca$ complex dominate Th(IV) speciation. The Eu(III) speciation however is dominated by the Eu(III)-GLU complex. Furthermore, Figure 17 and Figure 19 show that a GLU concentration of 10^{-7} M reduces the Eu(III) R_d value by a factor of 5. However, the R_d value for Th(IV) is not significantly reduced.

5.3.4.2 Effect of pH

The effect of pH is shown in Figure 24 to Figure 27. In the case of Eu(III), the influence of ISA and GLU complexes on speciation increases with increasing pH. For $[ISA]_{tot} = 10^{-5}$ M and $[GLU]_{tot} = 10^{-7}$ M, the concentrations of the Eu(III)–ISA and Eu(III)-GLU species are slightly higher than the $Eu(OH)_4^-$ concentration.

In the case of Th(IV), the concentrations of ISA and GLU complexes are independent of pH. For $[ISA]_{tot} = 10^{-5}$ M and $[GLU]_{tot} = 10^{-7}$ M, the concentrations of ISA and GLU complexes are always below the $Th(OH)_4$ concentration.

From these calculations we infer that

i) At maximum GLU and ISA concentrations in a disturbed far-field, i.e., 10^{-5} M for ISA and 10^{-7} M for GLU, Eu(III)-ISA and Eu(III)-GLU complexes are important species in the pore water. However, their effect on the Eu(III) sorption on calcite is minor, giving rise to a reduction of the R_d value only by a factor of 3 to 5.

ii) the maximum GLU and ISA concentrations in a disturbed far-field only slightly change Th(IV) speciation in ACW and, thus, Th(IV)-ISA and Th(IV)-GLU complexes have no influence on the retention of Th(IV) by calcite.

Table 12: Overview of the thermodynamic complexation constants for Eu(III)-ISA and Eu(III)-GLU complexes.

Reaction	$\log\beta$ (I=0)	$\log\beta$ (I=0.3)
$Eu^{3+} + H_4ISA^- \Leftrightarrow EuISA^{2-} + 4H^+$	-31.1±0.2	-31.4±0.2
$Eu^{3+} + H_5GLU^- \Leftrightarrow EuHGLU^{2-} + 4H^+$	-28.7±0.1	-29.0±0.1

Table 13: Overview of the thermodynamic complexation constants for Th(IV)-ISA and Th(IV)-GLU complexes.

Reaction	$\log\beta$ (I=0)	$\log\beta$ (I=0.3)
$Th^{4+} + 2H_4ISA^- + Ca^{2+} \Leftrightarrow Th(H_2ISA)_2\,Ca^0 + 4H^+$	-5.0±0.3	-7.4±0.3
$Th^{4+} + 2H_5GLU^- + Ca^{2+} \Leftrightarrow Th(H_3GLU)_2\,Ca^0 + 4H^+$	-2.14±0.01	-4.52±0.01

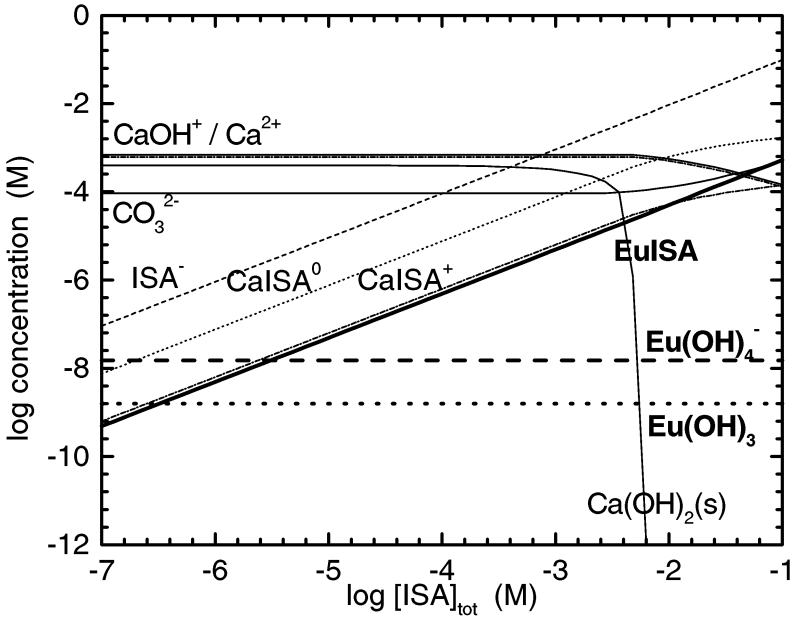

Figure 20: Eu(III) speciation in ACW at pH 13.3 as a function of the total ISA concentration in solution. The Ca concentration in solution is controlled by calcite.

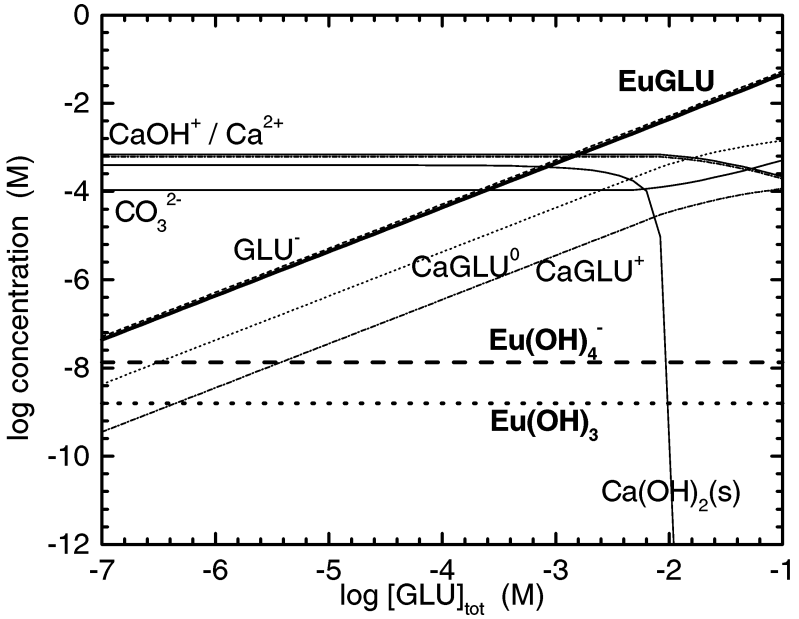

Figure 21: Eu(III) speciation in ACW at pH 13.3 as a function of the total GLU concentration in solution. The Ca concentration in solution is controlled by calcite.

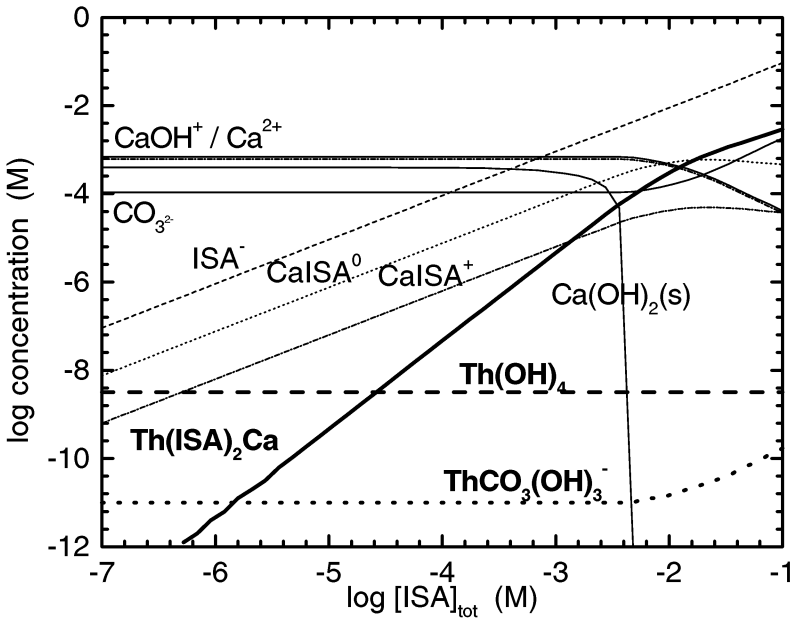

Figure 22: Th(IV) speciation in ACW at pH 13.3 as a function of the total ISA concentration in solution. The Ca concentration in solution is controlled by calcite.

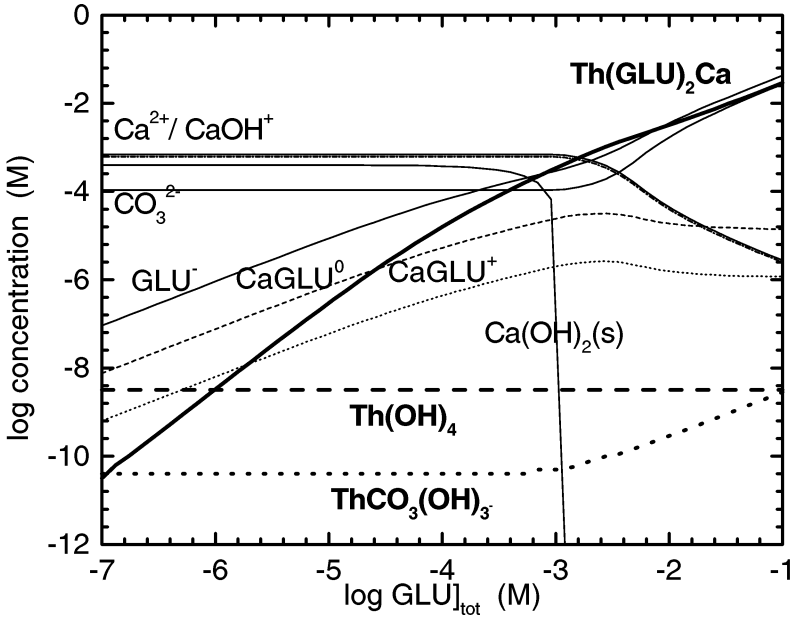

Figure 23: Th(IV) speciation in ACW at pH 13.3 as a function of the total GLU concentration in solution. The Ca concentration in solution is controlled by calcite.

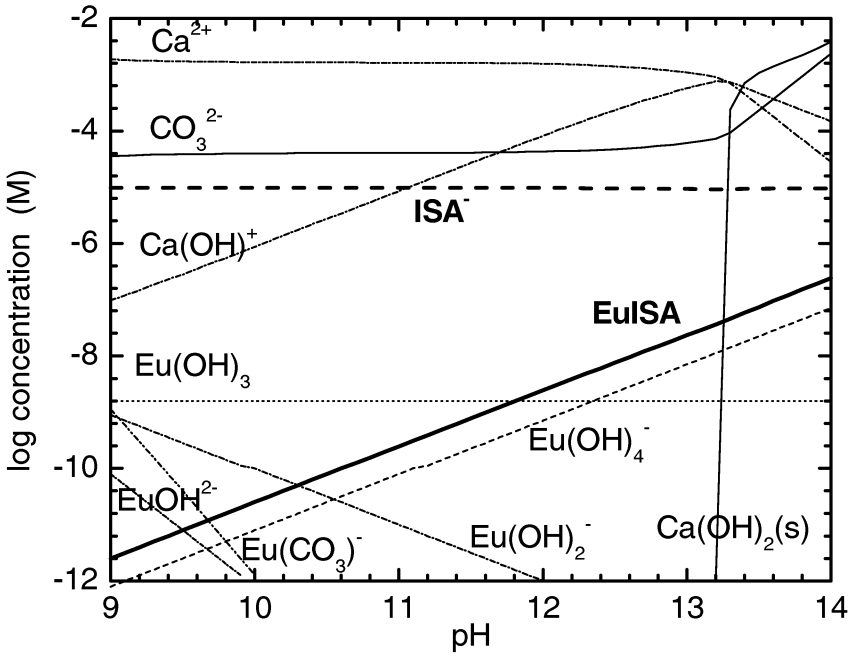

Figure 24: Eu(III) speciation as a function of pH in the presence of 10^{-5} M ISA. The Ca concentration in solution is controlled by calcite.

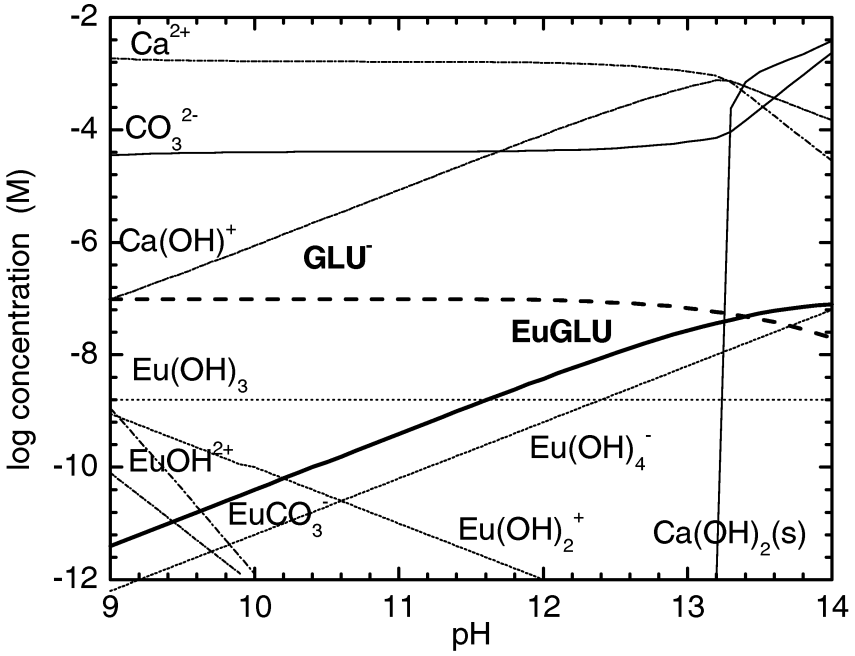

Figure 25: Eu(III) speciation as a function of pH in the presence of 10^{-7} M GLU. The Ca concentration in solution is controlled by calcite.

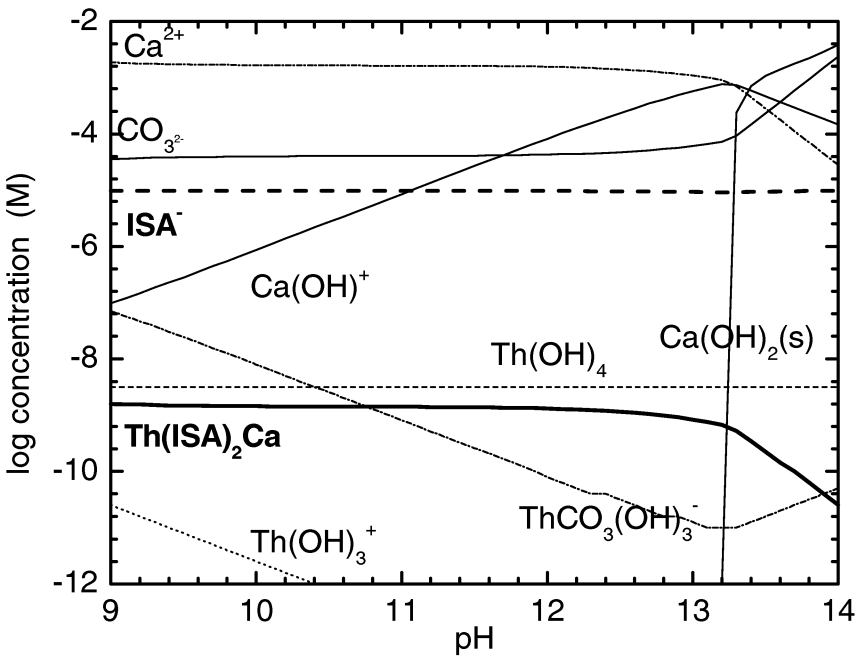

Figure 26: Th(IV) speciation as a function of pH in the presence of 10^{-5} M ISA. The Ca concentration in solution is controlled by calcite.

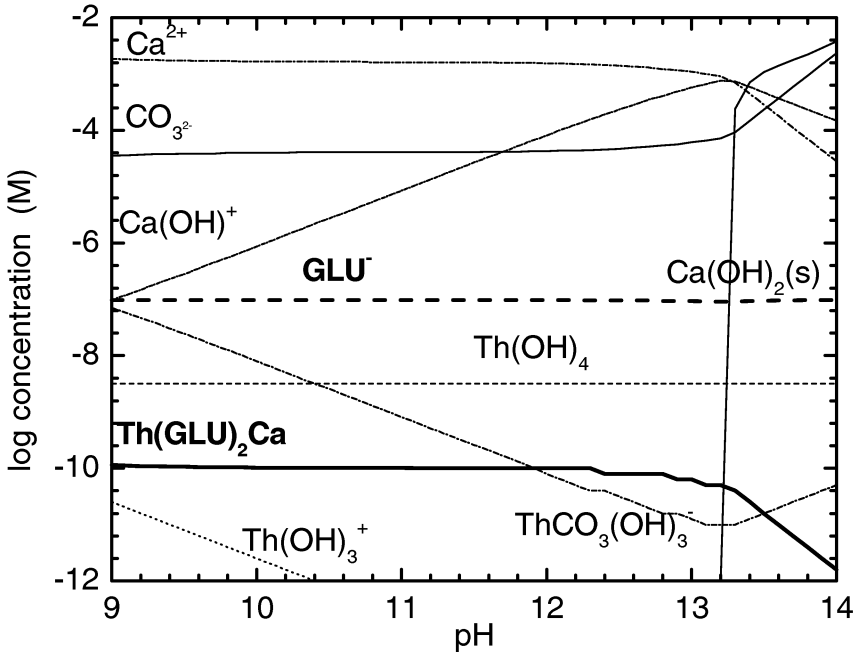

Figure 27: Th(IV) speciation as a function of pH in the presence of 10^{-7} M GLU. The Ca concentration in solution is controlled by calcite.

6. CONCLUSIONS

The study presented in this report has focused on three topics: 1) The sorption behaviour of Eu(III) and Th(IV) on Merck calcite under ACW conditions at a pH of 13.3, 2) the quantification of the effects of ISA and GLU on Eu(III) and Th(IV) sorption behaviour under ACW conditions, and 3) an assessment of the relevance of Eu(III) and Th(IV) complexation with ISA and GLU under estimated pore water conditions.

The sorption values for both elements under ACW conditions were found to be very high, i.e., in the range between 10^4 and 10^6 L kg^{-1} depending on the experimental conditions. The results indicate that the uptake of trace concentrations of Th(IV) by Merck calcite is consistent with an adsorption process. The data for Eu(III), however, cannot be interpreted in terms of an adsorption process. At the present time, solid solution formation with calcite combined with a variable calcite recrystallisation rate is proposed to explain the experimental data. A definitive answer requires significant additional experimental effort. The application of surface analysis techniques, e.g., X-ray absorption spectroscopy, could lead to a mechanistic understanding of Eu(III) uptake by calcite under alkaline conditions.

The experimental work on the effect of ISA and GLU on the Eu(III) uptake by calcite shows that R_d values for Eu(III) decrease strongly at ISA concentrations above 10^{-5} M and at GLU concentrations above 10^{-7} M. The results for Th(IV) show that the uptake of Th(IV) decreases at ISA concentrations above $2 \cdot 10^{-5}$ M and GLU concentrations above 10^{-6} M. Complexation constants for Eu(III)-ISA and Th(IV)-ISA-Ca complexes were estimated to be $\log\beta^0_{EuISA} = -31.1 \pm 0.2$ and $\log\beta^0_{ThISA} = -5.0 \pm 0.3$. These values agree well with those reported by VERCAMMEN (2000) and VERCAMMEN et al. (2001). Complexation constants for Eu(III)-GLU and Th(IV)-GLU-Ca complexes were estimated to be $\log\beta^0_{EuGLU} = -28.7 \pm 0.1$ and $\log\beta^0_{ThGLU} = -2.14 \pm 0.01$. Both cations form stronger complexes with GLU than with ISA. The complexation constants for the Eu(III)-GLU and Th(IV)-GLU complexes are 2 to 3 orders of magnitude larger than the corresponding values for the ISA complexes.

The impact of ISA and GLU on Eu(III) and Th(IV) complexation in the near-field and in the disturbed far-field of a repository can be assessed based on the available experimental data: The effect of both ligands on the uptake of Eu(III)

and Th(IV) by calcite is negligible at ISA and GLU concentrations in the pore waters, which are relevant to Swiss repository conditions, i.e., 10^{-5} M ISA and 10^{-7} M GLU.

7. ACKNOWLEDGEMENTS

The authors would like to thank R. Keil (PSI), Dr. C Moor (EMPA) and Dr. M. Glaus (PSI) for their assistance in the analytical work. Drs. E. Curti and M. Glaus are acknowledged for the many helpful discussions and suggestions, which helped to improve the quality of the report. Drs. J. Hadermann, I. Hagenlocher, P. Wersin and Prof. A. Maes are gratefully acknowledged for their careful review of the manuscript and their helpful comments. The authors would like to thank the National Cooperative for the Disposal of Radioactive Waste (Nagra) for partially financing this project.

8. REFERENCES

ADLER, M., MÄDER, U., & WABER, N. (1999): High-pH Alteration of Argilaceous Rocks: An Experimental Study. Schweiz. Mineral. Petrogr. Mitt. 79, 445-454.

BASTON, G.M.N., BERRY, J.A., BOND, K.A., BROWNSWORD, M. & LINKLATER, C.M. (1992): Effects of Organic Degradation Products on the Sorption of Actinides. Radiochim. Acta 52/53, 349-356.

BERNER, U. (1990): A Thermodynamic Description of the Evolution of Pore Water Chemistry and Uranium Speciation during the Degradation of Cement. PSI-Bericht 62, Paul Scherrer Institut, Villigen, Switzerland, and Nagra Technical Report NTB 90-12, Nagra, Wettingen, Switzerland.

BERNER, U. (1998): Geochemical Modelling of Repository Systems: Limitations of the Thermodynamic Approach. Radiochim. Acta 82, 423-428.

BERRY, J.A., BOND, K.A., FERGUSON, D.R. & PILKINGTON, N.J. (1991): Experimental Studies of the Effects of Organic Materials on the Sorption of Uranium and Plutonium. Radiochim. Acta 52/53, 201 - 209.

BRADBURY, M.H. & SAROTT, F.H. (1994): Sorption Databases for the Cementitious Near-Field of a L/ILW Repository for Performance Assessment. PSI Bericht 95-06, Paul Scherrer Institut, Villigen, Switzerland, and Nagra Technical Report NTB 93-08, Nagra, Wettingen, Switzerland.

BRADBURY, M.H. & BAEYENS, B. (1997a): Far-Field Sorption Databases for Performance Assessment of a L/ILW Repository in an Undisturbed Palfris Marl Host Rock. PSI Bericht 97-15, Paul Scherrer Institut, Villigen, Switzerland, and Nagra Technical Report NTB 96-05, Nagra, Wettingen, Switzerland.

BRADBURY, M.H. & BAEYENS, B. (1997b): Far-Field Sorption Databases for Performance Assessment of a L/ILW Repository in an Disturbed/Altered Palfris Marl Host Rock. PSI Bericht 97-16, Paul Scherrer Institut, Villigen, Switzerland, and Nagra Technical Report NTB 96-06, Nagra, Wettingen, Switzerland.

BRADBURY, M.H. & VAN LOON, L.R. (1998): Cementitious Near-Field Sorption Databases for Performance Assessment of a L/ILW Repository in a Palfris Marl Host Rock. CEM-94: UPDATE I, June 1997. PSI Bericht 98-01, Paul Scherrer Institut, Villigen, Switzerland, and Nagra Technical Report NTB 96-04, Nagra, Wettingen, Switzerland.

CRAWFORD, M.B. & SAVAGE, D. (1994): The Effects of Alkaline Plume Migration from a Cementitious Repository in Crystalline and Marl Host Rocks. Technical Report, WE/93/20C, Britisch Geological Survey, Nottingham, UK.

CURRIE, L.A. (1968): Limits for Detection and Quantitative Determination. Anal. Chem. 40(3), 586-593.

DAVIS, J.A., FULLER, C.C., & COOK, A.D. (1987): A Model for Trace Metal Sorption Processes at the Calcite Surface: Adsorption of Cd^{2+} and Subsequent Solid Solution Formation. Geochim. Cosmochim. Acta 51, 1477 - 1490.

DAVIS, J. & KENT, D.B. (1990): Surface Complexation Modelling in Aqueous Geochemistry. In: M. F. Hochella and A. F. White (eds.): Mineral-Water Interface Geochemistry, Mineral Society of America, Washington, USA.

DZOMBAK, D.A. & MOREL, F.M. (1986): Sorption of Cadmium on Hydrous Ferric Oxide at High Sorbate/Sorbent Ratios: Equilibrium Kinetics and Modelling. J. Colloid Interface Sci. 112, 588-598.

DZOMBAK, D.A. & MOREL, F.M. (1990): Surface Complexation Modeling. John Wiley and Sons, New York, USA.

EHMANN, W.D. & VANCE, D.E. (1991): Radiochemistry and Nuclear Methods of Analysis. John Wiley & Sons, New York, USA.

GANS, P. (1992): Data Fitting in the Chemical Sciences by the Method of Least Squares. John Wiley &Sons, New York, USA.

GILMORE, G. & HEMINGWAY, J. (1996): Practical Gamma-Ray Spectrometry. Wiley & Sons Inc. New York, USA.

GLAUS, M.A., VAN LOON, L.R., ACHATZ, S., CHODURA, A. & FISCHER, K. (1999): Degradation of Cellulosic Materials under the Alkaline Conditions of a Cementitious Repository for Low and Intermediate Level Waste. Part I: Identification of Degradation Products. Anal. Chim. Acta 398, 111-122.

GORGEON, L. (1994): Contribution à la Modélisation Physico-chimique de la Retention de Radioéléments à vie Longue par des Materiaux Argileux. PhD Thesis, Université Paris 6, Paris, France.

HUMMEL, W., BERNER, U., CURTI, E., PEARSON, F.J. & THOENEN, T. (2002): Nagra/PSI Chemical Thermodynamic Data Base 01/01. Nagra Technical report NTB 02-06, Nagra, Wettingen, Switzerland and Universal Publishers/uPublish.com, Parkland, Florida, in press.

MACAROVICI, C.G. & CZEGLEDI, L. (1964): Sur L'Obtention des Combinaisons du Thorium avec les Acides D-Gluconique et D-Saccharique. Rev. Roum. Chim. 9, 411 - 424.

McBRIDE, M.B. (1994): Environmental Chemistry of Soils. Oxford University Press, Oxford, UK.

NAGRA (1992): Nukleare Entsorgung Schweiz - Konzept und Realisierungsplan. Nagra Technical Report NTB 92-02, Nagra, Wettingen, Switzerland.

NAGRA (1993): Beurteilung der Langzeitsicherheit des Endlagers SMA am Standort Wellenberg (Gemeinde Wolfenschiessen, NW), Nagra Technical Report NTB 93-26, Nagra, Wettingen, Switzerland.

NAGRA (1994): Bericht zur Langzeitsicherheit des Endlagers SMA am Standort Wellenberg (Gemeinde Wolfenschiessen, NW), Nagra Technical Report NTB 94-06, Nagra, Wettingen, Switzerland.

NEALL, F.B. (1994): Modelling of the Near Field Chemistry of the SMA Repository at the Wellenberg Site. PSI Bericht 94-18, Paul Scherrer Institut, Villigen, Switzerland, and Nagra Technical Report NTB 94-03, Nagra, Wettingen, Switzerland.

NORDEN, M. & ALLARD, B. (1994): The Influence of Cellulose and its Degradation Products on the Adsorption of Europium on Cement. In: M. Norden: The Complexation of Some Radionuclides with Natural Organics: Implications for Radioactive Waste Disposal. PhD. Thesis, University of Linköping, Linköping, Sweden.

PFINGSTEN, W. & SHIOTSUKI, M. (1998): Modelling a Cement Degradation Experiment by a Hydraulic Transport and Chemical Equilibrium Coupled Code. In: I. G. McKinley and C. McCombie (eds.): Scientific Basis for Nuclear Waste Management, Vol. XXI, pp. 805-812. Materials Research Society, Warrendale, PA, USA.

PFINGSTEN, W. (2001): Indications for Self-Sealing of a Cementitious L&ILW Repository. PSI Bericht 01-09, Paul Scherrer Institut, Villigen, Switzerland, and Nagra Technical Report NTB 01-05, Nagra, Wettingen, Switzerland.

PUIGDOMENECH, I. (1983): INPUT-SED-PREDOM : "Computer Programs Drawing Equilibrium Diagrams". Technical Report TRITA-OOK-3010, Royal Institute of Technology, Stockholm, Sweden.

RAMACHANDRAN, V.S. (1984): Concrete Admixtures Handbook. Noyes Publication, Park Ridge New Jersey, USA.

SAWYER, D.T. & AMBROSE, R.T. (1962): Cerium(IV) Gluconate Complexes. Inorg. Chem. 1(2), 296-303.

SCHUBERT, J. & LINDENBAUM, A. (1952): Stability of Alkaline Earth Organic Acid Complexes Measured by Ion Exchange. J. Am. Chem. Soc. 74, 3529 - 3532.

SCHWARZENBACH, R.P., GSCHWEND, P.M. & IMBODEN, D.M. (1993): Environmental Organic Chemistry. John Wiley & Sons, Inc., New York, USA.

SPOSITO, G. (1984): The Surface Chemistry of Soils. Oxford University Press, New York, USA.

SPOSITO, G. (1986): Distinguishing Adsorption from Surface Precipitation. In: J. A. Davis and K. F. Hayes (eds.): Geochemical Processes at Mineral Surfaces, pp. 217-228. American Chemical Society, Washington, USA.

SPOSITO, G. (1989): The Chemistry of Soils. Oxford University Press, New-York, USA.

STIPP, S.L.S., EGGLESTON, C.M. & NIELSEN, B.S. (1994): Calcite Surface Structure Observed at Microtopographic and Molecular Scales with Atomic Force Microscopy. Geochim. Cosmochim. Acta 58(14), 3023-3033.

STUMM, W. & MORGAN, J.J. (1996): Aquatic Chemistry. John Wiley & Sons, inc., New York, USA.

TITS, J., BAEYENS, B. & BRADBURY, M.H. (1996): The Influence of Organics on the Sorption of Americium on Far-Field Minerals at high pH. In: J. Birchley, R. Rösel, and R. Van Doesburg (eds.): PSI Annual Report 1995, Annex IV, Paul Scherrer Institut, Villigen, Switzerland.

TITS, J., BAEYENS, B. & BRADBURY, M.H. (1997): Sorption Behaviour of Americium on Calcite under Alkaline Conditions. The Influence of Organic Ligands. PSI Internal Report TM-44-97-11, Paul Scherrer Institut, Villigen, Switzerland.

VAN DUIN, M., PETERS, J.A., KIEBOOM, A.P.G. & VAN BEKKUM, H. (1989): A General Coordination-Ionization Scheme for Polyhydroxy Carboxylic Acids in Water. Recl. Trav. Chim. Pays-Bas 108, 57-60.

VAN LOON, L.R., GLAUS, M.A., STALLONE, S. & LAUBE, A. (1997): Sorption of Isosaccharinic Acid, a Cellulose Degradation Product, on Cement. Environ. Sci. Technol. 31(4), 1243-1245.

VAN LOON, L.R. & GLAUS, M.A. (1998): Experimental and Theoretical Studies on Alkaline Degradation of Cellulose and its Impact on the Sorption of Radionuclides. PSI Bericht 98-07 Paul Scherrer Institut, Villigen, Switzerland, and Nagra Technical Report NTB 97-04, Nagra, Wettingen, Switzerland.

VAN LOON, L.R., GLAUS, M.A. & VERCAMMEN, K. (1999): Solubility Products of Calcium Isosaccharinate and Calcium Gluconate. Acta Chem. Scand. 53, 235-240.

VERCAMMEN, K., GLAUS, M.A. & VAN LOON, L.R. (1999): Complexation of Calcium by α-Isosaccharinic Acid under Alkaline Conditions. Acta Chem. Scan. 53, 241-246.

VERCAMMEN, K., GLAUS, M.A. & VAN LOON, L.R. (2000): Evidence for the Existence of Complexes between Th(IV) and α-Isosaccharinic Acid under Alkaline Conditions. Radiochim. Acta 87, 221-224.

VERCAMMEN, K. (2000): Complexation of Calcium, Thorium and Europium by α-Isosaccharinic Acid under Alkaline Conditions. Ph.D. Thesis, Swiss Federal Institute of Technology, Zürich, Switzerland.

VERCAMMEN, K., GLAUS, M.A. & VAN LOON, L.R. (2001): The Complexation of Th(IV) and Eu(III) with α-Isosaccharinic Acid under Alkaline Conditions. Radiochim. Acta 89, 393-401.

WERSIN, P., CHARLET, L., KARTHEIN, R. & STUMM, W. (1989): From Adsorption to Precipitation: Sorption of Mn^{2+} on $FeCO_3$(s). Geochim. Cosmochim. Acta 53, 2787-2796.

WIELAND, E., TITS, J., SPIELER, P. & DOBLER, J.P. (1998): Interaction of Eu(III) and Th(IV) with Sulphate-Resisting Portland Cement. Mat. Res. Soc. Symp. Proc. 506, 573 - 578.

WIELAND, E. & VAN LOON, L. (2002): Near-Field Sorption Database for Performance Assessment of a LL-ILW Repository in Opalinus Clay and Crystalline Host Rock. PSI Bericht, Paul Scherrer Institut, Villigen, Switzerland (in Review).

WIELAND, E., TITS, J., DOBLER, J.P., & SPIELER, P. (2002): The Effect of α-Isosaccharinic Acid on the Stability of and Th(IV) Uptake by Hardened Cement Paste. Radiochim. Acta, In press.

ZACHARA, J.M., KITTRICK, J.A. & HARSH, J.B. (1988): The Mechanism of Zn^{2+} Adsorption on Calc0ite. Geochim. Cosmochim. Acta 52, 2281-2291.

ZHONG, S. & MUCCI, A. (1995): Partitioning of Rare Earth Elements (REEs) between Calcite and Seawater Solutions at 25°C and 1 atm, and High Dissolved REE Concentrations. Geochim. Cosmochim. Acta 59(3), 443-453.

Appendix A: Experimental uncertainties and reproducibility

Sorption measurements are subject to several sources of uncertainties giving rise to an overall uncertainty on the sorption values. These uncertainties may be either random (non-systematic) or systematic. The latter category originates from, e.g., wrongly calibrated equipment, and arises due to a principal lack of theoretical comprehension of the process of measurement. Such uncertainties can only be detected by independent measurements and result in a systematic deviation between expected and measured values. Random uncertainties on sorption measurements originate mainly from three sources: 1) the heterogeneity of the solid sample, 2) the manipulations of a sample (weighting procedures, dilutions…) and 3) the measurement of radioactive decay.

Uncertainty considerations require an estimate of the arithmetic mean and the standard deviation of n measurements. The arithmetic mean, $\overline{x}$, of a limited number of n observations taken from an infinite set of observations (population) $\{x_i\}$, I=1,2,…,n, is given by:

$$\overline{x} = \frac{1}{n}\sum_{i=1}^{n} x_i \quad . \tag{A.1}$$

The standard deviation σ_x of the measurements expresses how closely the data are clustered around the sample mean. σ_x is defined by

$$\sigma_x = \sqrt{\frac{1}{n-1}\sum_{i=1}^{n}(x_i - \overline{x})^2} \quad . \tag{A.2}$$

As it is impossible to find the true population mean μ from a limited number of measurements, the standard deviation of the mean, $\sigma_{\overline{x}}$ measures the quality of the mean $\overline{x}$, as an estimator of the population mean, μ. $\sigma_{\overline{x}}$ is given by:

$$\sigma_{\overline{x}} = \frac{\sigma_x}{\sqrt{n}} = \sqrt{\frac{1}{n(n-1)}\sum_{i=1}^{n}(x_i - \overline{x})^2} \quad . \tag{A.3}$$

For an increasing number of measurements, σ_x, does not change much, but $\sigma_{\overline{x}}$ slowly decreases.

With the help of the confidence interval of the measurements, *T,* where $T = t \cdot \sigma_x$, the quality of the data can be assessed[3]. The meaning of *T* is that *p* % of all measurements are located within the interval ($x \pm T$). The corresponding confidence interval $T_{\bar{x}}$ of the mean, $\bar{x}$, is given by

$$T_{\bar{x}} = \frac{T}{\sqrt{n}} = t \cdot \sigma_{\bar{x}} \quad . \tag{A.4}$$

With the Student's factor, t, it is considered that the standard deviation of the mean becomes larger due to a statistical insufficient number of single measurements.

To estimate the uncertainty (the confidence interval) on the final results, e.g. R_d values and equilibrium concentrations, the uncertainty on a function *f*, a non-linear combination of physical quantities ($\bar{x}_i$), which are subject to uncertainties, has to be evaluated (GANS, 1992). To calculate the uncertainty on *f,* the assumption is made that the confidence intervals, $T_{\bar{x}_i}$, are small compared to the value of $\bar{x}_i$. The reason for this assumption is that the function f has to be linearized using a truncated Taylor series and this truncation is only allowed for small uncertainties. Furthermore, it is assumed that all measured quantities are uncorrelated, so that the covariance term can be omitted. When these two assumptions are fulfilled the uncertainty on the function *f* can be calculated according to the following expression for the error propagation:

$$T_f(\bar{x}_1, \bar{x}_2, \bar{x}_3, \ldots, \bar{x}_N) \cong \sqrt{\sum_{i=1}^{N} \left(\frac{\partial f}{\partial \bar{x}_i} \right)^2 T_{\bar{x}_i}^2} \quad . \tag{A.5}$$

For some sorption tests presented here, R_d values were deduced from activity measurements of the supernatant solution (A_l in equation 2.6), which were close to the detection limit of the counting equipment. In other sorption tests, i.e., when the sorption was very weak, calculation of the R_d value was based on the subtraction of two values of similar magnitude (A_{susp} and A_l in equation 2.6). Both cases resulted in very large uncertainties. Therefore, a procedure is proposed in this study, which allows a critical assessment of the very high, and very low sorption values. This procedure consists of the definition of a

---

[3] *t* is the so-called Student's factor which is dependent on the degree of freedom (*n* - 1) and the statistical probability *p* [%].

maximum sorption value ($R_{d,max}$) and a minimum sorption value ($R_{d,min}$) in each experiment. The determination of $R_{d,max}$ and $R_{d,min}$ is based upon the experimental conditions in each experiment, i.e., total activity, background activity and S:L ratio.

Once the two limits are fixed, the uncertainties on measured R_d values lying in between these limits can be determined and are given as 95% confidence intervals. Calculation of $R_{d,max}$ and $R_{d,min}$ and the 95% confidence interval will be discussed in detail below.

A.1 Determination of the maximum sorption value, ($R_{d,max}$)

Radioactive decay is a statistically random process (EHMANN & VANCE, 1991; GILMORE & HEMINGWAY, 1996). The decay of a single atom cannot be predicted. Hence, each counting rate has a statistical error, which decreases with the number of counts measured. In most activity measurements this source of errors is negligible compared to the other sources of errors mentioned before because the measured number of counts is high. However, in the case of Eu(III) and Th(IV) sorption on solids under highly alkaline conditions, the remaining activity in solution after sorption can become so low that it is not significantly different from the background activity (noise level). The statistical error on the counts can then become significant.

The probability P(n), that in a sample of N atoms, n atoms will decay in time t, given that the true number of decays is μ, can be described by the Poisson distribution function (CURRIE, 1968; EHMANN & VANCE, 1991 ; GILMORE & HEMINGWAY, 1996):

$$P(n) = \frac{\mu^n}{n!} e^{-\mu} \quad . \tag{A.6}$$

The Poisson distribution can be applied in those cases where the probability of a single event is very small compared to the total number of cases. This is true for most radioactive isotopes. Only isotopes with very short half-lives, are exceptions.

For a single decay measurement, the best estimate of μ is n, the measured number of decays in 1 L. Furthermore, it is a mathematical property of the Poisson distribution that the standard deviation, σ, may be estimated from μ.

These two properties of the Poisson distribution are summarised in the two following equations :

$$\mu = n \quad . \tag{A.7}$$

$$\sigma = [\mu]^{1/2} = (n)^{1/2} \quad \text{or} \quad \sigma^2 = n \quad . \tag{A.8}$$

In practice, the decay of a radionuclide is measured by a counting device which has a counting efficiency, ε. In the further course of the discussion it is assumed that ε is constant for all the measurements. Hence:

$$C = \varepsilon \cdot n \quad , \tag{A.9}$$

C: measured number of decays, expressed in counts L^{-1}.

Equations A.7 and A.8 can then be rewritten as:

$$\mu = C \quad , \tag{A.10}$$

$$\sigma = [\mu]^{1/2} = (C)^{1/2} \quad \text{or} \quad \sigma^2 = C \quad . \tag{A.11}$$

$R_{d,max}$ is determined by $C_{l,min}$, that is the lowest number of counts in the supernatant solution that can be measured. It is the minimum number of counts required to obtain a result with a relative uncertainty, α, which is below an a priori fixed value. Generally, α is allowed to be at maximum 10 %. This value of 10% is arbitrarily chosen, but is widely accepted in the literature (CURRIE, 1968; EHMANN & VANCE, 1991; GILMORE & HEMINGWAY, 1996). Thus, the relative uncertainty on the net number of counts, α, must meet the following condition:

$$\alpha = \frac{\sigma_1}{C_1} \leq 0.1 \quad , \tag{A.12}$$

C_l: measured net number of counts in the supernatant solution, i.e., the measured gross number of counts of sample X, minus the number of counts of blank B, expressed in counts L^{-1}.

σ_l: standard deviation on the measured net number of counts.

Note that α only accounts for the uncertainty originating from counting of the radioactive decay. It does not take into account uncertainties originating from sample manipulation or sample inhomogeneity.

In the following discussion C_l is expressed in counts per ml sample. The volume usually analysed in radioassays is 5 ml. Hence, the actually measured activities are 5 times higher.

The minimum net number of counts in solution, $C_{l,min}$, can be estimated using equation A.12:

$$C_{l,min} = \alpha_{l,min}^{-1} \cdot \sigma_{l,min} \text{ [counts ml}^{-1}\text{]} \quad . \tag{A.13}$$

$\sigma_{l,min}$: standard deviation of $C_{l,min}$,

$\alpha_{l,min}$: relative uncertainty of $C_{l.min}$.

With $\alpha_{l,min} = 0.1$, $C_{l.min}$ can be written as follows:

$$C_{l,min} = 10 \cdot \sigma_{l,min} \quad \text{[counts ml}^{-1}\text{]} \quad . \tag{A.14}$$

$C_{l,min}$ is obtained by subtracting the number of background counts, B [counts/ml], detected in time t, from X [counts ml^{-1}], which is the gross number of counts detected in time t.

$$C_{l,min} = X - B \qquad \text{[counts ml}^{-1}\text{]} \quad . \tag{A.15}$$

The variance of $C_{l,min}$, $(\sigma_{l,min})^2$ is then:

$$\sigma^2_{l,min} = \sigma^2_{(X-B)} = \sigma^2_X + \sigma^2_B \quad . \tag{A.16}$$

We only consider here the uncertainty originating from the random decay process. Hence, we can apply equation (A.11) to the right hand side of equation (A.16) resulting in the following equation:

$$\sigma_{l,min}{}^2 = X + B \quad , \tag{A.17}$$

Replacing "X" by "$C_{l,min}$ + B" (equation A.15) and combining equation A.17 with equation A.13, yields:

$$C_{l,min} = \left(\alpha_{l,min}\right)^{-1} \cdot \left(C_{l,min} + 2B\right)^{1/2} \text{[counts ml}^{-1}\text{]} \, . \tag{A.18}$$

The solution of this quadratic equation is:

$$C_{l,min} = \frac{1}{2(\alpha_{l,min})^2} \cdot \left(1 + \left(1 + 8(\alpha_{l,min})^2 B\right)^{1/2}\right) \text{ [counts ml}^{-1}\text{]} . \quad (A.19)$$

Substituting $\alpha_{l,min}$ by 0.1 gives:

$$C_{l,min} = 50 \cdot \left(1 + (1 + 0.08 \cdot B)^{1/2}\right) \quad \text{[counts ml}^{-1}\text{]} . \quad (A.20)$$

$C_{l,min}$ can be expressed in terms of a minimum measurable activity, $A_{l,min}$ determined for the time period t (counts per minute /ml or cpm ml^{-1}):

$$A_{l,min} = C_{l,min}/t \quad \text{[cpm ml}^{-1}\text{]} . \quad (A.21)$$

The following calculations for ^{152}Eu illustrate the importance of $C_{l,min}$ for an assessment of activity measurements and R_d values. All the data used in the following are based on measurements on 5 ml samples. As the background activity is not necessarily proportional to the sample volume, all the calculations will refer to 5 ml samples.

In general, the background activity is ~150 cpm/5ml. Thus, the value for the blank, B, amounts to 4500 counts/5ml for a measuring time t, of 30 minutes. Allowing a maximum uncertainty of 10%, $C_{l,min}$ takes a value of 1000 counts/5ml or, expressed per unit counting time, ~33.3 cpm/5ml. This means that, by accepting a relative uncertainty of 10% on the net counts and accepting a background of 150 cpm/5ml in 30 minutes counting time, activities below 183.3 cpm/5ml (background + $A_{l,min}$) must be rejected from a statistical point of view.

Based on the minimum net numbers of counts, a value for the maximum distribution ratio, $R_{d,max}$, that is, the highest distribution ratio which is measurable with a sufficient precision, can be given. This maximum distribution ratio, $R_{d,max}$, can be calculated as follows:

$$R_{d,max} = \frac{\left(A_{susp} - A_{l,min}\right)}{A_{l,min}} \cdot \frac{V}{m} \quad \text{[L kg}^{-1}\text{]} , \quad (A.22)$$

A_{susp}: total initial activity in the suspension taking part in the sorption reaction [cpmml^{-1}].

M: mass of solid [kg],

V: volume of solution [L].

In this study, $R_{d,\,max}$ was estimated for each sorption experiment.

Note that for constant A_{susp} and $A_{l,min}$, $R_{d,max}$ depends only on the S:L ratio (m/V).

A.2 Determination of the minimum sorption value ($R_{d,min}$)

The activity of sorbed tracer expressed in counts, C_s, is obtained by subtracting the number of counts in solution, C_l, from the total number of counts in the suspensions, C_T.

$$C_s = C_T - C_l \ . \ [\text{counts}] \ . \qquad (A.23)$$

When the sorption of a radionuclide is weak, C_T and C_l take similar values and, thus, the uncertainty on the difference, C_s (and therefore on the R_d), becomes very large.

The lowest measurable sorption value, $R_{d,min}$, can be deduced in a similar manner to the procedure described for $R_{d,max}$. For this, the minimum activity of sorbed tracer, $C_{s,min}$, required to deduce $R_{d,min}$ can be estimated as follows:

The relative uncertainty on the net number of counts "sorbed", is set to 10% at a maximum. The relative uncertainty, α, must meet the following condition:

$$\alpha = \frac{\sigma_s}{C_s} \leq 0.1 \quad . \qquad (A.24)$$

σ_s: standard deviation of C_s.

From equation A.24 the minimum net number of counts "sorbed", $C_{s,min}$ can be estimated:

$$C_{s,min} = \left(\alpha_{s,min}\right)^{-1} \cdot \sigma_{s,min} \, [\text{counts ml}^{-1}] \ . \qquad (A.25)$$

$\sigma_{s,min}$: standard deviation of $C_{s,min}$,

$\alpha_{s,min}$: relative uncertainty of $C_{s.min}$,

with $\alpha_{s,min} = 0.1$, $C_{s.min}$ can be written as:

$$C_{s,min} = 10 \cdot \sigma_{s,min} \quad [\text{counts ml}^{-1}] \ . \tag{A.26}$$

$C_{s,min}$ is obtained by subtracting the number of counts in supernatant solution (C_l) from the total input number of counts (C_T), taking into account the background counts:

$$C_{s,min} = (C_T - B) - (C_l - B) = C_T - C_l \ . \tag{A.27}$$

C_T: total number of counts taking part in the sorption reaction [counts ml^{-1}].

C_l: number of counts remaining in the supernatant solution after sorption [counts ml^{-1}].

B: number of counts measured in a blank [counts ml^{-1}].

The rules for arithmetic operations with standard deviations allow us to write the following expression:

$$\sigma_s = \sigma_{(T-l)} = \left(\sigma_T^2 + \sigma_l^2\right)^{1/2} \ , \tag{A.28}$$

σ_T: standard deviation on C_T,

σ_l: standard deviation on C_l.

Combining equation A.25 with equation A.27 and A.28 yields:

$$\left(C_T - C_l\right) = \left(\alpha_{s,min}\right)^{-1} \cdot \left(\sigma_T^2 + \sigma_l^2\right)^{1/2} \ . \tag{A.29}$$

When sorption is weak, both C_T and C_l are large. Close examination of the experimental data showed that uncertainties on C_T and C_l, originating from the random decay process under such conditions, are smaller than 1%, or, conservatively, $\sigma_T = 0.01 \cdot C_T$ and $\sigma_{sol} = 0.01 \cdot C_{sol}$. Equation A.29 can then be rewritten as follows:

$$C_T - C_l = \left(\alpha_{s,min}\right)^{-1} \cdot \left((0.01 \cdot C_T)^2 + (0.01 \cdot C_l)^2\right)^{1/2} \ . \tag{A.30}$$

The solution of this quadratic equation using $\alpha_{s,min} = 0.1$ gives:

$$C_l = 0.87 \cdot C_T \ , \tag{A.31}$$

or:

$$C_{s,min} = C_T - C_I = 0.13 \cdot C_T \quad . \qquad (A.32)$$

$C_{s,min}$ can be expressed in terms of a minimum measurable activity "sorbed", $A_{s,min}$, determined within measuring time t (counts per minute/ml or cpm ml^{-1}):

$$A_{s,min} = C_{s,min}/t \qquad [cpm\ ml^{-1}] \quad . \qquad (A.33)$$

From equation A.32 it follows that approximately 13% of the total net counts must be "sorbed" in order to reach the required relative standard deviation of 10%.

The minimum sorption value $R_{d,\,min}$ is given by:

$$R_{d,min} = \frac{A_{s,min}}{A_{susp} - A_{s,min}} \cdot \frac{V}{m} \quad [L\ kg^{-1}] \quad . \qquad (A.34)$$

Combining equations A.32, A.33 and A.34 results in the following expression for $R_{d,min}$:

$$R_{d,min} = \frac{0.13}{0.87} \cdot \frac{V}{m} = 0.15 \cdot \frac{V}{m} \qquad [L\ kg^{-1}] \quad . \qquad (A.35)$$

Thus, $R_{d,min}$ is only determined by the S:L ratio of the system.

A.3 Determination of $R_{d,max}$ and $R_{d,min}$ for the sorption experiments

The experimental parameters of the different sorption experiments necessary to calculate $R_{d,max}$ and $R_{d,min,}$ are summarized and given together with the estimated values for $R_{d,max}$ and $R_{d,min}$ in the following tables.

In the case of the sorption isotherms, two values for $R_{d,max}$ are given; one for the lowest value of A_{susp} and the other one for the highest value of A_{susp}. Note that the variation of the value of A_{susp} does not necessarily reflect the variation of the total element concentration because the radionuclide concentrations are at trace levels whereas the total element concentration is determined by the concentration of the non-radioactive stable isotopes.

Two $R_{d,max}$ values and two $R_{d,min}$ values, one for the lowest and one for the highest S:L ratio, are given for the sorption experiments, where the S:L ratio was varied. Note that both values, $R_{d,max}$ and $R_{d,min}$, depend on the S:L ratio.

Table A-1: Calculation of the $R_{d,max}$ and $R_{d,min}$ values for Eu(III) sorption experiments.

Experiment	Counting time [minutes]	S:L [kg L^{-1}]	Background [counts (5 ml)$^{-1}$]	$A_{l,min}$ [cpm ml^{-1}]	A_{susp} [cpm ml^{-1}]	$R_{d,max}$ [L kg^{-1}]	$A_{s,min}$ [cpm ml^{-1}]	$R_{d,min}$ [L kg^{-1}]
Sorption kinetics	30	$2 \cdot 10^{-4}$	4500	33.3	20000	$3.0 \cdot 10^{6}$	2600	750
		$2 \cdot 10^{-4}$	4500	33.3	4000	$5.9 \cdot 10^{5}$	520	750
		$2 \cdot 10^{-3}$	4500	33.3	40800	$5.9 \cdot 10^{4}$	520	75
Sorption isotherms	30	$5 \cdot 10^{-4}$	4770	34.3	12225	$7.1 \cdot 10^{5}$	1590	300
		$5 \cdot 10^{-4}$	4770	34.3	167190	$9.8 \cdot 10^{6}$	21735	300
Effect of the S:L ratio	30	$1 \cdot 10^{-4}$	4890	34.7	92000	$2.6 \cdot 10^{7}$	11960	1500
		$2 \cdot 10^{-2}$	4890	34.7	165840	$2.4 \cdot 10^{5}$	21560	7.5
Effect of [ISA]	30	$4 \cdot 10^{-4}$	3600	30	18500	$1.5 \cdot 10^{6}$	2105	375
		$4 \cdot 10^{-3}$	3600	30	31500	$2.6 \cdot 10^{5}$	4095	37.5
Effect of [GLU]	30	$2 \cdot 10^{-3}$	3600	30	30000	10^{5}	3900	75
		$4 \cdot 10^{-4}$	3600	30	19750	$1.6 \cdot 10^{6}$	2565	375
		$4 \cdot 10^{-3}$	3600	30	28500	$2.4 \cdot 10^{5}$	3705	37.5

Table A-2: Calculation of the $R_{d,max}$ and $R_{d,min}$ values for Th(IV) sorption experiments.

Experiment	Counting time [minutes]	S:L [kg L^{-1}]	Background [counts (5 ml)$^{-1}$]	$A_{l,min}$ [cpm ml^{-1}]	A_{susp} [cpm ml^{-1}]	$R_{d,max}$ [L kg^{-1}]	$A_{s,min}$ [cpm ml^{-1}]	$R_{d,min}$ [L kg^{-1}]
Sorption kinetics	30	$4 \cdot 10^{-4}$	10500	50	180000	$8.9 \cdot 10^{6}$	24300	75
		$2 \cdot 10^{-3}$	10500	50	17000	$1.7 \cdot 10^{5}$	2210	375
Sorption isotherms	30	10^{-3}	5442	36.5	22765	$6.2 \cdot 10^{5}$	3537	150
		10^{-3}	5442	36.55	2740	$7.4 \cdot 10^{4}$	3537	150
Effect of the S:L ratio	30	$1 \cdot 10^{-4}$	5115	35.4	92505	$2.6 \cdot 10^{7}$	11960	1500
		$2 \cdot 10^{-2}$	5115	35.4	166780	$2.3 \cdot 10^{5}$	21560	7.5
Effect of [ISA]	30	$4 \cdot 10^{-4}$	4800	34.5	14000	$1.0 \cdot 10^{6}$	1820	375
		$2 \cdot 10^{-3}$	4800	34.5	17000	$2.5 \cdot 10^{5}$	2210	35
		$4 \cdot 10^{-3}$	4800	34.5	15000	$1.1 \cdot 10^{4}$	1950	37.5
		$1 \cdot 10^{-2}$	4800	34.5	37000	$1.1 \cdot 10^{4}$	4810	15
Effect of [GLU]	30	$4 \cdot 10^{-4}$	4800	34.5	80000	$5.7 \cdot 10^{6}$	10400	375
		$2 \cdot 10^{-3}$	4800	34.5	80000	$1.2 \cdot 10^{6}$	10400	75
		$4 \cdot 10^{-3}$	4800	34.5	92500	$6.7 \cdot 10^{5}$	12025	37.5

A.4 Evaluation of the 95% confidence interval for measured R_d values

Based on the expression used to calculate the distribution ratio R_d, (equation 1.2) and taking into account error propagation (equation A.5), the relative uncertainty (the confidence interval) on the R_d value can be calculated as follows:

$$\frac{T_{R_d}}{R_d} = \sqrt{\left(\frac{\sqrt{\left(T_{A_{susp}}\right)^2 + \left(T_{A_B^{susp}}\right)^2 + \left(T_{A_l}\right)^2 + \left(T_{A_B^l}\right)}}{A_{susp} - A_B^{susp} - A_l + A_B^l}\right)^2 + \left(\frac{\sqrt{\left(T_{A_l}\right)^2 + \left(T_{A_B^l}\right)^2}}{A_l - A_B^l}\right)^2 + \left(\frac{T_V}{V}\right)^2 + \left(\frac{T_m}{m}\right)^2} \quad \text{(A.36)}$$

with:

T_x: confidence interval on variable x,

A_{susp}: activity in the homogeneous suspension [cpm ml^{-1}],

A_l: activity in the supernatant solution [cpm ml^{-1}],

A_B^{susp}: background activity for activity measurements of the suspension,

A_B^l: background activity for activity measurements of the supernatant solution.

Note that the background activities for activity measurements of total suspensions and for activity measurements for supernatant solutions must not necessarily be similar, as, for γ emitters, these background activities are caused mainly by the activity of the neighbouring samples in the counter equipment.

The main uncertainties on the R_d value originate from uncertainties on the mass of solid phase (m) used in the experiments and the activity measurements of the suspension (A_{susp}) and the equilibrium solution (A_l). By contrast, the uncertainties on the activities of the blank samples (A_B^{susp} and A_B^l) as well as on the volume, V, were found to be negligibly small. The uncertainties in m and A_{susp} are mainly caused by the preparation of the calcite suspensions. The very low quantities of solid required for the experiments do not allow weighting of the calcite material. Calcite suspensions were prepared by pipetting an aliquot of a concentrated suspension into a centrifuge tube and diluting it with the ACW to the desired S:L ratio. Note that preparation of diluted suspensions strongly depends on the homogeneity of the concentrated suspension. Due to the high

ionic strength of the ACW, it was very difficult to make sure that the calcite suspensions were homogeneous during pipetting due to coagulation effects. This effect leads to very large uncertainties on the mass of solid used in the experiments.

An estimate of the uncertainty caused by the variation in the mass of solid can be deduced from multiple measurements of the suspension activity, A_{susp}. This was done for a typical ^{152}Eu sorption experiment[4] (Table A-3 and Table A-4). Note that any variation in the amount of calcite in the test tubes results in a proportional variation of the ^{152}Eu activity measured in the calcite suspension.

The data in Table 3 and Table 4 show that the relative 95% confidence intervals for A_{susp} and, consequently, for the mass, m, at a S:L ratio of $2 \cdot 10^{-4}$ kg L^{-1} is approximately 48%. At a S:L ratio of $2 \cdot 10^{-3}$ kg L^{-1}, this relative 95% confidence interval decreases to approximately 29%. The relative confidence intervals for the activities in the equilibrium solutions are ~43% and ~44% at S:L ratios of $2 \cdot 10^{-4}$ kg L^{-1} and $2 \cdot 10^{-3}$ kg L^{-1}, respectively.

Applying the uncertainties obtained in Table A-3 and Table A-4 in equation A.36 yields relative 95% confidence intervals for the R_d values of 67% and 62%, respectively. Note that due to the large uncertainties on the variables in equation A.5 and A.36, the first assumption made in deriving these equations is not strictly fulfilled anymore. Hence, estimates of uncertainties based on these equations only are an approximation of the real uncertainties.

Note that the relative uncertainty on A_l includes contributions from the radioactive decay as well from other possible sources such as pipetting, sample heterogeneity etc. Therefore, this uncertainty differs from the maximum allowed uncertainty, α, defined in section A.1 and A.2, which only accounts for the uncertainty on the radioactive decay.

In most experiments the number of replicates was too small to allow us to estimate the correct 95% confidence intervals (T) on the R_d values and aqueous radionuclide concentrations. In these cases, relative 95% confidence intervals of 67% and 48%, respectively, were assumed.

---

[4] See section 4.5.1 and 5.2.1 for the description and the results of this experiment. No effect of time on ^{152}Eu sorption was observed, so measurements made after increasing equilibration times can be treated as replicates.

Table A-3: Statistics of the ^{152}Eu activity in suspension of two series of replicate measurements. The Student's factor t for n=10, p=95% is 2.26.

S:L ratio [kg L^{-1}]	Number of measurements	$\overline{A_{susp}}$ [cpm ml^{-1}]	$\sigma_{A_{susp}}$	$T_{A_{susp}}$	$\frac{T_{A_{susp}}}{\overline{A_{susp}}} \cdot 100$
$2 \cdot 10^{-4}$	10	3159	672.4	1519.6	48
$2 \cdot 10^{-3}$	10	3347	438.2	990.3	29

Table A-4: Statistics of the ^{152}Eu activity in solution of two series of replicate measurements . The Student's factor t for n=10, is 2.26.

S:L ratio [kg L^{-1}]	Number of measurements	$\overline{A_l}$ cpm ml^{-1}	σ_{A_l}	$T_{\overline{A_l}}$	$\frac{T_{A_l}}{\overline{A_l}} \cdot 100$
$2 \cdot 10^{-4}$	10	148.8	28.2	63.6	43
$2 \cdot 10^{-3}$	10	59	11.6	26.2	44